LUND UNIVERSITY

Proteogenomic profiling of metastatic melanoma. From protein expression to patient stratification.

Kuras, Magdalena

2023

Document Version:
Publisher's PDF, also known as Version of record

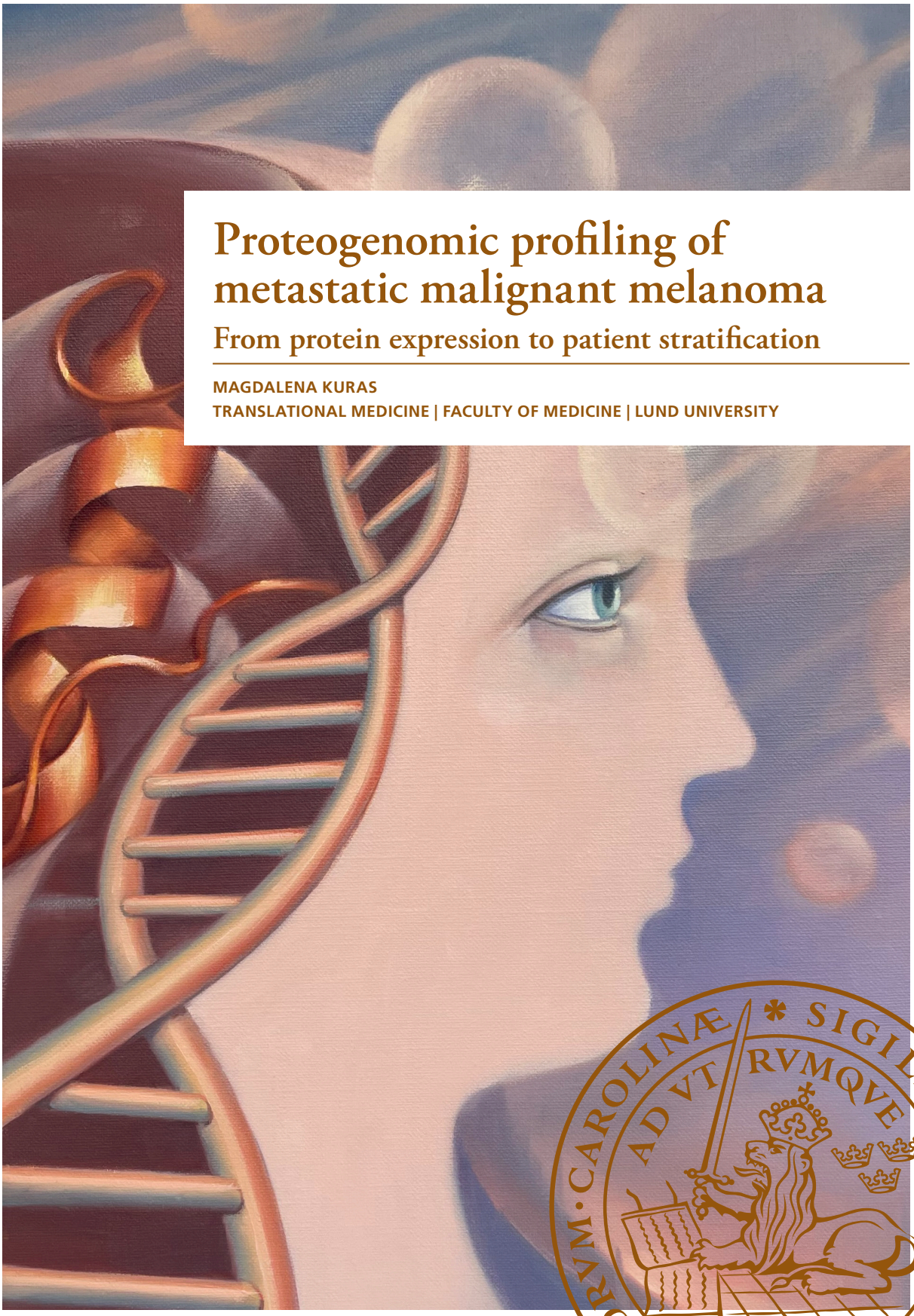

Proteogenomic profiling of metastatic malignant melanoma

From protein expression to patient stratification

MAGDALENA KURAS
TRANSLATIONAL MEDICINE | FACULTY OF MEDICINE | LUND UNIVERSITY

Printed by Media-Tryck, Lund 2023 NORDIC SWAN ECOLABEL 3041 0903

MAGDALENA KURAS received her master's degree in Medical Science from Lund University in 2017. She then started her scientific career in clinical proteomics focusing on malignant melanoma, and pursued her doctoral studies at the Department of Translational Medicine at Lund University.

The understanding of melanoma biology has increased profoundly during the last two decades, leading to the emergence of immunotherapy and targeted therapy, revolutionising the treatment of patients with disseminated disease. As new therapies are continuously being developed, there is an urgent need for patient stratification and prognostic and predictive biomarkers. This thesis brings novel insights into the molecular mechanisms of melanoma progression with a particular focus on patient stratification.

LUND UNIVERSITY

FACULTY OF MEDICINE

Department of Translational Medicine

Lund University, Faculty of Medicine
Doctoral Dissertation Series 2023:39
ISBN 978-91-8021-378-3
ISSN 1652-8220

Proteogenomic profiling of metastatic malignant melanoma
From protein expression to patient stratification

Proteogenomic profiling of metastatic malignant melanoma

From protein expression to patient stratification

Magdalena Kuras

LUND
UNIVERSITY

DOCTORAL DISSERTATION

by due permission of the Faculty of Medicine, Lund University, Sweden.
To be defended at Belfragesalen, BMC D15, Lund
Friday, March 31st, 2023, at 14.00

Faculty opponent
Jennifer van Eyk, PhD, FAHA, FISHR
Advanced Clinical BioSystems Research Institute,
Cedars-Sinai Medical Center, Los Angeles, CA, USA

Organization LUND UNIVERSITY	**Document name** Doctoral dissertation
Department of Translational Medicine	**Date of issue:** 2023-03-31
Author Magdalena Kuras	Sponsoring organization

Title and subtitle
Proteogenomic profiling of metastatic malignant melanoma – From protein expression to patient stratification

Abstract
Malignant melanoma is a very aggressive skin cancer due to its heterogeneous nature and strong metastatic potential. The incidence is continuously increasing worldwide, and it is one of the most common cancers seen in young adults. In the last twenty years, our understanding of melanoma biology has increased profoundly, leading to the emergence of immunotherapy and targeted therapy. Thus, revolutionising the treatment of patients with disseminated disease. However, a large fraction of patients relapses or do not respond. As new therapies are continuously being developed, there is a prominent need for patient stratification and prognostic and predictive biomarkers.

The first three papers of this thesis established robust high-throughput sample preparation workflows for analysing the proteome of clinical tissue samples. In papers four and five, the developed workflows were applied to analyse treatment-naïve frozen metastases from 137 patients with malignant melanoma, followed by integrating and interpreting the data to understand melanoma biology better.

We propose several ways of stratifying melanoma metastases based on protein expression, histopathology, and patient outcome. Our analyses identified five proteomic subtypes, displaying differences in phenotype switching, immune surveillance, levels of known melanoma markers, and significant associations with patient outcomes. About 50% of melanoma tumours harbour mutations in the BRAF gene. In the fourth paper, the protein expression of BRAF V600E mutated tumours was linked to survival and used for subsequent identification of BRAF V600 mortality-based risk groups, proposing a more individualised treatment approach.

Furthermore, we present a melanoma-associated signature of single amino acid variants enriched mainly in proteins related to different extracellular matrix functions, suggesting a contribution of these variants to the formation of a pro-tumourigenic microenvironment. Lastly, we classified patients into subgroups based on the composition of the tumour microenvironment in lymph node metastases, improving prognosis prediction.

We are just beginning to understand the complex signalling between the tumour, its microenvironment and the immune system, giving rise to particular melanoma phenotypes essential for disease progression. As we move forward, our ever-increasing knowledge will enable the successful treatment of most patients with disseminated melanoma.

Keywords: Proteomics, mass spectrometry, malignant melanoma

Classification system and/or index terms (if any)

Supplementary bibliographical information		**Language:** English
ISSN and key title: 1652-8220		**ISBN:** 978-91-8021-378-3
Recipient's notes	**Number of pages:** 124	Price
	Security classification	

Signature Date 2022-02-23

Proteogenomic profiling of metastatic malignant melanoma

From protein expression to patient stratification

Magdalena Kuras

LUND
UNIVERSITY

Cover by Fathi Kasraian

Figures 1, 3-10 and 12 were created with BioRender.com

Faculty of Medicine
Department of Translational Medicine

ISBN 978-91-8021-378-3
ISSN 1652-8220
Lund University, Faculty of Medicine Doctoral Dissertation Series 2023:39

Printed in Sweden by Media-Tryck, Lund University
Lund 2023

Nothing in life is to be feared,
it is only to be understood.
Now is the time to understand more,
so that we may fear less.
– Marie Curie

Table of Contents

List of papers included in the thesis

Paper I. **Kuras, M.**, Betancourt, L. H., Rezeli, M., Rodriguez, J., Szasz, M., Zhou, Q., Miliotis, T., Andersson, R., & Marko-Varga, G. (2019). Assessing Automated Sample Preparation Technologies for High-Throughput Proteomics of Frozen Well Characterized Tissues from Swedish Biobanks. J Proteome Res, 18(1), 548-556.

Paper II. Murillo, J. R., **Kuras, M.**, Rezeli, M., Miliotis, T., Betancourt, L., & Marko-Varga, G. (2018). Automated phosphopeptide enrichment from minute quantities of frozen malignant melanoma tissue. PLoS One, 13(12), e0208562.

Paper III. **Kuras, M.***, Woldmar, N.*, Kim, Y., Hefner, M., Malm, J., Moldvay, J., Dome, B., Fillinger, J., Pizzatti, L., Gil, J., Marko-Varga, G., & Rezeli, M. (2021). Proteomic Workflows for High-Quality Quantitative Proteome and Post-Translational Modification Analysis of Clinically Relevant Samples from Formalin-Fixed Paraffin-Embedded Archives. J Proteome Res, 20(1), 1027-1039.

Paper IV. Betancourt, L. H., Szasz, A. M., **Kuras, M.**, Rodriguez Murillo, J., Sugihara, Y., Pla, I., Horvath, Z., Pawlowski, K., Rezeli, M., Miharada, K., Gil, J., Eriksson, J., Appelqvist, R., Miliotis, T., Baldetorp, B., Ingvar, C., Olsson, H., Lundgren, L., Horvatovich, P., Welinder, C., Wieslander, E., Kwon, H. J., Malm, J., Nemeth, I. B., Jonsson, G., Fenyo, D., Sanchez, A., & Marko-Varga, G. (2019). The Hidden Story of Heterogeneous B-raf V600E Mutation Quantitative Protein Expression in Metastatic Melanoma-Association with Clinical Outcome and Tumor Phenotypes. *Cancers (Basel)*, *11*(12).

Paper V. **Kuras, M.***, Betancourt, L. H.*, Hong, R.*, Szadai, L., Rodriguez, J., Horvatovich, P., Pla, I., Eriksson, J., Szeitz, B., Deszcz, B., Welinder, C., Sugihara, Y., Ekedah, H., Baldetorp, B., Ingvar, C., Lundgren, L., Lindberg, H., Oskolas, H., Horvath, H., Rezeli, M., Gil, J., Appelqvist, R., Keméeny, L. V., Malm, J., Sanchez, A., Szasz, M. A., Pawłowski, K., Wieslander, E., Fenyö, D., Balazs Nemeth, I., & Marko-Varga, G. Histopathology-assisted proteogenomics provides foundations for a comprehensive stratification of melanoma metastases. *Unpublished.*

*Contributed equally as first authors

List of papers not included in the thesis

1) Woldmar, N.*, Schwendenwein, A.*, **Kuras, M.***, Szeitz, B., Boettiger, K., Tisza, A., László, V., Reiniger, L., Bagó, A. G., Szállási, Z., Moldvay, J., Szász, A. M., Malm, J., Horvatovich, P., Pizzatti, L., Domont, G. B., Rényi-Vámos, F., Hoetzenecker, K., Hoda, M. A., Marko-Varga, G., Schelch, K., Megyesfalvi, Z., Rezeli, M., & Döme, B. (2022). Proteomic analysis of brain metastatic lung adenocarcinoma reveals intertumoral heterogeneity and specific alterations associated with the timing of brain metastases. ESMO Open, 8(1), 100741.

2) Betancourt, L. H., Gil, J., Sanchez, A., Doma, V., **Kuras, M.**, Murillo, J. R., Velasquez, E., Cakir, U., Kim, Y., Sugihara, Y., Parada, I. P., Szeitz, B., Appelqvist, R., Wieslander, E., Welinder, C., de Almeida, N. P., Woldmar, N., Marko-Varga, M., Eriksson, J., Pawlowski, K., Baldetorp, B., Ingvar, C., Olsson, H., Lundgren, L., Lindberg, H., Oskolas, H., Lee, B., Berge, E., Sjogren, M., Eriksson, C., Kim, D., Kwon, H. J., Knudsen, B., Rezeli, M., Malm, J., Hong, R., Horvath, P., Szasz, A. M., Timar, J., Karpati, S., Horvatovich, P., Miliotis, T., Nishimura, T., Kato, H., Steinfelder, E., Oppermann, M., Miller, K., Florindi, F., Zhou, Q., Domont, G. B., Pizzatti, L., Nogueira, F. C. S., Szadai, L., Nemeth, I. B., Ekedahl, H., Fenyo, D., & Marko-Varga, G. (2021). The Human Melanoma Proteome Atlas-Complementing the melanoma transcriptome. Clin Transl Med, 11(7), e451.

3) Betancourt, L. H., Gil, J., Kim, Y., Doma, V., Cakir, U., Sanchez, A., Murillo, J. R., **Kuras, M.**, Parada, I. P., Sugihara, Y., Appelqvist, R., Wieslander, E., Welinder, C., Velasquez, E., de Almeida, N. P., Woldmar, N., Marko-Varga, M., Pawlowski, K., Eriksson, J., Szeitz, B., Baldetorp, B., Ingvar, C., Olsson, H., Lundgren, L., Lindberg, H., Oskolas, H., Lee, B., Berge, E., Sjogren, M., Eriksson, C., Kim, D., Kwon, H. J., Knudsen, B., Rezeli, M., Hong, R., Horvatovich, P., Miliotis, T., Nishimura, T., Kato, H., Steinfelder, E., Oppermann, M., Miller, K., Florindi, F., Zhou, Q., Domont, G. B., Pizzatti, L., Nogueira, F. C. S., Horvath, P., Szadai, L., Timar, J., Karpati, S., Szasz, A. M., Malm, J., Fenyo, D., Ekedahl, H., Nemeth, I. B., & Marko-Varga, G. (2021). The human melanoma proteome atlas-Defining the molecular pathology. Clin Transl Med, 11(7), e473.

4) Sanchez, A.*, **Kuras, M.***, Murillo, J. R., Pla, I., Pawlowski, K., Szasz, A. M., Gil, J., Nogueira, F. C. S., Perez-Riverol, Y., Eriksson, J., Appelqvist, R., Miliotis, T., Kim, Y., Baldetorp, B., Ingvar, C., Olsson, H., Lundgren, L., Ekedahl, H., Horvatovich, P., Sugihara, Y., Welinder, C., Wieslander, E., Kwon, H. J., Domont, G. B., Malm, J., Rezeli, M., Betancourt, L. H., & Marko-Varga, G. (2020). Novel functional proteins coded by the human genome discovered in metastases of melanoma patients. Cell Biol Toxicol, 36(3), 261-272.

5) Gil, J., Betancourt, L. H., Pla, I., Sanchez, A., Appelqvist, R., Miliotis, T., **Kuras, M.**, Oskolas, H., Kim, Y., Horvath, Z., Eriksson, J., Berge, E., Burestedt, E., Jonsson, G., Baldetorp, B., Ingvar, C., Olsson, H., Lundgren, L., Horvatovich, P., Murillo, J. R., Sugihara, Y., Welinder, C., Wieslander, E., Lee, B., Lindberg, H., Pawlowski, K., Kwon, H. J., Doma, V., Timar, J., Karpati, S., Szasz, A. M., Nemeth, I. B., Nishimura, T., Corthals, G., Rezeli, M., Knudsen, B., Malm, J., & Marko-Varga, G. (2019). Clinical protein science in translational medicine targeting malignant melanoma. Cell Biol Toxicol, 35(4), 293-332.

6) Mendonca, C. F., **Kuras, M.**, Nogueira, F. C. S., Pla, I., Hortobagyi, T., Csiba, L., Palkovits, M., Renner, E., Dome, P., Marko-Varga, G., Domont, G. B., & Rezeli, M. (2019). Proteomic signatures of brain regions affected by tau pathology in early and late stages of Alzheimer's disease. Neurobiol Dis, 130, 104509.

7) Betancourt, L. H., Sanchez, A., Pla, I., **Kuras, M.**, Zhou, Q., Andersson, R., & Marko-Varga, G. (2018). Quantitative Assessment of Urea In-Solution Lys-C/Trypsin Digestions Reveals Superior Performance at Room Temperature over Traditional Proteolysis at 37 degrees C. J Proteome Res, 17(7), 2556-2561.

*Contributed equally as first authors

Thesis at a glance

Malignant melanoma is a very aggressive skin cancer due to its heterogeneous nature and strong metastatic potential. The incidence is continuously increasing worldwide, and it is one of the most common cancers seen in young adults. In the last twenty years, our understanding of melanoma biology has increased profoundly, leading to the emergence of immunotherapy and targeted therapy. Thus, revolutionising the treatment of patients with disseminated disease. However, a large fraction of patients relapses or do not respond. As new therapies are continuously being developed, there is a prominent need for patient stratification and prognostic and predictive biomarkers.

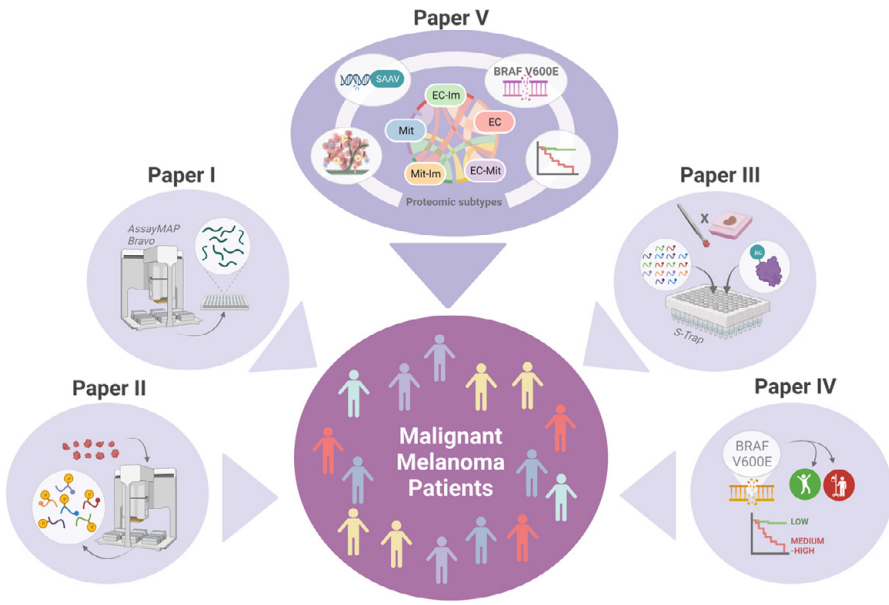

The first three papers of this thesis established robust high-throughput sample preparation workflows for analysing the proteome of clinical tissue samples. In papers four and five, the developed workflows were applied to analyse treatment-

naïve frozen metastases from 137 patients with malignant melanoma, followed by integrating and interpreting the data to understand melanoma biology better.

We propose several ways of stratifying melanoma metastases based on protein expression, histopathology, and patient outcome. Our analyses identified five proteomic subtypes, displaying differences in phenotype switching, immune surveillance, levels of known melanoma markers, and significant associations with patient outcomes.

About 50% of melanoma tumours harbour mutations in the BRAF gene. In the fourth paper, the protein expression of BRAF V600E mutated tumours was linked to survival and used for subsequent identification of BRAF V600 mortality-based risk groups, proposing a more individualised treatment approach.

Furthermore, we present a melanoma-associated signature of single amino acid variants enriched mainly in proteins related to different extracellular matrix functions, suggesting a contribution of these variants to the formation of a pro-tumourigenic microenvironment. Lastly, we classified patients into subgroups based on the composition of the tumour microenvironment in lymph node metastases, improving prognosis prediction.

We are just beginning to understand the complex signalling between the tumour, its microenvironment and the immune system, giving rise to particular melanoma phenotypes essential for disease progression. As we move forward, our ever-increasing knowledge will enable the successful treatment of most patients with disseminated melanoma.

Abbreviations

ACN	Acetonitrile
Adj.	Adjusted
AJCC	American Joint Committee on Cancer
ALM	Acral lentiginous melanoma
Ambic	Ammonium bicarbonate
CAF	Cancer-associated fibroblast
CPTAC	Clinical Proteomic Tumor Analysis Consortium
CT	Connective tissue
CTLA4	Cytotoxic T-lymphocyte-associated antigen 4
CV	Coefficient of variation
DC	Dendritic cell
DDA	Data-dependent acquisition
DIA	Data-independent acquisition
DNA	Deoxyribonucleic acid
DTT	Dithiothreitol
ECM	Extracellular matrix
EMA	European Medicine Agency
EMT	Epithelial-mesenchymal transition
FDA	Food and drug administration
FDR	False discovery rate
FFPE	Formalin-fixed and paraffin-embedded
GO	Gene ontology
HCT	High connective tissue
HE	Haematoxylin and eosin
HLA	Human leukocyte antigen
HLN	High lymph node
HR	Hazard ratio
HPLC	High-performance liquid chromatography
IA	Iodoacetamide
ICA	Independent component analysis
IL	Interleukin
IMAC	Immobilised metal ion affinity chromatography
KEGG	Kyoto Encyclopedia of Genes and Genomes
KM	Kaplan-Meier
LCT	Low connective tissue

LC-MS/MS	Liquid chromatography-tandem mass spectrometry
LDH	Lactate dehydrogenase
LM	Lentigo maligna melanoma
LLN	Low lymph node
LN	Lymph node
MAPK	Mitogen-activated protein kinase
MDSC	Myeloid-derived suppressor cells
MHC	Major histocompatibility complex
mRNA	Messenger RNA
MS	Mass spectrometry
NK cells	Natural killer cells
NM	Nodular melanoma
OIS	Oncogene-induced senescence
OS	Overall survival
PD1	Programmed cell death 1
PD-L1	Programmed cell death ligand 1
PI3K	Phosphoinositide 3-Kinases
PTM	Posttranslational modification
RNA	Ribonucleic acid
ROC	Receiver operating characteristic
RP	Reversed phase
RT	Room temperature
RTK	Receptor tyrosine kinase
SAAV	Single amino acid variant
SDS	Sodium dodecyl sulfate
SSM	Superficial spreading melanoma
S-Trap	Suspension trap
TAM	Tumour-associated macrophage
TCGA	The Cancer Genome Atlas Network
TEAB	Tetraethylammonium bromide
TFA	Trifluoroacetic acid
TIL	Tumour infiltrating lymphocytes
TME	Tumour microenvironment
TMT	Tandem mass tags
TNM	Tumour-node-metastasis
TSA	Tumour-specific antigen
UV	Ultraviolet
VAf	Variant Allele Frequency
WHO	World health organisation
WNT	Wingless-related integration site
wt	Wild-type

Introduction

Malignant melanoma

Epidemiology and aetiology

Melanoma of the skin is a very aggressive type of cancer originating from cells called melanocytes. It has a heterogeneous nature and a strong propensity to metastasise to other organs [1,2]. The incidence of melanoma is continuously rising globally, and it is one of the most common cancers seen in young adults. According to the Swedish cancer foundation (2019), malignant melanoma is the fifth most common cancer in both men and women. A yearly increase of above four percent has occurred in the last twenty years. The continuous increase in melanoma prevalence is becoming a significant clinical problem and will be associated with even higher treatment costs in the coming years. Over 4,000 people are diagnosed with invasive melanoma yearly in Sweden, meaning the tumour has grown through the basement membrane into the dermis, causing around 500 deaths (Figure 1). According to WHO (2020), melanoma incidence and mortality due to melanoma are the highest in Australia and New Zealand, followed by North America and Northern and Western Europe. The main reason is believed to be intermittent sun exposure, characterised by a history of sunburns. Other risk factors include a fair skin type, many nevi, and advanced age, where the median age of diagnosis is around 65 to 70 years.

A weakened immune system, family history, and prior removal of melanomas are also considered essential risk factors [2,3]. Between 25 and 30% of melanoma tumours arise from a pre-existing nevus. Therefore, not only the total number of nevi but also the size and type of nevi are associated with melanoma development [4]. Melanoma only accounts for about 1–4% of all skin cancers globally. Although it is less frequent, it is much deadlier than other skin tumours [3]. However, in early-stage melanoma, surgical removal of the tumour has a curable outcome in around 90% of the patients.

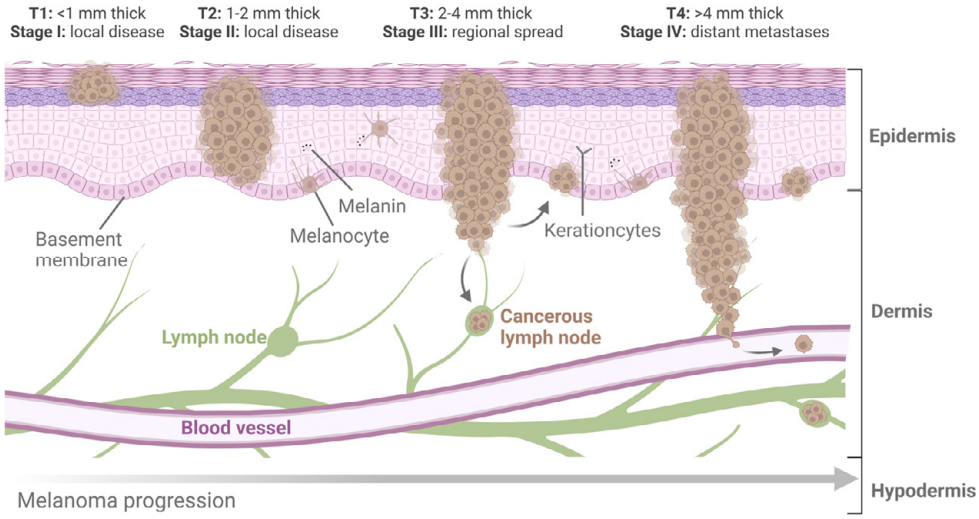

Figure 1. Melanoma development. Melanoma progression is characterised by a series of steps where normal melanocytes progressively develop a malignant phenotype by acquiring various features such as decreased differentiation and loss of melanoma markers. In the first disease stage (T0 or stage 0 – not shown), the melanoma is restricted to the outer part of the epidermis. In the early disease stages I–II (T1–2), the melanoma is confined to the top layer of the skin (the epidermis), and if detected at this point, the five-year survival is above 98%. In the later stages, the melanoma breaches through the basement membrane and invades the deeper layer of the skin (the dermis) (T3–T4). During this vertical-growth phase, melanoma cells may attain a migratory phenotype and enter the nearby lymph nodes or capillaries, forming regional (stage III) or distant (stage IV) metastases. If melanoma is detected at the later stages, the five-year survival is about 70% for stage III and just below 30% for stage IV.

Melanoma classification, staging and diagnosis

The four main histological subtypes of melanoma

Melanoma is, in many ways, one of the most heterogeneous tumour types. It can develop in the skin (cutaneous), in mucosal membranes (mucosal) and in the eye (ocular). The most common form is cutaneous melanoma, which can be divided into four main histological subtypes, including superficial spreading melanoma (SSM), nodular melanoma (NM), lentigo maligna melanoma (LM) and acral lentiginous melanoma (ALM) [5]. SSM is the most prevalent, accounting for 70–80% of all diagnosed melanoma cases. It is also the most common among younger individuals. In women, it is frequently found on the lower extremities and, in men, on the trunk. Histological characteristics of SSM include a pagetoid and nested spread within the epidermis (Figure 2A) [6]. NM is the second most prevalent and accounts for 15–30% of diagnosed cases, and it is considered one of the most aggressive types [5]. The most common anatomical location includes the trunk, head and neck. Histologically, epidermal proliferation is often minimal. Instead, intradermal nests are frequently observed (Figure 2B). LM is commonly seen in older people with sun-damaged faces and often appears on the nose and cheeks. The histological features include widespread melanocytic proliferation, observed in the dermal-epidermal junction and by intradermal nests of epithelioid or spindled-shaped cells. ALM is less

common and is usually found in African Americans [6,7]. It mainly develops on the palms of the hands and soles of the feet, and the histological characteristics include restricted lentiginous growth of nested tumour cells. Other types include desmoplastic, polypoid, primary dermal, verrucous and amelanotic melanomas [5,8].

Tumour-node-metastasis (TNM) staging

The most used staging system for clinical decision-making of patients with cutaneous melanoma is the tumour-node-metastasis (TNM) classification. The assessment contains three parts: T refers to the thickness of the primary tumour and the presence or absence of ulceration (Figure 1). N includes the number of involved lymph nodes and the presence or absence of in-transit, satellite or microsatellite metastases. Finally, M indicates the presence of distant metastases and the patient's serum levels of LDH [9]. Although the TNM staging system helps to classify the patient, complementary approaches which consider tumour cell morphology, expression of molecular pathway effectors, genetic mutations, tumour immune response (immunoscoring) and tumour microenvironment composition (stroma-to-tumour ratio) would give additional valuable information in predicting outcome, assessing prognosis and guide treatment selection. A more in-depth analysis, evaluating such parameters, could generate deeper knowledge of patient-specific tumour properties, help to guide treatment selection, and potentially improve the therapeutical response.

Melanoma diagnosis

To diagnose melanoma, surgical excision with appropriate margins is the preferred method, after which a histological examination of the skin lesion is performed. Parameters such as histological subtype, number of mitoses and tumour thickness or Breslow thickness, which is the depth of the melanoma from the surface of the skin down to the deepest point of the tumour, are determined, as well as the presence or absence of ulceration and microsatellites. Additional information regarding the growth phase (horizontal or vertical) and the presence or absence of tumour infiltrating lymphocytes (TILs), regression, and vascular or perineural involvement may also be assessed. If there are uncertainties regarding the diagnosis, immunohistochemical melanoma markers can be examined, including the proteins involved in melanin production MLANA, TYR and HMB45 (PMEL), or SOX10, S100 and the proliferation marker MIB-1, which recognises the Ki67 antigen (Figure 3) [5 9]. These markers are used to diagnose primary and metastatic melanoma and distinguish it from other cancer types such as carcinomas (epithelioid origin), neuroendocrine tumours, sarcomas, lymphomas and germ cell tumours [10,11]. However, most currently used diagnostic markers of melanoma rely on the detection of melanocytes, meaning that they can determine melanocytic lineage rather than melanoma [12]. Additionally, their expression is often determined as present or absent and not quantified in detail. Melanoma patients would strongly benefit from

additional markers that can predict prognosis and therapy response, and efforts towards finding and introducing such markers would be valuable in many aspects.

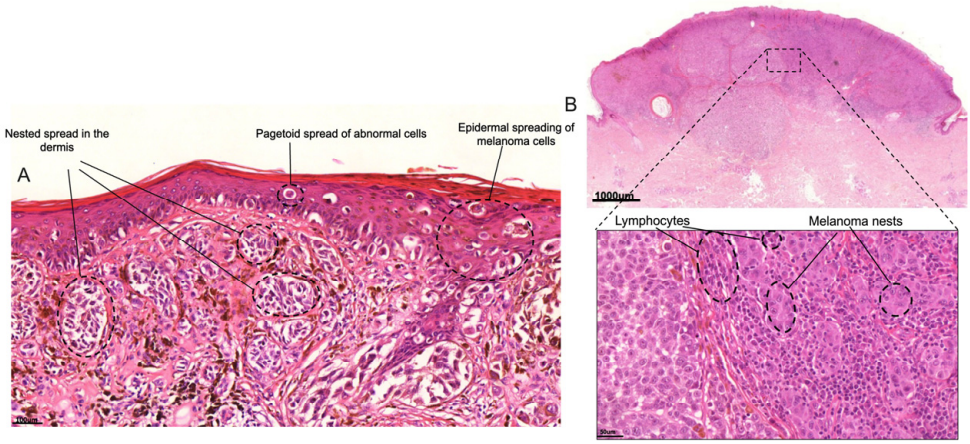

Figure 2. HE stained images of primary melanoma. (A) Superficial spreading melanoma, with epithelial and dermal spreading, including dermal nests and pagetoid spread (B) Nodular melanoma growing vertically with melanoma nests surrounded by lymphocytes.

Melanocyte function and the emergence of melanoma

Melanoma, a word derived from the Greek melas "dark" and oma "tumour", emerges from melanocytes, a type of specialised dendritic cells of neural crest origin, which can be found in the epidermis of the skin, along the choroidal layer of the eye, on mucosal surfaces and in the meninges[13]. Within the melanocytes, melanosomes produce the pigment melanin[14]. Two main types of melanin exist in the animal kingdom, yellow and red-brown pheomelanin and brown and black eumelanin, where eumelanin offers better protection against UV radiation than pheomelanin[15]. Melanosomes that primarily harbour pheomelanin differ in structure, composition and size from melanosomes mainly comprised of eumelanin. One melanocyte interacts with around 36 keratinocytes and supplies them with melanin[16] (Figure 1). In response to UV-induced DNA damage, keratinocytes in the skin produce a melanocyte-stimulating hormone (αMSH) that binds to the melanocortin receptor 1 (MC1R) on melanocytes, which then produces and release melanin (Figure 3).

Melanin shields the cells against UV radiation, thus preventing further DNA alterations[17,18]. Melanin and the distribution of melanosomes in the epidermis are among the most critical factors in protecting human skin from the harmful effects of UV radiation[14]. Predominantly UVB (280–315 nm) radiation is considered a primary mutagen since it is absorbed directly by DNA and induces DNA base damage. At the same time, UVA (315–400 nm) is mainly responsible for indirect

DNA damage by generating reactive oxygen species (ROS)[19,20]. The damage to the DNA can cause mutations in genes involved in melanoma development and is thought to be the first step towards disease formation. Due to UV-induced DNA damage, melanocytes transform and start to grow and proliferate uncontrollably compared to the normal surrounding tissue. Melanoma development is a multistep process caused by genetic and epigenetic modifications [21]. Eventually, the melanoma cells may invade the dermis and the hypodermis, and penetrate the endothelium of capillaries to enter the bloodstream or the lymphatic system and finally form distant metastases (Figure 1) [22 23].

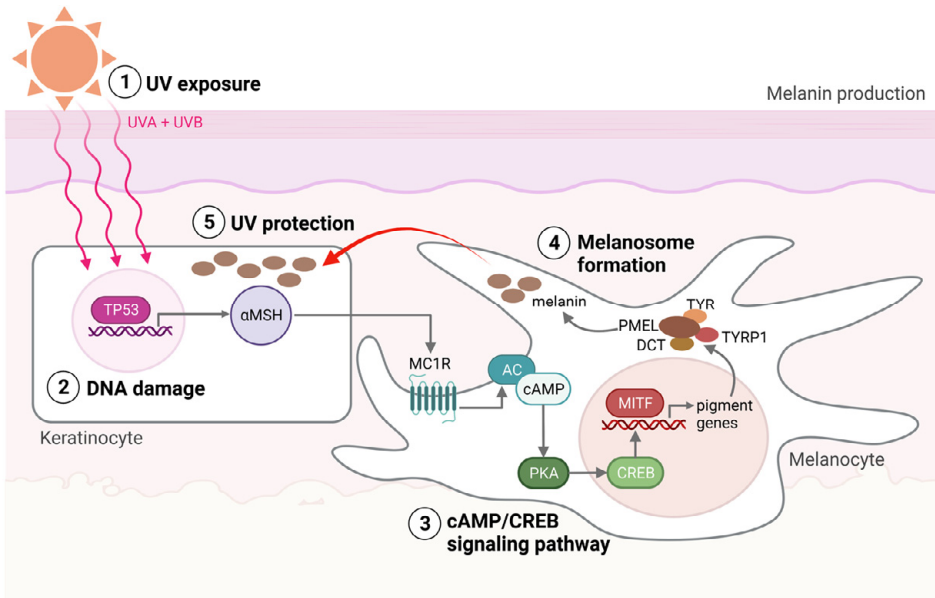

Figure 3. Melanin production. (1) The production of melanin, a process called melanogenesis, is activated upon UV exposure. (2) UV radiation damages the DNA in the keratinocytes, activating the TP53 pathway, which results in the production of αMSH that is secreted from the keratinocytes and binds to the MC1R on the melanocyte. (3) cAMP levels are then increased within the melanocytes, activating protein kinase A (PKA), which induces CRE-binding (CREB) protein and thereby the transcriptional activity of MITF. (4) MITF activates the transcription of pigment genes, including TYR, TYRP1, DCT, and PMEL, which are transported to the membrane-bound melanosome. (5) Matured melanosomes are then transferred from melanocytes to keratinocytes to protect them against UV light.

Genetic susceptibility to melanoma

About 10% of melanoma cases occur in patients with a family history of melanoma [24]. Although most genetic alterations associated with melanoma development are somatic, the underlying presence of heritable melanoma risk genes is essential to disease occurrence. It is thought to be so even in "sporadic" melanoma [25,26]. In the familial atypical multiple mole-melanoma (FAMMM) syndromes and the melanoma-astrocytoma syndrome (MAS), germline mutations in CDKN2A and

CDK4 are the most frequent genetic abnormalities [27]. CDKN2A encodes two crucial tumour suppressor proteins, $p16I^{NK4A}$ and $p14^{ARF}$, which, together with CDK4, function as cell cycle regulators (Figure 4) [28,29]. Germline mutations in CDKN2A or CDK4, and in BAP1 (enzyme), TERT (RNP enzyme), POT1 (RNP), ACD (regulates telomere length) and TERF2IP (transcriptional regulator) are considered high penetrance melanoma predisposition mutations. Together with MITF and MC1R, they are important components of melanoma susceptibility [2,26]. Medium and low penetrance alleles such as MITF and MC1R are more prevalent in the population, but alone, they are unlikely to result in melanoma development. However, a combination of mutations in several of these genes may be enough to promote disease development.

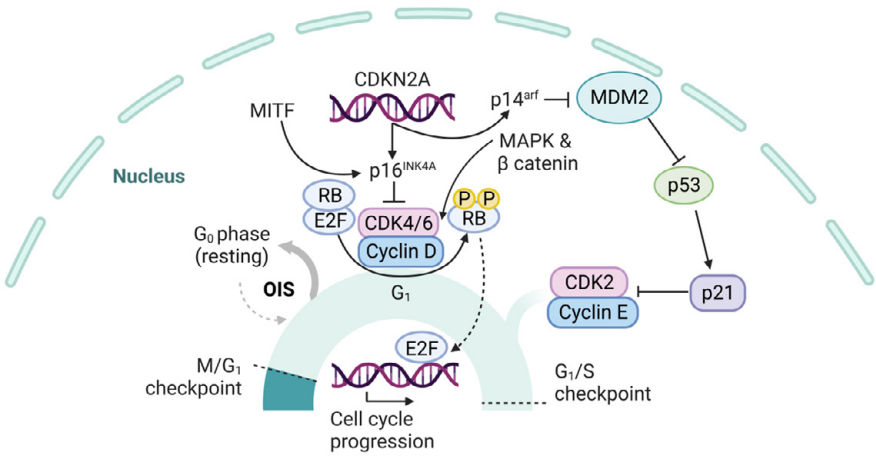

Figure 4. Cell cycle regulation. The proteins p16INK4A, p14ARF and Rb mainly govern progression through the G1-S phase of the cell cycle. On the contrary, cyclins bound to cyclin-dependent kinases facilitate cell cycle progression. CDK4/6 associates with Cyclin D and drive the cell cycle by phosphorylating Rb, releasing it from its inhibitory interaction with the E2F transcription factor and thereby allowing the expression of E2F-related genes and progression through the cell cycle. $p16^{INK4A}$ and $p14^{ARF}$ are the two most important proteins that govern the G1-S checkpoints, and in the absence of these proteins, by, i.e., a mutation in the CDKN2A gene, the tumour cells can progress through these checkpoints with minimal control. Alternatively, as a result of oncogenic stimulus such as DNA damage due to mutations or through ROS, cells may enter the G0 phase, a phenomenon referred to as oncogene-induced senescence, upheld mainly by retinoblastoma (Rb) and p53 signalling pathways, to prevent tumour development [34,35].

Polymorphism of the MC1R gene has been found to play a significant role in sporadic skin melanoma. MC1R, as described above, is the key regulator of skin pigmentation, and more than 200 coding region variants have been identified, many within the European population [30]. Polymorphisms in the MC1R gene give rise to diverse skin pigmentation phenotypes, among which red hair, freckles and fair skin express low pigmentation and show vulnerability to melanoma. This is thought to be a consequence of a quantitative shift of melanin synthesis from eumelanin to pheomelanin [30]. Furthermore, specific variants of MC1R are believed to increase the penetrance of CDKN2A mutations, doubling the risk of melanoma compared to a

CDKN2A mutation alone. Likewise, the coexistence of certain MC1R variants and a somatic BRAF V600E mutation increases tumour growth [31,32]. An interaction between MC1R and the tumour suppressor PTEN has also been proposed, where wild-type MC1R but not the variants associates with PTEN and protects it from degradation, thereby stimulating an immune response [33].

Commonly dysregulated pathways in melanoma

The mutation rate in melanoma tumours, measured as the number of mutations per Mb, exceeds that of all other cancers according to The Cancer Genome Atlas (TCGA) data [1]. The high rate of somatic mutations makes it particularly difficult to distinguish between causative (driver) mutations and bystander (passenger) mutations. The major players involved in melanoma formation include cell-autonomous mutations of the MAPK, PI3K and WNT signalling pathways [23] (Figure 5).

The Mitogen-Activated Protein Kinase (MAPK) pathway

The most common mutations in melanoma involve the MAPK signalling pathway. They include acquired mutations in the genes encoding two kinases, BRAF and NRAS, resulting in continuous activation and aberrant cell proliferation. Constant activation of MAPK signalling can lead to increased expression of cyclin D1, which interacts with CDK4/6 to promote phosphorylation and inhibition of the retinoblastoma (Rb) family of transcriptional repressors, enhancing E2F-dependent transcription of S-phase genes, facilitating G1-S phase transition and consequently cell cycle progression (Figure 4) [36]. However, upon acquirement of a BRAF mutation, a benign melanocytic lesion does not switch to malignancy. Instead, it enters a state of oncogene-induced senescence (OIS), leading to cell-cycle arrest (Figure 4) [2,37]. OIS facilitates tumour suppression by blocking cell proliferation and recruitment of immune cells to eliminate the damaged melanocytes [35].

Furthermore, BRAF mutations are found in about half of all melanocytic lesions and are thought to occur early in the disease. Most mutations occur at the V600 position, where a valine-to-glutamate substitution (V600E) is the most common (~ 80–90%), while V600K, V600D, and V600R account for another 10% to 15%. BRAF mutations are more frequent in melanomas that develop in sun-exposed skin. The mutated BRAF kinase can activate its downstream effector MEK, independent of RAS activation (Figure 5). MEK then activates ERK, which relocates to the nucleus and alters gene transcription by increasing the expression of various transcription factors (TFs), such as c-MYC and MITF [38,39]. MITF coordinates many different signalling pathways in melanoma, including cell-cycle regulation, differentiation, and migration, depending on its expression levels [40]. Generally, low MITF activity promotes invasion and cell cycle arrest, while high activity favours proliferation and differentiation by upregulation of pigmentation genes (Figure 3)

[41,42]. Amplification in MITF is present in about 20% of melanomas and is associated with a reduced five-year survival [43].

NRAS and BRAF mutations are almost always mutually exclusive, where NRAS mutations occur in about 20% of melanoma cases. In addition to MAPK pathway activation, oncogenic RAS acts as a positive upstream regulator of the PI3K pathway (Figure 5) [44]. Thus, activation of RAS transcription leads to downstream activation of two interconnected pathways. While both cause cell proliferation, dissemination, and survival of tumour cells, the PI3K-AKT signalling pathway contributes stronger to apoptosis prevention. In contrast, the RAF-MEK-ERK pathway is more active in proliferation and invasion [45,46]. Patients with NRAS mutations, often at the Q61 position, tend to have a worse prognosis and shorter median overall survival due to the aggressive nature of this mutation [47].

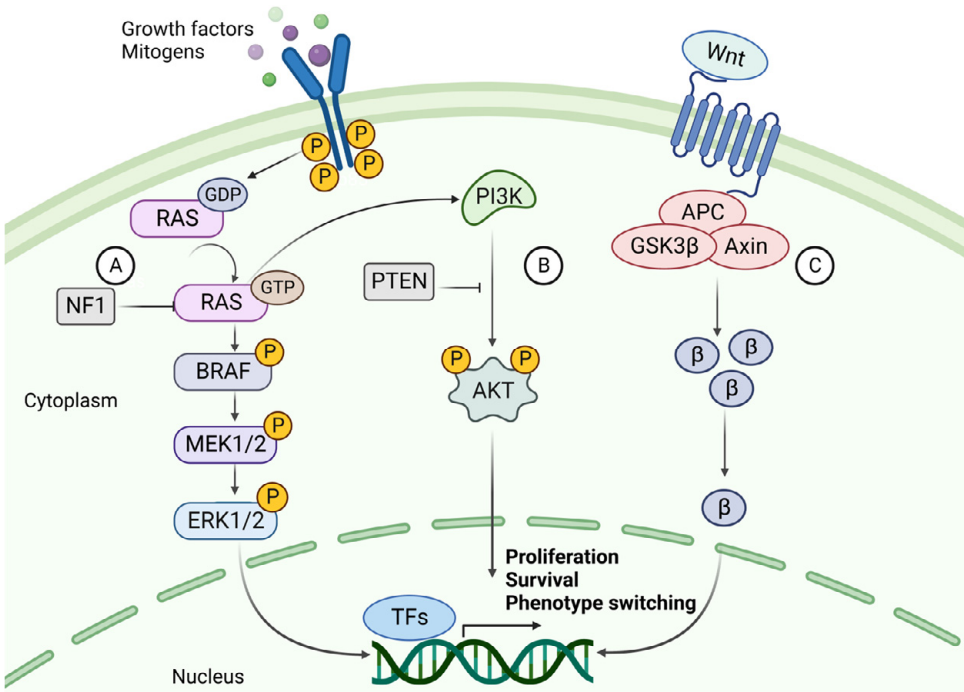

Figure 5. The signalling cascades of MAPK, PI3K and canonical WNT pathways. (A) The NRAS-BRAF MAPK pathway is activated by binding a growth factor (GF) or mitogen to a receptor tyrosine kinase. Upon activation, the RAS protein phosphorylates (P) MEK1/2, phosphorylating ERK1/2. ERK can then translocate to the nucleus and activate transcription factors which promote proliferation and progression through the cell cycle. NF1 hampers this cell cycle progression by converting RAS to its inactive GDP-bound form. (B) The activation of PI3K signalling by GTP-bound RAS. PI3K activates AKT through phosphorylation using a second messenger (PIP3 not shown). AKT is a kinase that mediates the phosphorylation of protein substrates, subsequently affecting the cell cycle and survival of the tumour cell. PTEN acts as a suppressor of this pathway by dephosphorylating PIP3, thereby blocking the activation of AKT. (C) The canonical WNT signalling pathway and its main effector, β catenin (β). β catenin is activated upon binding a WNT ligand to the G-protein coupled receptor (GPCR), whereby it is prevented from degradation and instead accumulates in the cytoplasm. β catenin then relocates to the nucleus, where it acts as a co-activator of transcription of genes related to EMT-like phenotype switching, among others.

The PI3K/AKT signalling pathway

To overcome OIS in a BRAF-mutated melanocytic lesion, subsequent mutations of the PI3K pathway are frequently acquired [37]. The coexistence of mutations in these pathways has been shown to overcome BRAFV600E OIS by losing PTEN expression or by overexpression of AKT3, a downstream target of PI3K (Figure 5). PTEN-negative or AKT3-overexpressing melanomas do not undergo apoptosis in response to BRAF inhibition. Both high activity of AKT3 and loss of PTEN function have been shown to promote the progression of BRAFV600E-positive nevi to melanoma [48]. PTEN is also thought to inhibit MAPK signalling by decreasing the phosphorylation of MEK and ERK [49]. Interestingly, BRAF mutations were found in both the nevi- and melanoma parts in melanoma biopsies, while activation of the PI3K pathway was detected in the melanoma portions only [33,50]. This indicates that the PI3K/AKT pathway is activated during the progression to malignant melanoma, most likely as means to overcome OIS.

Canonical and non-canonical WNT signalling

Normal WNT signalling is required to develop melanocytes, while aberrant WNT signalling is known to contribute to melanoma formation [23]. The canonical WNT pathway mainly contributes to the development of primary melanoma by suppressing $p16^{INK4A}$, overcoming OIS, and increasing proliferation. In contrast, the non-canonical pathway is primarily involved in metastasis formation by disrupting cell polarity and increasing migration capabilities [40]. Moreover, constitutively activated canonical WNT signalling via β-catenin has been shown to act synergistically with the MAPK pathway by suppressing the expression of $p16^{INK4A}$ and cooperating with NRAS in the transformation of a melanocytic lesion into melanoma. In a melanoma mouse model with a BRAFV600E mutation and inactivated PTEN, β-catenin acted as the central mediator of metastasis development and a regulator of both the MAPK and PI3K pathways[51]. Additionally, WNT signalling is known to be one of the key regulators of epithelial-mesenchymal transition (EMT). Therefore, it plays an important role in the EMT-like phenotype switching that occurs during melanoma progression [52].

The role of KIT, NF1, TERT and TP53 in melanoma

Other essential effector molecules in melanoma formation include KIT, NF1, TERT and p53. KIT is a proto-oncogene that encodes a receptor tyrosine kinase and is considered a driver mutation in melanoma. It is found to be mutated in about 1–3% of melanoma tumours [53]. KIT activates the MAPK and PI3K pathways leading to cell proliferation and survival. NF1 is a tumour suppressor that negatively regulates the MAPK and PI3K pathways. NF1 mutations are prevalent in melanomas that are wt for BRAF and NRAS and are considered driver mutations in these patients (Figure 5) [54]. Mutations in the TERT gene increase transcription from the TERT promoter, thereby preventing cancer cells from undergoing apoptosis [55]. Mutations

in the promoter region of TERT are considered driver mutations because of their association with familial melanoma and high frequency (70–80%) in sporadic melanoma. Lastly, mutations in the well-known tumour suppressor TP53 are also present within melanoma tumours (Figure 4). However, it is not as common compared with other cancers. Point mutations are found in about 10–20% of melanomas, suggesting that this cancer type uses different mechanisms to evade tumour suppression by the p53 protein [33,54].

The tumour microenvironment

The tumour microenvironment (TME) is known to have a central role in melanoma progression rather than acting as a bystander, and a pro-tumourigenic microenvironment is essential for a tumour's survival and progression [56]. Compared to the microenvironment surrounding normal tissue, the TME differs in architecture, including extracellular matrix (ECM) composition, metabolism, nutritional status, pH and oxygen levels [57]. The TME consists of a complex mixture of fibroblasts, immune cells and endothelial cells embedded in the ECM. There is continuous reciprocal communication between tumour cells and the microenvironment, where tumour cells secrete stimulatory growth factors, chemokines and cytokines and change glucose and oxygen levels [23,56,57]. This results in the recruitment of stromal cells, immune cells and vascular cells, which remodels the surroundings, creating a pro-tumourigenic microenvironment (Figure 6). The mechanisms behind the ability of the TME to drive melanoma progression, invasion and metastasis include increased cell proliferation and survival of the tumour cells, changed cellular plasticity including the acquirement of stem-like properties, where the melanoma cells become more neural crest-like, and by metabolic reprogramming [58].

Reprogramming of the tumour microenvironment

Oncogenic reprogramming of cellular metabolism is an essential feature of melanoma progression. It is triggered by genetic alterations and adaptation, forming a microenvironment that lacks nutrients and oxygen [57,59,60]. A metabolic shift from oxidative phosphorylation (OXPHOS) to a glycolytic phenotype has long been considered a hallmark of cancer [61]. Indeed, a key feature of BRAFV600E melanoma is the metabolic switch from mitochondrial respiration to glycolysis [60]. However, there is increasing evidence linking mitochondrial pathways to cancer development and progression [62-64]. Mitochondrial metabolism is thought to impact tumour development by increasing ROS as a by-product of OXPHOS, supporting the genomic instability required for transforming a melanocytic lesion into a melanoma tumour [60]. ROS is also thought to trigger oncogenic signalling of the MAPK pathway [63]. It is becoming evident that melanoma cells are dependent on mitochondria after inhibition of oncogenic MAPK signalling, linking mitochondrial dynamics, oncogenic MAPK signalling, and metabolism to tumourigenesis.

Furthermore, tumour cells secrete growth factors, transcription factors and cytokines to modify the microenvironment by reprogramming fibroblasts to cancer-associated fibroblasts (CAFs) (Figure 6). Although CAFs can originate from epithelial cells, endothelial cells, HSCs and CSCs, among others, fibroblasts represent the largest population of stromal cells within the TME [65]. In the early stages of tumourigenesis, activated fibroblasts act as tumour suppressors. As the disease progresses, they eventually develop into CAFs, characterised by the expression of α-smooth muscle actin, vimentin, desmin and fibroblast-activation protein (FAP) [56,66]. CAFs supply the tumour with growth factors, cytokines and metabolites and stimulate blood vessel formation. They rely upon aerobic glycolysis, a characteristic of highly proliferating cells, which promotes the metabolic adaptation of the progressing tumour. The tumour stroma can impact the aggressiveness of cancer cells not only through signalling but also through mechanical pressure and tissue stiffness, mainly stimulated by the LOX proteins [67,68]. A high frequency of CAFs and ECM proteins in the stroma forms a physical barrier surrounding the tumour, increasing the interstitial pressure and hypoxia within the tumour, partly explaining why a tumour with a high stromal content often is associated with an inadequate response to therapy and a poor outcome [69,70]. In response to the low oxygen levels, the cancer cells upregulate HIF1α, a transcription factor that controls genes involved in angiogenesis, migration, metabolism, and metastasis [71].

Phenotypic switch

The tumour stroma further contributes to melanoma progression by initiating a "phenotypic switch", where the melanocytic characteristics are lost and exchanged in favour of a more undifferentiated phenotype [72]. The undifferentiated mesenchymal-like melanoma cells almost completely lose their melanocytic features and appear nearly undistinguishable from epithelial tumours undergoing EMT, suggesting a resemblance between the two processes [73,74] [75]. Given that melanocytes derive from neural crest cells, which underwent EMT during their development into melanocytes, it is not surprising that phenotype switching mimics this process [76]. The phenotypic transition of melanoma cells includes the acquisition of a spindle-like morphology, upregulation of mesenchymal markers and release of ECM degrading proteins, such as matrix metalloproteinases (MMPs), which further support the invasive features (Figure 7). An additional downregulation of the epithelial cell surface protein E-cadherin in favour of N-cadherin accompanies the phenotypic switch. As a result, the keratinocytes lose control over the melanoma cells, which gain properties to grow vertically through the epidermis (Figure 1) [77]. A parallel upregulation of the TGF-β signalling pathway and the above-described pathways (MAPK, PI3K/AKT3 and Wnt/β-catenin) increase the abundance of transcription factors such as MITF, SOX, Snai1/2, Slug, Twist1, Zeb1/2, and NFκB, markers facilitating the phenotype switching in melanoma [78,79]. Melanoma is believed to progress and metastasise by alternating between the melanocytic

(proliferative) and undifferentiated (invasive) states, including intermediate, transitory and neural crest-like states (Figure 7) [72,80]. In several studies, the two extreme conditions are characterised by a high expression of MITF, and a low expression of a receptor tyrosine kinase (RTK) named AXL in the melanocytic state and a low MITF and high AXL expression in the undifferentiated state. The different phenotypes often coexist in the same tumour [42,80,81]. When a more undifferentiated phenotype is acquired, it may cause modification of tumour-specific antigens (TSA) and a different repertoire of expression, accelerating the escape from immune surveillance. That is why targeting TSAs, common to melanocytic (proliferative), intermediate and undifferentiated (invasive) phenotypes, should be considered when developing new treatment approaches to increase the likelihood of a more efficient and prolonged treatment response.

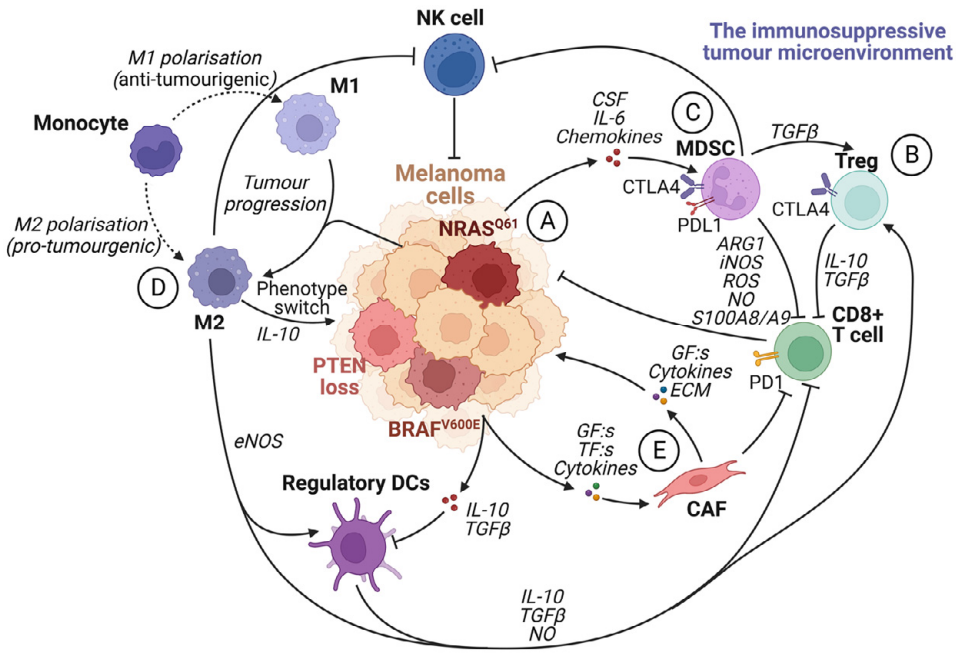

Figure 6. The immunosuppressive tumour microenvironment. The recruitment of various cells modulates the tumour microenvironment by the secretion of cytokines and chemokines by tumour cells and other infiltrating cells. Most cells within an immunosuppressive tumour microenvironment inhibit the activation and function of cytotoxic CD8+ T cells. (A) Tumour cells can induce the activity of Treg cells, tumour-associated macrophages (M2) and MDSCs by secreting growth factors such as VEGF. They also facilitate the transformation of fibroblasts into cancer-associated fibroblasts and enhance the expression of PD1 on CD8+ T cells. (B) Treg cells inhibit CD8+ T cells and NK cells by upregulating CTLA4 and releasing IL-10 and TGFβ. (C) MDSCs, whose expression of PDL1 inhibits T cell activation by binding to PD1. Furthermore, MDSCs promote Treg cell proliferation in a TGFβ-dependent manner, boost angiogenesis in the tumour microenvironment, and contribute to the phenotypic switch in melanoma cells. In addition, MDSCs hinder CD8+ T cells by releasing arginase I and S100A8/A9 and metabolites such as ROS, NO and iNOS. (D) TAMs promote regulatory DC maturation, inhibition of CD8+ T cells and NK cells, and facilitate phenotype switching in melanoma cells by IL-10 signalling. (E) Cancer-associated fibroblasts (CAFs) can induce immunosuppression by inhibiting CD8+ T cells. In addition, CAFs secrete TGFβ, CXCL12, matrix metalloproteinase 2 (MMP2) and IL-6, which promote tumour proliferation and invasion.

The immune system

The immune system has a vital role in the fight against cancer. The last decade's advances in immunotherapy have led to an old yet obvious approach to cancer treatment based on activating the endogenic immune system and recognising the tumour [82,83]. The relevance of the immune system in the battle against cancer was further emphasised by the 2018 Nobel Prize in Physiology or Medicine, awarded to James P. Allison and Tasuku Honjo for their discovery of immune checkpoint inhibitor antagonists as means of treating cancer [84,85]. However, the treatment of melanoma is still troublesome, mainly due to the plasticity of melanoma cells, which often gives rise to a phenomenon called immune evasion, whereby the tumour cells become invisible to the immune cells and are thus able to escape [57].

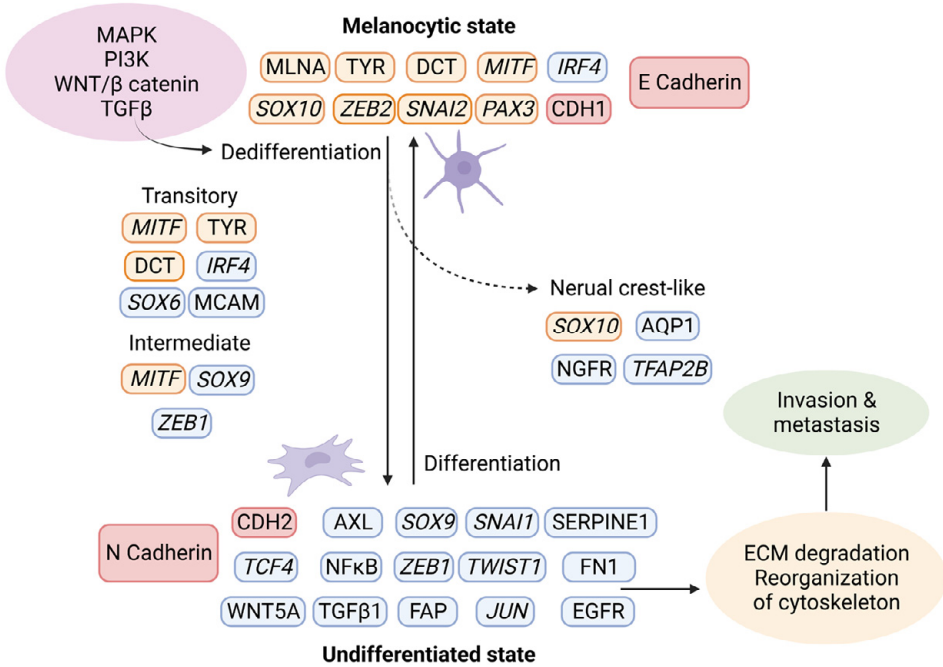

Figure 7. Phenotypic switching in melanoma. Upon activation of the signalling pathways MAPK, PI3K, WNT, and TGFβ, a changed expression of specific markers leads to ECM degradation and reorganisation of the cytoskeleton, which facilitates invasion and metastasis. Using single-cell approaches, it has become evident that phenotype switching is not binary but rather a multistep process in which cells transit through a series of intermediate cell states expressing combinations of epithelial and mesenchymal phenotypes. Furthermore, these intermediate states can simultaneously display proliferation, invasion, and stemness features. Transcriptional regulators are highlighted in italic. The red indicates the switch between E- and N-cadherin and the responsible genes CDH1 and CDH2. Melanocytic markers are highlighted in orange, and other markers are in blue.

Three phases can describe the interplay between melanoma cells and the immune system: elimination, equilibrium, and escape [86]. During the early stages of tumour formation, the neoplastic cells are recognised and eliminated by NK (natural killer)

cells and cytotoxic CD8+ T-cells, hampering tumour initiation [87]. Eventually, as the tumour acquires additional mutations and epigenetic alterations, subpopulations of cells evade the immune system. During the equilibrium phase, the resistant, "invisible" clones expand. However, the immune system can keep the melanoma cells in check by continuously eliminating the "visible" clones [57]. In the last phase of immune evasion, the best-adapted clones can grow without restraint, causing the disease to progress.

The roles of the different immune cells in melanoma development

In the TME, various innate and adaptive cells can be found. Macrophages constitute a large pool of immune cells in solid tumours, and other cell types include NK cells, lymphocytes (B cells and T cells), dendritic cells (DCs), mast cells and neutrophils [57,83]. Macrophages present within a tumour can have very different functions, and they are frequently divided into two main groups: pro-tumourigenic (M2) and anti-tumourigenic (M1) (Figure 6). The M1 macrophages are often more active in the earlier stages of tumour formation and exert immune activation, apoptosis and inflammatory functions. On the other hand, the M2 macrophages are often the most dominant in the later disease stages. The M2 macrophages promote tumour growth, angiogenesis, invasiveness and immune suppression. Macrophages utilising tumour-suppressive functions are often called tumour-associated macrophages (TAMs). TAMs can switch between M1 and M2 depending on the stimulus from the surrounding tissue [57]. Although macrophages are often the most dominant immune cell type, the presence, localisation and activity of TILs in melanoma tumours are the most important features of successful immune surveillance. TILs recognise antigens presented by the tumour cells and mediate cytotoxicity, thus keeping the tumour growth in check. However, the tumour's ability to uphold an immunosuppressive environment can instead promote tumour progression by the release of interferons (IFN), interleukins (IL), growth factors and colony-stimulating factors (CFSs), which recruit suppressive immune cells such as regulatory T (Treg) cells, myeloid-derived suppressor cells (MDSCs), and TAMs (Figure 6) [88,89]. In general, melanoma tumours are considered highly antigenic, meaning they more often have a high infiltration of TILs compared to other cancer types. Melanomas also show a better immune checkpoint inhibitor therapy response rate than other cancers [83].

Additionally, Tregs and MDSCs often express a high amount of immune checkpoint molecules such as PD1, PD-L1 and CTLA4, further enhancing immunosuppression. However, by continuously expressing immune checkpoint molecules, the CD8+ T cells may become exhausted, creating a vicious cycle of immunosuppressive signals, facilitating further disease progression [66]. Additionally, it has been shown that a high Treg cell to CD8+ T cell ratio in the tumour microenvironment of melanoma is often associated with an unfavourable outcome [90]. Furthermore, the existence of highly organised tertiary lymphoid structures (TLSs) within the tumour,

including B cells, T cells and DCs, is another way of promoting an immune response. These cells form specialised immune aggregates surrounding high endothelial venules (HEVs), enabling the recruitment of naive B cells and T cells. Both tumour-infiltrating B cells and TLSs can activate an immune response in patients with melanoma [91].

As outlined, melanoma tumours display a complex landscape, including a high mutational load, resulting in subpopulations of clones with different mutations combined with a constantly changing TME. An outcome of this is an exceptional intratumoural heterogeneity observed in both primary tumours and metastases from melanoma patients. Moreover, metastases within a patient can originate from different clones, further complicating treatment planning and, most importantly, achieving therapeutic efficacy.

Treatment of malignant melanoma

The understanding of melanoma pathobiology and treatment of melanoma patients, particularly patients with metastatic disease, has dramatically changed during the last two decades. A disease once untreatable may now be controlled and even regressed. Melanoma management has evolved rapidly, and 2011 was a landmark when the FDA approved two new types of agents for treating metastatic melanoma: BRAF V600E-targeted therapy and anti-CTLA4 immunotherapy [9,92]. Around the turn of the millennium, the median survival for a patient with stage IV melanoma was about seven months. In contrast, upon the introduction of immune checkpoint inhibitors, the median survival has increased and is now above six years, which is quite remarkable [93,94]. The currently available treatments for melanoma are surgery, radiotherapy, chemotherapy, immunotherapy and targeted therapy. The most appropriate treatment for a patient depends on the disease stage, melanoma location, and mutation status. Parameters such as age and health status are also considered [95].

Surgery

Surgical resection of early melanoma (stage I and II), with adequate margins, is the standard treatment. Surgery is also an option for melanoma patients with more advanced disease (stage III and IV), with sentinel lymph node positivity or distant metastases. Still, alone, it has limited curative potential. Thus, it is combined with radiotherapy, chemotherapy, immunotherapy, or targeted therapy [96 92].

Chemotherapy

Before 2011, chemotherapy was the only systemic treatment for stage IV melanoma [92]. Although chemotherapy remains a therapeutic option for melanoma management, especially in palliative or relapsed situations, new therapeutic choices are preferred in the advanced stages of the disease. However, in patients with resistance to immunotherapy, severe toxicity towards immunotherapy or when there

are no applicable targets for targeted therapy, chemotherapy is considered [9]. The main disadvantages of chemotherapy are the low specificity towards the tumour cells and the low capacity of drug accumulation in the TME. Therefore, the therapeutic benefits are limited, and the side effects are usually prominent [9].

Radiotherapy

Radiotherapy is rarely performed on primary melanomas and is only considered a first-line treatment when surgery is not an alternative due to a tumour's location or the patient's health status. On the other hand, radiotherapy is widely used as a palliative treatment for patients with bone and brain metastases [9,92].

Immune checkpoint therapy

The increased knowledge of the molecular mechanisms responsible for melanoma formation and progression, together with the known importance of the immune system and TME has transformed the treatment of patients with disseminated disease. Melanoma tumours are considered one of the most immunogenic tumours with a high mutational burden and are thereby well suited for immunotherapy[92]. Indeed, melanoma was the first cancer type treated with immune checkpoint therapy [97]. There are currently four approved targets, including CTLA4 (2011, FDA and EMA), PD1 (2014, FDA and EMA), PD-L1 (2020, FDA) and LAG-3 (2022, FDA and EMA). These proteins are expressed on the surface of T cells, among other cell types and are involved in signalling pathways that lead to immune suppression. LAG-3 negatively regulates CD4+ T cell activation and function while enhancing Treg activity and was the most recently approved immune checkpoint target.

Additionally, LAG-3 has the potential to act synergistically with PD1 targets [98]. The approved immune checkpoint inhibitors, monoclonal IgG antibodies, exert their function by binding to these proteins and blocking their activity, thereby re-establishing an anti-tumourigenic immune environment [99]. In patients with unresectable melanoma, PD1 antagonists, either as monotherapy or in combination with CTLA4, are often considered a first-line treatment, independent of BRAF status. However, in some cases, targeted therapy might be more appropriate [92]. Apart from the approved target proteins, novel immune checkpoint inhibitors are being explored, including TIM-3, TIGIT, VISTA, and BTLA, especially their function in combination with currently approved immune checkpoint inhibitor therapy [86,98]. Despite the major advances regarding immune checkpoint therapy, approximately half of the melanoma patients do not respond, alternatively relapse due to primary or acquired resistance [86]. Therefore, we should continue the investigation of combinatorial therapies of existing drugs and explore novel targets. For example, the MDSCs constitute a promising target to convert the pro-tumourigenic microenvironment into a normal tissue microenvironment [57].

Targeted therapy

Approximately 70% of melanoma patients harbour a genetic alteration in one of the main signalling pathways previously described. The MAPK signalling pathway consists of an RTK and the proteins RAS, RAF, MEK and ERK. Small molecule inhibitors of BRAF and MEK are approved as targets for melanoma therapy [40]. Targeted therapies aim to stop the signalling and thereby inhibit uncontrolled proliferation. However, resistance to these inhibitors is pronounced, but when used in combination, an increase in efficacy combined with reduced toxicity is observed. Additionally, combining BRAF and MEK inhibitors offers greater inhibition of MAPK signalling coupled with a more extended response [99]. Additional targeted therapy includes inhibitors of KIT [100].

Oncolytic virus therapy

A relatively novel approach to treating local unresectable cutaneous, subcutaneous and nodal melanoma lesions is through oncolytic viruses. The approved drug (T-VEC) consists of a genetically modified herpes simplex type 1 virus. Upon injection, it can infect and kill the melanoma cells but also stimulate a local and systemic immune response [9,99]. In preclinical studies, oncolytic viruses increased the tumour cell sensitivity against immune checkpoint inhibitors in melanoma [101].

Novel treatments

Novel promising therapies to fight melanoma include cancer vaccines based on predicted neoantigens. A neoantigen is a tumour-specific antigen, a product of somatic mutations, presented solely by tumour cells and not by normal cells [98]. Due to the high mutational frequency in melanoma, the mutational landscape does not overlap too much between patients. Therefore, how this technology induces T cell reactivity is based on the genome of a particular tumour. From there, potential neoantigens are predicted in a patient-specific way [98,102]. However, although T cell reactivity is induced, the long-term efficacy still relies on the continuous activation of these cells, which a suppressive TME might hamper. Therefore, combining cancer vaccines with immune checkpoint inhibitors may produce a more efficient therapy response. Additionally, a cancer vaccine has the potential of being highly specific with fewer adverse effects due to the tumour-restricted expression of neoantigens, which might result in a higher proportion of responders to immunotherapy, both among melanoma patients as well as other cancer types.

Another novel approach includes nanosystems, aiming to improve drug efficacy by personalised and targeted drug delivery by associating a current melanoma treatment, such as immune checkpoint inhibitors or targeted treatments, with a nanoparticle delivery system [100]. The most researched nanoparticles within melanoma therapy include polymeric nanoparticles liposomal formulation, with several ongoing clinical trials [9].

Adoptive T cell transfer (ATT) of TILs is another therapy under intense investigation as an alternative for patients with resistance towards immune checkpoint inhibitors [103]. In ATT, ex vivo-expanded TILs are administered to melanoma patients following lymphodepletion with high doses of IL-2 [104]. However, constructing TILs is challenging, and IL-2 is often accompanied by substantial toxicity [92].

The potential synergistic effects of combining CAR-T cell therapy with anti-PD1 and anti-CTLA4 are being explored [98]. Treatment using CAR-T cells works by first removing the T-cells from a patient, followed by in vitro culturing and genetically engineering the cells to express the CAR antigen receptor, a fusion protein. This allows T-cell activation and infiltration of the tumour and subsequent killing of tumour cells. However, their function can be inhibited by a pro-tumourigenic or cold TME, partially induced by the upregulation of immune checkpoint molecules, which immune checkpoint inhibitors can reverse.

Finally, therapies aiming to reverse the suppressive signals from the TME are also being investigated [105]. One approach includes targeting TAMs, specifically, the reprogramming of pro-tumourigenic M2 macrophages to anti-tumourigenic M1 macrophages or by killing TAMs or minimising their recruitment to the tumour site [57] [98]. Additionally, the combination of anti-angiogenic modulators and immune checkpoint therapy is also under intense investigation [106]. However, despite the numerous molecular targets and delivery strategies, most cancer patients do not respond adequately to therapy. Melanoma, with its response rate to immune checkpoint therapy of about 58%, is one of the cancer types that elicit the highest response rate [107].

Molecular classification of melanoma

Besides the clinical and pathological classifications of melanoma described previously, there is an increasing interest in molecular classifications aiming at stratifying patients into clinically meaningful subgroups to guide treatment selection, prediction, and patient outcome.

In 2006, Hoek et al. outlined a transcriptional taxonomy for melanoma using cell lines based on gene expression profiling [80]. They propose three groups with different metastatic potentials. Subclass A and B were proliferative with weak metastatic potential and displayed a neural crest-like transcriptomic signature, while subclass C was less proliferative but with high metastatic potential (Figure 7). The subtypes were primarily driven by Wnt- and TGFβ-like signalling. Furthermore, in 2010, Jönsson et al. proposed a molecular stratification of metastatic melanoma samples based on gene expression profiling, dividing tumours into four distinct subtypes: high-immune, proliferative, pigmentation and normal-like, as reflected by their characteristic gene expression [108]. This classification was further developed by

Harbst et al. in 2012, where they demonstrated that the classification of primary tumours could be accomplished using the same subclasses. They combined the subtypes high-immune with normal-like and proliferative with pigmentation to obtain low-grade and high-grade subtypes, which were significantly associated with survival [109]. In a work by TCGA in 2015, melanoma tumours were divided based on transcriptomic analyses [110]. Three clusters emerged from their analysis: immune, keratin and MITF-low. Among the metastatic melanoma samples in the cohort, the patient's survival was significantly different between the three subtypes, with the patients from the immune subtype surviving longer, followed by the keratin subtype and MITF-low.

Furthermore, Rambow and colleagues utilised a single-cell RNA approach to identify molecular subtypes in melanoma, and they found four different subtypes related to drug resistance [111]. Tsoi et al. used cells to investigate the diverse stages of melanoma dedifferentiation and found four distinct subclasses named C1–C4 [42]. The C1 subtype was considered the most undifferentiated due to the enrichment of genes related to invasive capabilities such as cell adhesion, motility and inflammation, similar to what was observed by Hoek et al. [80] and Konieczkowski et al. [112]. The C2 subtype shared the invasive and inflammatory features of C1 but presented additional characteristics of a neural crest-like phenotype. As expected, both C1 and C2 displayed low levels of MITF and high levels of AXL. C3 was described as an intermediate subtype with enrichment in neural crest-related genes and genes associated with a more differentiated phenotype. The last subtype, C4, was defined as the melanocytic subtype with high levels of MITF and other pigment-related genes. Although different samples and approaches were applied in these studies, the different molecular subtypes show similarities, with MITF, AXL and SOX10 being some of the common transcriptional elements. While the proportion of overlapping genes within the various states of differentiation varies among the studies, similar mechanisms seem to be involved.

Many promising ways of stratifying melanoma have been proposed at the level of transcripts. However, classifications still need to be presented at the protein level. Although studies have shown a moderate correlation between transcripts and proteins [113-117], proteins are the main functional entities in the human body and the targets of most drugs. This highlights the importance of studying protein expression levels within a disease setting. Additionally, the involvement of the TME, including the immune cells, emphasises the importance of studying clinical melanoma specimens where all aspects of the disease can be viewed together with all its complexity.

Clinical proteomics

Why study proteins?

Proteins represent the most important biomolecules in understanding human biology. They are the executors of most biological processes, including catalysing chemical reactions, providing structural support, regulating the passage of substances across the cell membrane, transporting oxygen, and coordinating cell signalling pathways. Proteins include, among others, antibodies, enzymes, hormones, cytokines, and transcription factors. Often their expression changes as a response to different physiological conditions, and therefore, they should be at the centre of developing new, more efficient and personalised therapies. Furthermore, with their unique proximity to phenotype and pathophysiology, proteins are excellent biomarkers with crucial and wide-ranging applications across biological research, clinical care and drug development, such as tailoring treatments, predicting responses and foreseeing patient outcomes.

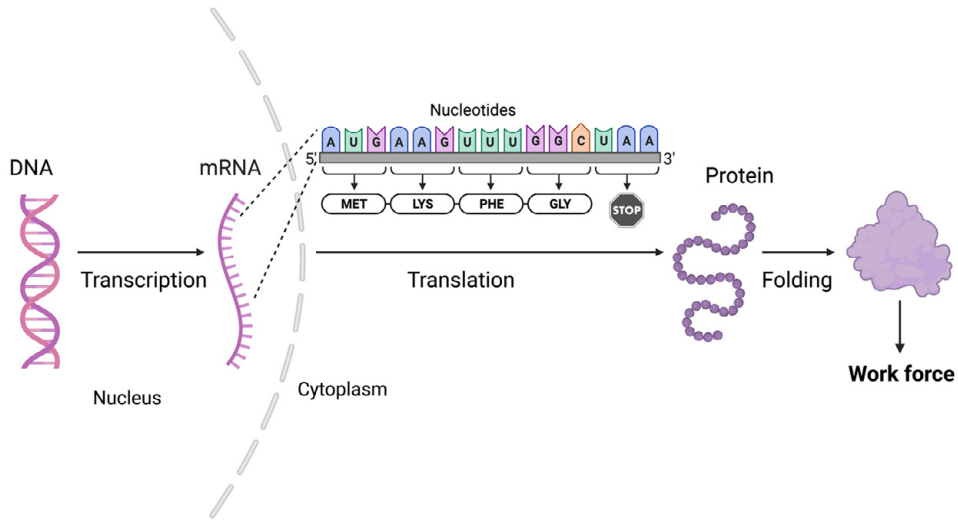

Figure 8. From genes to proteins. The DNA contains the information needed to make the proteins through a multi-step process consisting of two major steps: transcription and translation, which are referred to as gene expression. The information within the gene's DNA is passed on to the messenger RNA (mRNA) during transcription, and when studying transcriptomics, the mRNA levels are most often measured. The mRNA carries the information to the cytoplasm, where the ribosome initiates the translation. Three nucleotides usually code for a particular amino acid, and the proteins are assembled one amino acid at a time until a stop codon is reached. As a last step, the protein is folded to become stable and biologically functional.

The proteome and the study of proteins – proteomics

The word proteome was first described by Wilkins in 1994 and is defined as the complete set of proteins made by an organism, which are translated at different times and in different amounts, depending on their function and how they interact with other proteins inside and outside the cell [118-120]. Each protein can have many variants, so-called proteoforms. Proteoforms can be distinguished by as little as an amino acid change, a post-translational modification (PTM) or by alternative splicing [121]. How many of the 1 million theoretical human proteoforms expressed in an organism remain to be elucidated?

Proteomics is the large-scale study of proteins within cells, tissues or entire organisms, with the objective of acquiring knowledge of cellular processes that occur under specific conditions [122,123]. Proteomic studies intend to identify and quantify as many proteins as possible in a given sample and might include identifying single amino acid variants (SAAVs) or mutations and PTMs. In clinical proteomics, specimens, including body fluids and tissues, can be analysed from healthy and diseased patients to identify novel biomarkers associated with different diseases. Clinical proteomics can comprise a wide range of experimental processes, utilising well-characterised clinical samples accompanied by clinical data. This can ultimately lead to the identification of novel drug candidates that can be studied in clinical trials to improve treatment options. Finally, clinical proteomics can assist in personalised medicine to ensure the patient's disease is fully comprehended [124,125].

The role of single amino acid variants in cancer

A SAAV describes an amino acid substitution in the protein sequence resulting from genetic polymorphism. There is an implication of a functional role for SAAV in several cancer types that may affect signalling pathways and help cancer cells adapt to their environment [126-129]. Accumulation of somatic mutations is a hallmark of cancer, and melanoma is the cancer type with the highest frequency of these mutations [130]. The importance of studying these mutations is underscored by the possibility of targeting tumour tissue by engineering neoantigens found exclusively in tumour cells but not in normal tissue. In principle, any genetic change affecting a protein-coding region has the potential to generate mutated peptides presented by HLA class I proteins on the surface, which can be recognised by cytotoxic T cells, making them potential cancer vaccine immunogens [126,127].

Post-translational modifications

About 250 different post-translational modifications exist, and nearly all proteins can be post-translationally modified [121,131]. Some of the essential PTMs to study within the field of cancer are phosphorylation and acetylation [132]. Phosphorylation generally occurs enzymatically in the endoplasmic reticulum and the Golgi apparatus. It is one of the most common post-translation modifications, and occurs at the amino acid residues of serine, threonine, and tyrosine, and it is considered

crucial in cancer cell signalling [133,134]. Often, phosphorylation is used as a surrogate for monitoring kinase activity [132]. For example, many signalling transducers in melanoma depend on phosphorylation upon activation. Aberrant signalling of the MAPK, PI3K and WNT pathways are known features of melanoma and may result from mutations, overexpression of kinases, or defects in the negative feedback mechanisms. Hence, comprehensive characterisation of protein phosphorylation is crucial [135]. However, the task is complex since protein phosphorylation is often of low stoichiometry and covers a wide dynamic range, imposing considerable strains upon detection by mass spectrometry [52].

Lysine acetylation, where histone acetylation is the most well-studied, is thought to play a vital role in cancer by altering gene transcription and chromatin remodelling [136,137]. It is a reversible PTM, controlled by acetyltransferases (KATs) and deacetylases (KDACs), and changes in these proteins, such as mutations, has been linked to cancer [138,139]. Small molecule inhibitors targeting KDACs are approved as cancer therapies [140]. However, lysine acetylation stoichiometry is not well studied in cancer, making it a promising field to explore further.

Mass spectrometry-based proteomics

Mass spectrometry (MS) coupled with high-performance liquid chromatography is the key analytical technology in proteomics. Today's mass spectrometers generate large amounts of high-quality data that allow protein identification, annotation of post-translational modifications, and determination of the absolute or relative abundance of individual proteins. MS-based proteomics can be divided into two main categories, specifically bottom-up and top-down approaches, the latter including the analysis of intact proteins [141].

Bottom-up proteomics

Various bottom-up approaches are widely used to analyse complex biological samples for discovery purposes. This includes the digestion of proteins into peptides by sequence-specific proteases, which are then separated by liquid chromatography before being introduced to the mass spectrometer [141]. Peptides are more easily separated, ionised, and fragmented using liquid chromatography-tandem mass spectrometry than proteins (LC-MS/MS) (Figure 9) [142]. A very attractive aspect of bottom-up proteomics is the ability to quantify proteins over a wide dynamic range since proteins span approximately seven orders of magnitude in tissues and over ten in body fluids [143].

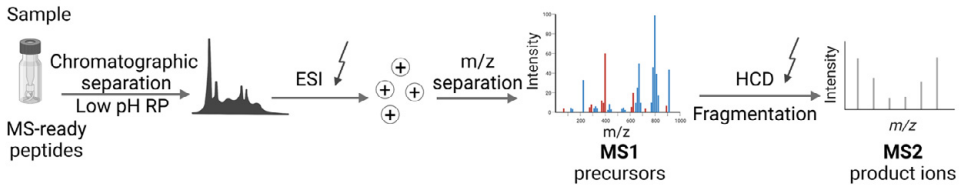

Figure 9. LC-MS/MS. A typical setup for bottom-up proteomics includes liquid chromatography-tandem mass spectrometry (LC-MS/MS). When using a quadrupole-orbitrap analyser, an MS-ready peptide mixture is separated online using RP low-pH fractionation and eluted into an electrospray ion source. Peptides are then ionised in tiny, charged droplets, most often in positive mode. After evaporation, multiple positively charged peptides enter the mass spectrometer, and a mass spectrum of the peptides eluting at each point is recorded (MS1 spectrum). Generally, the most abundant peptides are prioritised for fragmentation by collision with an inert gas in the collision cell, and a series of tandem mass spectra (MS2) are recorded.

The importance of sample preparation

Sample preparation is the step preceding the MS analysis, and unlike genomic and transcriptomic research, there is no universal sample preparation method for proteomics. A balance between sensitivity and scalability must be considered in proteomic experiments since strategies to improve proteome coverage often come at the expense of throughput. Therefore, the approach that produces the most relevant data to answer the biological questions in a given study should be chosen. Additional parameters to consider when developing sample preparation methods are the reproducibility between replicates and the over-time variability of the technique to acquire consistent and reliable results. Any variability associated with the sample preparation should be addressed and evaluated before drawing biological conclusions from the data.

A sample preparation workflow for "bottom-up" proteomics of tissue samples

The tissue samples used for proteomic analyses are divided into two main categories, fresh frozen or formalin-fixed and paraffin-embedded (FFPE). There are advantages and disadvantages to both tissue types. The additional costs of collecting and storing frozen tissues, often resulting in smaller sample numbers, must be weight against the more straightforward sample preparation and the opportunity to study almost any post-translational modification. On the other hand, FFPE samples can easily be stored at room temperature for years [144], and large cohorts with longer follow-up times and hence more comprehensive clinical information are often available [145,146]. On the other hand, although no large effects have been seen in protein abundance between frozen and FFPE tissues, the sample preparation is often associated with difficulties, including proteins which are hard to extract and harsh buffer conditions, which can be challenging to remove prior to MS analysis [147,148].

A "bottom-up" sample preparation workflow using frozen or FFPE samples can be performed using different protocols, equipment and chemicals. However, some common steps permeate the process (Figure 10). For example, deparaffinisation and antigen retrieval is the first step of the sample preparation of FFPE tissues. During

the fixation process, formaldehyde introduces crosslinks between molecules such as proteins, RNA and DNA, which need to be broken to enable protein extraction from the tissue [148]. A widely used method for deparaffinisation includes xylene followed by rehydration with ethanol [149]. However, due to the health hazards of xylene, other approaches are also commonly used, such as high pH and temperature-based deparaffinisation with Tris-EDTA solutions [150,151]. To unmask hidden epitopes and retrieve antigens, FFPE samples are often heated in high pH buffers containing Tris-EDTA or SDS before further processing [147,152].

When working with frozen samples, the first step of the sample preparation includes protein extraction. The protein extraction is often carried out with strong chaotropic agents such as urea or with detergents such as SDS. This causes the proteins to denature, and combined with ultrasound technology, the extraction process is even more efficient, mainly by improved extraction of membrane proteins [153]. Low urea concentrations (0.5–1.5 M) are compatible with the subsequent protein digestion with proteases, while detergents such as SDS should be removed before digestion. This can be accomplished through suspension trapping [154] or precipitation [155], among other methods. Digestion can be performed in various ways, such as in-solution, in-gel and on-filter and with different proteases [156]. The most widely used is trypsin, a serine protease, which cleaves exclusively at the carboxyl terminal of arginine and lysine. Another commonly used enzyme is endoproteinase Lys-C, which, as the name suggests, cleaves at the carboxyl-terminal of lysine residues. Lys-C is preferably used as the first enzyme in a two-enzyme digestion protocol since it can handle somewhat harsher conditions than trypsin, for example, a higher urea content.

By carefully optimising the digestion conditions, the number of missed cleaved sites is minimised, resulting in a high amount of fully cleaved peptides and a more reliable and reproducible protein quantification. Following digestion, peptides are usually cleaned to remove salts and other buffer constituents. The most widely used method for sample clean-up is RP C18 desalting. Following desalting, the eluted peptides are ready for LC-MS/MS. However, samples are commonly subjected to prefractionation to increase proteome coverage and reduce the co-elution of peptides with similar mass.

Many different fractionation approaches exist, such as RP high pH, Strong Cation Exchange (SCX) [157], and hydrophobic interaction liquid chromatography (HILIC). The chosen pre-fractionation method should have high resolution and be orthogonal to the separation used for the LC-MS/MS analysis. RP high pH fractionation generally performs better than SCX due to well-separated peptides. Additionally, in RP high pH fractionation, low or no-salt-containing buffers produce cleaner samples, while another desalting step is needed following SCX, resulting in sample loss [158]. The RP high pH fractionation and the second dimension RP low pH separation, which is the standard setup of the LC-MS/MS system in proteomics, provides better orthogonality compared to SCX-RP low pH [157].

Large-scale proteomic experiments often include analysis of post-translational modifications such as phosphorylation, where an enrichment strategy is employed. Commonly used methods include immobilised metal ion affinity chromatography (IMAC) and metal oxide affinity chromatography (MOAC) [52]. In IMAC, metal ions such as Fe3+ are used, while in MOAC, TiO2 is the metal oxide of choice [159]. The phosphopeptides bind to the immobilised metal ions/oxide and can be eluted with a high pH buffer such as ammonium hydroxide, followed by MS analysis.

MS acquisition methods

The most common acquisition methods for bottom-up proteomics are data-dependent acquisition (DDA), data-independent acquisition (DIA) and targeted approaches, the latter where the proteins of interest are predetermined and known and not infrequently selected based on a hypothesis-free discovery experiment using DDA or DIA.

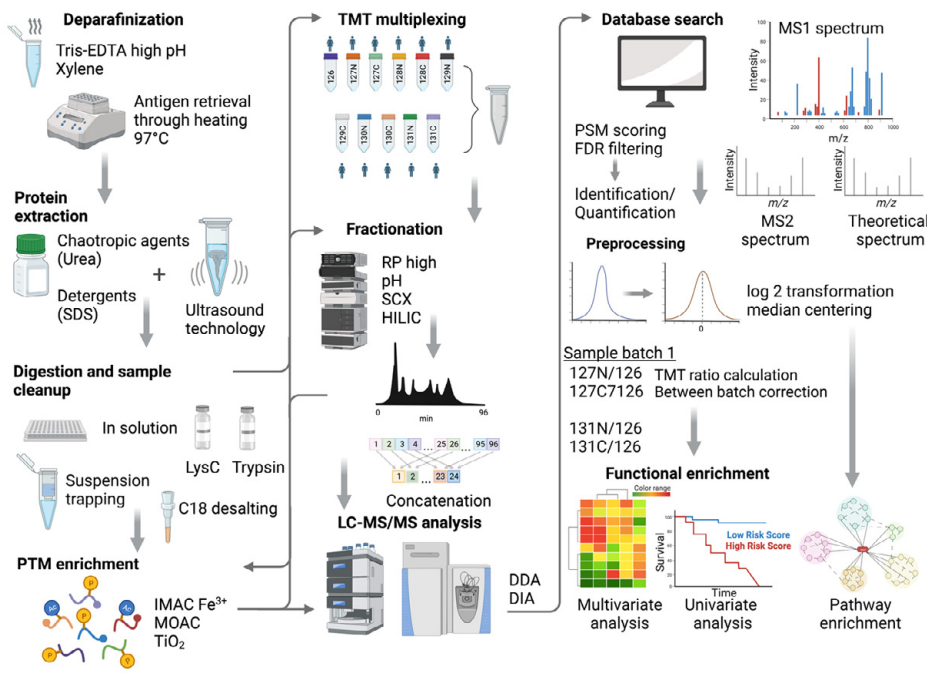

Figure 10. Workflow for bottom-up proteomics. Overview of steps commonly included in a data-driven discovery approach using bottom-up proteomics.

The Data-Dependent Acquisition

In DDA methods, the top N most intense precursor ions from the full MS1 scans are selected using narrow isolation windows (~ 1 Da). Then, these ions are fragmented, and individual MS2 scans are recorded. Therefore, the selection of precursor ions is somewhat stochastic, favouring the more abundant ions, causing missing values and less reproducible measurements.

A missing value may arise for several reasons, including at random, meaning that the peptide is present in the sample at a detectable level but is not detected nor correctly identified. Alternatively, the peptide is present but at an abundance below the instrument's detection limit, and lastly, the peptide is not present [160].

This can be addressed to some extent by the so-called "match between runs" approach, where a peptide sequence identified by MS2 can be transferred to a peptide peak from another measurement based on precursor ion mass to charge ratio (m/z) and peak retention time [161,162]. There are many possible instrument configurations for DDA methods; however, the quadrupole-orbitrap hybrid instruments are the most used [163,164].

Quantification in DDA mode can be either label-free, performed at the MS1 level, or based on stable-isotope labelling such as tandem mass tags (TMT) using MS2 reporter ions. Isobaric tags enable multiplexing using stable heavy isotopes. The tags contain an amine-reactive, a balancer, and a reporter ion group, resulting in an equal mass. Therefore, identical peptides from different samples elute simultaneously and appear as a single peak in the MS1 spectrum, resulting in the possibility of multiplexing up to 16 samples in a single TMT experiment without increasing the complexity of the MS1 spectrum considerably [165]. However, at the MS2 level, the reporter ions released upon fragmentation enable relative quantification. Peptide and protein quantification is accomplished by comparing the intensities of the reporter ions in the MS2 spectra [166]. Multiplexing has the advantage of being less sensitive to instrumentation variability since all samples are analysed simultaneously; also, in combination with extensive fractionation, it is possible to achieve a deeper proteome coverage in a time-efficient manner compared with a label-free approach. Additionally, the TMT methodology is well suited for studying the many existing proteoforms, including various post-translational modifications [166,167].

Other labelling strategies include isobaric tags for relative and absolute quantitation (iTRAQ) [168] and stable isotope labelling by amino acids in cell culture (SILAC) [169]. In iTRAQ, isobaric reagents label the primary amines of peptides and proteins. The iTRAQ reagents consist of an N-methyl piperazine reporter group, a balancer group, and an N-hydroxy succinimide ester group that reacts with the primary amines of peptides. The quantification is achieved by analysing reporter ions generated upon fragmentation in the mass spectrometer, similar to TMT. SILAC uses a non-radioactive isotopic strategy where cells are labelled by growing in light and heavy

medium, containing regular and heavy arginine or lysine. Metabolic incorporation of the amino acids into the proteins results in a mass shift of the corresponding peptides, which a mass spectrometer can detect. By combining the two samples, the ratio of the peak intensities in the mass spectrum reflects the relative protein abundance.

Data-Independent Acquisition

In contrast to DDA, where precursor ion selection is somewhat stochastic, in DIA methods, all ions within the selected mass range are isolated and fragmented sequentially, potentially resulting in fewer missing values. Quantification in DIA mode can be performed on both MS1 and MS2 levels, though MS2 quantification is more frequently used [162]. However, MS1-based quantification can be advantageous since it can utilise the high-resolution capacity (120,000) of a quadrupole-orbitrap mass spectrometer, a method called high-resolution DIA (HR-DIA). One challenge when designing a DIA method based on MS1 or MS2 quantification is determining the optimal number of isolation windows and ensuring enough sampling points across a peak, as under-sampling can result in unreliable quantification. Therefore, optimising the method by considering both the cycle times and peak widths is essential.

Computational and bioinformatics analysis

Data generated by mass spectrometry is extensive, and the computational analysis is often time-demanding and generally consists of several consecutive steps. A database search is usually the first step. For DDA, the most common approach is to use a classical search engine containing theoretical spectra such as SEQUEST [170] together with Proteome Discoverer, Andromeda [161,171] together with MaxQuant or Pulsar [172] together with Spectronaut. The most common approach in DIA is to create an experimental library based on DDA runs or an in-silico library [173,174]. Also, direct DIA approaches can be applied without constructing a library. This can be accomplished in software such as DIA-NN [175,176] and Spectronaut [172].

For peptide identification, the software generally assigns a score to the peptide-spectrum match; this is then followed by the estimation of false discovery rates (FDRs), often using the targeted-decoy approach [177-179]. Peptides are then assigned to proteins. To avoid redundant identifications and ambiguous quantification, proteins which are very similar and cannot be distinguished based on the identified peptides are reported at the group level [161]. Finally, abundances are calculated, often based on the average intensity of the top N peptides, and the final outputs are matrixes containing peptide and protein abundances.

Before performing statistical analyses and addressing biological questions, the data needs to be pre-processed to correct for experimental variability, missing values,

and batch effects. This includes filtering and imputing missing values, transformations, and standardisation strategies, including ratio calculations for TMT data. Different statistical methods for handling missing values should be applied depending on the assumed reason behind the missing value. If the peptide truly exists at a detectable level, using observed values to impute missing values or simply filtering out a few missing values is appropriate. However, imputations based on observed values are not appropriate if the peptide abundance is below the instrument's detection limit or not present [160]. The goal of pre-processing large proteomic data sets is to obtain a final matrix that can be confidently used for further statistical analyses and functional enrichment.

Since the multi-omics era, the view on data analysis has changed a lot. The hypothesis-driven approach is often substituted for a data-driven approach with the incentive that when data are sufficient, they are self-explanatory. However, in big data, the number of significant features is often sparse, and several feature extraction methods are employed depending on the objective. Often combinations of univariate and multivariate analyses are exploited to answer questions about patient stratification, diagnosis, and prognosis [180] [181]. The selected significant omics signatures are then annotated using different bioinformatic tools such as Toppcluster [182], STRING [183], PANTHER [184], and DAVID [185] together with public databases, for example, KEGG (Kyoto Encyclopedia of Genes and Genomes) [186], Gene Ontology (GO) [187], Reactome pathway database [188] and Gene Set Enrichment Analysis Hallmark gene set [189].

The proteomic field is continuously evolving, primarily because of improvements in MS technology, methodology, and the availability of new bioinformatics tools, enabling researchers to advance and gain further insight into disease biology, thereby improving patient care. Today, melanoma represents a severe public health problem. It is a heterogeneous and unpredictable tumour that annually takes thousands of lives worldwide. The emergence of immunotherapy and targeted therapy has prolonged numerous lives, but many patients relapse or do not respond. A prominent obstacle is selecting the target leading to immune activation, whether it is an approved drug or a newly found potential drug target. This will require the parallel examination of different aspects of the tumour cells and their microenvironment, such as mutations, transcripts, proteins, neoantigens, and PTMs, often referred to as multi-omics.

Aims

There were two main objectives of the studies encompassed in this thesis. The first included the development of robust and high-throughput sample preparation methods for proteomic analysis of clinical tissue samples. The second objective comprised the integration and interpretation of transcriptomic, proteomic, phosphoproteomic and clinical and histopathological data for a better understanding of melanoma biology and, ultimately, contributing to improved disease management through better-informed clinical decisions.

The specific aims of the included papers were to:

I. Establish a semi-automated sample preparation workflow for the proteomic analysis of large cohorts of sectioned frozen tissues;

II. Optimise an automated phosphopeptide enrichment protocol for phosphoproteomic analysis of small amounts of tissue, followed by integration into the workflow developed in the first study;

III. Establish workflows to process Formalin-Fixed and Paraffin-Embedded tissues for studying global proteomes and endogenous lysine acetylation;

IV. Study the expression of the BRAF V600E mutated protein by mass spectrometry in melanoma metastases and its association with tumour phenotypes and patient survival; and

V. Characterise treatment naïve melanoma metastases through proteogenomic approaches combined with clinical and histopathological data.

Material and Methods

Study design and overview

The studies encompassed in this thesis consist of consecutive works (except paper III), intending to answer biological questions related to the molecular mechanisms responsible for developing and progressing malignant melanoma. An additional aim was to stratify melanoma patients into clinically relevant and functional groups that consider different aspects of the disease, such as the protein expression differences related to clinical and histopathological features, BRAF mutations, the presence of single amino acid variants, the compositions of the tumour microenvironment and in the involvement of the immune system (Figure 11). In the first three studies, robust and reproducible sample preparation protocols were developed that were later applied to the main cohort of melanoma lymph node metastases (described in detail below). Finally, the results were analysed using different statistical approaches and bioinformatic tools and summarised in papers IV and V.

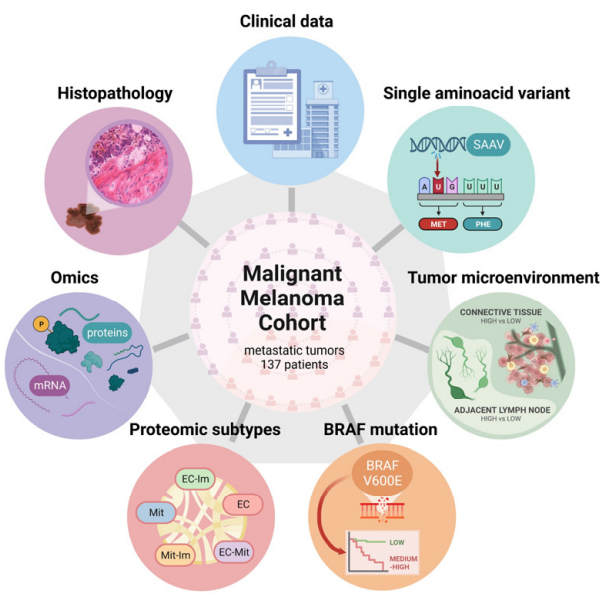

Figure 11. An overview of the studied aspects of malignant melanoma covered in this thesis.

The cohort or the patient samples

Throughout this thesis, samples of different types and tissue origins were analysed, including frozen samples from melanoma patients (papers I–V), samples from patients with pancreatic cancer (paper I) and rat spleen tissue (paper I). In paper III, FFPE samples from malignant melanoma and lung adenocarcinoma patients and samples originating from tonsils were included. The biological interpretations and conclusions are based on the analysis of a cohort of 137 malignant melanoma patient samples collected at the university hospital in Lund. The collection and usage of the sporadic samples throughout the studies were done in agreement with specific ethical considerations for each sample type.

Main cohort

Tissue collection and clinical information

The patient samples were collected between 1975 and 2011, before the era of modern cancer therapy. The tissue specimens were put on dry ice with a small amount of isopentane in liquid nitrogen within 30 minutes of surgery. The samples were then stored at -80°C until further processing. Initially, the tumours were classified as stages I, II, III and IV (Table 1). However, for 80 % of the patients, a reclassification, according to the 8th edition of the AJCC8, of the pathological stage was possible. The samples were treatment naïve.

Ethical consideration

The study was approved by the Regional Ethical Committee at Lund University, Southern Sweden (DNR 191/2007, 101/2013 (BioMEL biobank), 2015/266 and 2015/618). All patients provided written informed consent.

Table 1. Patient characteristics of the main cohort analysed in papers IV and V.

Age at diagnosis		**Survival from sample collection**		**Overall survival**	
Range	23–96 years	Range	0.1–25.2 years	Range	0.2–42.5 years
Median ± SD	64 ± 13.9 years	Median ± SD	2 ± 5.1 years	Median ± SD	4.9 ± 7 years
Gender		**Disease stage (patients)**		**Localization**	
Female	47	I-II	3	Lymph node	121
Male	87	III	97	Cutaneous	1
NA	3	IV	34	Subcutaneous	7
		NA	3	Visceral	3
				NA	5
Mutational status		**Type of BRAF mutation**		**Status/Remarks**	
wt	36	V600E	45	Alive	26
BRAF	49	V600K	2	Dead	91
NRAS	35	V600R	1	Unknown cause	16
NA	17	V600A	1	NA	4

Sample processing and LC-MS/MS analysis

Tissue sectioning and histological assessment

The tissue samples processed through papers I–V were sectioned stepwise according to Figure 12 [190]. Every eleventh section was placed on a glass slide and stained with haematoxylin and eosin using a standard staining protocol [191,192]. The tissue content was evaluated, and the percentage of tumour cells, necrosis, connective tissue, and adjacent tissue were determined. In addition, a morphological assessment, including the degree of lymphocytic infiltration in terms of distribution and density, was assigned, where scores from zero to three were given for each parameter (Table 2).

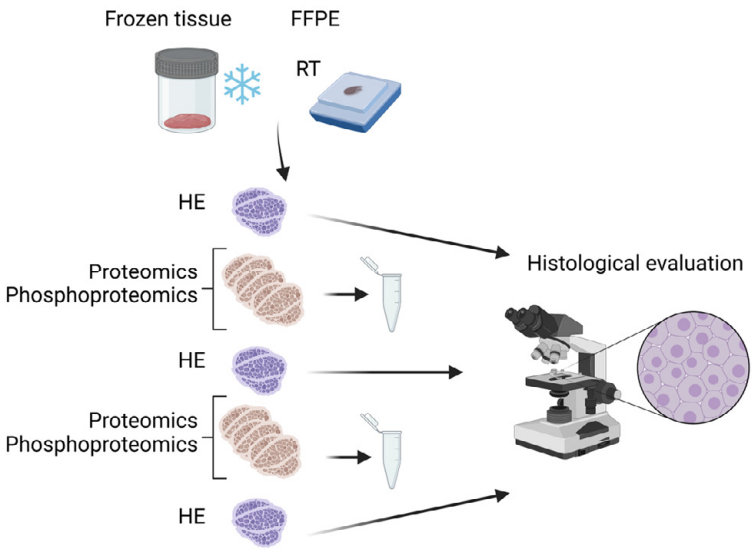

Figure 12. Tissue preparation. The first step of the tissue sectioning protocol includes the sectioning of thin (4–10 μm) sections, where the first is attached to a microscope slide and stained with haematoxylin and eosins. The following sections (between 1 and 30) are placed in tubes and stored appropriately until further analysis. The stained sections, immediately neighbouring both sides of the sections placed in tubes, undergo histological examination. The tissue composition is assessed for each section, and the percentage of tumour cells, necrosis, connective tissue, and adjacent tissue is determined. In addition, various morphological assessments were considered, including tumour cell size, predominant tumour cell shape, pigmentation, predominant cytoplasm, and parameters such as the distribution and density of lymphocytic infiltration.

Table 2. Summary of the histological annotations of the main cohort.

Histological features	Median	Mean ± SD
Tumour %	80	67.2 ± 30.7
Adjacent lymph node %	0	11.8 ± 21.7
Connective tissue %	6.25	16.7 ± 26.8
Necrosis %	0	5.75 ± 11.5
Lymphocyte distribution (0-3)	1	1.41 ± 1.1
Lymphocyte density (0-3)	1	1.30 ± 0.94
Lymphatic score (0-6)	2.67	2.70 ± 1.89
Pigment score (0-3)	0	0.95 ± 1.19
Tumour cell size (0-3)	0	0.04 ± 0.23
Predominant cell shape (0-3)	0	0.23 ± 0.48
Predominant cytoplasm (0-3)	2	1.45 ± 0.69

Protein extraction

The protocol developed in paper I was applied for protein extraction of the main cohort, including 137 frozen melanoma tissues (papers IV and V) and for the samples included in paper II. From each patient sample, 30 sections (10 µm thickness) were used, and 100 µL of lysis buffer containing 4 M Urea in 100 mM Ambic was added, followed by protein extraction using ultrasound technology. The samples were then centrifuged, and the protein content in the supernatant was determined using a colourimetric micro-BCA assay. For digestion, the protein concentrations were equalised, and 100 µg of protein from each sample was taken out and reduced with 10 mM DTT for 1 h at room temperature (RT) and sequentially alkylated with 20 mM iodoacetamide for 30 min in the dark at RT.

In paper III, where FFPE tissues were processed, deparaffinisation and antigen retrieval were performed with a xylene-free approach using a high pH Tris-EDTA buffer prior to protein extraction. Antigen retrieval was induced, and the amino acid cross-links were broken in two different ways. The first protocol utilised an SDS-based extraction buffer containing 25 mM DTT and 10 % SDS in 100 mM TEAB (pH 8), and 50 µL of extraction buffer was added per tissue section to each sample. The samples were incubated at 99 °C for 1 h with shaking. In the second protocol, the samples were first incubated with 1 mL of 500 mM Tris−HCl (pH 8.6) at 99 °C for 1 h, which was then removed, and 50 µL of extraction buffer containing 8M urea in 100 mM AmBic was added per tissue section. After antigen retrieval, the samples were subjected to sonication to reduce viscosity, followed by centrifugation to clear the lysates. Proteins extracted with the urea protocol were reduced with 25 mM DTT at 37 °C for 1 h, protein determination was performed for all samples using a Pierce TM 660 nm protein assay. An ionic detergent compatibility reagent for the samples containing SDS was added before the protein determination. Prior to digestion, the lysates were alkylated with 50 mM iodoacetamide for 30 min at RT in the dark.

Protein digestion and sample clean-up

The urea in-solution digestion protocol developed in paper I was applied for the main cohort (papers IV and V) and the samples included in paper II. First, the urea concentration was decreased by diluting the samples with 100 mM Ambic to a urea concentration of about 1.5 M. Digestion was performed in two steps at RT. Proteins were first incubated with Lys-C at a 1:50 (w/w) ratio (enzyme/protein) for 5 h, and then trypsin was added at a 1:50 (w/w) ratio (enzyme/protein) followed by an overnight incubation. The reaction was quenched by adding 20% TFA to a final concentration of ~ 1%. Next, peptides were desalted on the AssayMAP Bravo platform using C18 cartridges and then dried in a centrifugal evaporator.

In paper III, suspension trapping (S-Trap) was used for digestion. First, phosphoric acid was added to a final concentration of 1.2% in each sample. Then, S-Trap binding buffer (90% methanol, 100 mM TEAB) was added to a final volume of eight times the lysate volume. Next, the samples were loaded onto the S-Trap filter, followed by a short centrifugation, and then the captured proteins were washed with S-Trap binding buffer. Next, digestion buffer (50 mM TEAB) containing Lys-C at a 1:50 w/w ratio (enzyme/protein) was added onto the filter and incubated at 37°C for 2 h. Then, digestion buffer (50 mM TEAB) containing trypsin at a 1:50 w/w ratio (enzyme/ protein) was added on top, and the samples were incubated overnight at 37°C. The following day, the peptides were eluted with three buffers; digestion buffer; 0.2% formic acid; 50% acetonitrile containing 0.2% formic acid. Finally, the eluted peptides were acidified with 50% formic acid to a final pH of ~ 3 and dried in a centrifugal evaporator. Dried peptides were stored at -80°C until further downstream analyses, including TMT labelling and phosphopeptide enrichment.

Multiplexing by isobaric labelling with TMT

In papers III, IV, and V, isobaric labelling with TMT was used for sample multiplexing. The peptide amount in each sample was estimated using a colourimetric peptide assay kit. In the main cohort (papers IV and V), equal amounts of peptides were labelled with TMT 11-plex reagents within each batch. Peptides were resuspended in 100 µL of 200 mM TEAB, and individual TMT 11-plex reagents were dissolved in 41 µL of anhydrous acetonitrile and mixed with the peptide solution. The internal reference sample, a pool of 40 melanoma patient samples, was labelled as channel 126 in each batch. After one hour of incubation, the reaction was quenched by adding 8 µL of 5% hydroxylamine, followed by 15 min incubation at RT. The labelled peptides were mixed in a single tube, and the volume was reduced using a centrifugal evaporator.

Then, the peptides were cleaned up using a Sep-Pak C18 96-well plate. The eluted peptides were dried in a centrifugal evaporator and resuspended in water before high pH RP HPLC fractionation. For TMTpro 16 plex (paper III), the same protocol was

applied except for the quenching of the labelling reaction, which was performed by adding hydroxylamine to a final concentration of ~ 3 %.

Fractionation to reduce sample complexity

In papers III, IV and V, the TMT batches were fractionated using an XTerra Shield RP18 Column (125 Å, 3.5 µm, 2.1 mm × 150 mm) from Waters (paper III) and an Aeris Widepore XB-C8 (3.6 µm, 2.1 × 100 mm) column from Phenomenex (papers IV and V) on an 1100 Series HPLC from Agilent, operating at 80 µL/min and a detection wavelength of 220 nm. Solvents A and B consisted of 20 mM ammonium formate (pH 10) and 80% ACN in 20 mM ammonium formate (pH 10), respectively. Approximately 200 µg of labelled peptides were separated at RT using the following gradient: 0 min 5% B; 1 min 20% B; 60 min 40% B; 90 min 90% B; 120 min 90% B. In total, 96 fractions were collected at 1 min intervals and concatenated into 24 or 25 fractions by combining four fractions that were 24 fractions apart so that #1, #25, #49, #73; and so forth, were concatenated and then dried in a centrifugal evaporator.

In papers I and II, automated off-line high pH step-fractionation was performed. Malignant melanoma digests were fractionated in the AssayMAP Bravo using the RPS cartridges. The pH of the samples was adjusted to pH 10 with ammonium formate. Six fractions were collected using step-elution consisting of 30 µL of 4%, 10%, 15%, 20%, 25%, and 80% ACN in 20 mM ammonium formate. The flow-through was collected and analysed as a seventh fraction.

Analysis of post-translational modifications

Phosphorylation

From the main cohort of 137 melanoma tissues, 118 samples were subjected to phosphopeptide enrichment using the protocol developed in paper II. In total, 100 µg of proteins were digested, and the cleaned peptides were subjected to phosphopeptide enrichment by applying the optimised Phospho Enrichment protocol on the AssayMAP Bravo platform using Fe(III)-NTA cartridges. The enriched peptides were then dried in a centrifugal evaporator and stored at -80°C until analysis by LC-MS/MS.

Acetylation

In paper III, a protocol for studying endogenous lysine acetylation was developed using S-Trap. First, the proteins were loaded onto the S-Trap Mini Spin Columns (nominal capacity 100–300 µg), followed by complete acetylation of the protein's free amino groups by two consecutive additions of 5 µmol of N-acetoxisuccinimide carrying three deuterium atoms (NAS-d3), dissolved in 20 µL of DMSO and 100

μL of 100 mM TEAB. The mixture was incubated for 1.5 h at RT following each addition step. Next, undesired O-acetylation was reversed by incubating the proteins with 120 μL of 5% hydroxylamine for 20 min. The lysine-acetylated proteins were then digested with trypsin 1:50 w/w ratio (enzyme/proteins) in 50 mM TEAB overnight. Next, the peptides were eluted with three buffers; digestion buffer; 0.2% formic acid; 50% acetonitrile containing 0.2% formic acid. The eluted peptides were then acidified with 50% formic acid to a final pH of ~ 3 and dried in a centrifugal evaporator.

LC-MS/MS analysis

The data presented throughout this thesis was generated by mass spectrometry. Samples were analysed by nLC-MS/MS on an Ultimate 3000 HPLC coupled to a Q Exactive HF-X mass spectrometer from Thermo Scientific equipped with an EASY-Spray ion source. Approximately 1 μg of peptides was injected for most global proteomic analyses, loaded onto an Acclaim PepMap 100 C18 trap column, and then separated on an Acclaim PepMap RSLC C18 25 cm analytical column. For the analysis of phosphopeptides, an iRT (indexed Retention Time) peptide mix was added to each sample prior to MS analysis. A flow rate of 300 nL/min and a column temperature of 45°C were used for all experiments. The solvents used for the gradients were A (0.1% formic acid) and B (0.08% formic acid in 80% ACN). All samples were analysed in random order. Three different approaches were used for data acquisition: label-free DDA (papers I, II and III), DDA including the TMT node (papers III, IV and V) and DIA (paper V). Details of each LC-gradient and MS parameters, such as gradient length, mass range, resolution, AGC target, injection time, isolation window, dynamic exclusion, and normalised collision energy, can be found in the respective paper.

Computational analysis

Database search

Proteome discoverer

Most of the data presented throughout papers I–V were processed with Proteome Discoverer from Thermo Scientific. The search was performed using the SEQUEST HT search engine against the Uniprot Homo sapiens revised database, including isoforms. Cysteine carbamidomethylation was set as a fixed modification, and variable modifications included in the search were the oxidation of methionine residues and N-terminal protein acetylation. Mass tolerance for the precursor and

fragment ions were 10 ppm and 0.02 Da, respectively. Two missed cleavage sites were permitted with a minimum peptide length of six amino acids. A maximum FDR of 1% was used for identification at peptide and protein levels. The peptides that could be uniquely mapped to a protein were used to calculate protein abundance.

For the TMT experiments, a TMT label at the peptide N-terminus and lysine residues was included as a static modification, and isotope correction factors were added to each batch. The search for phosphopeptides in paper II included variable phosphorylation of serine, threonine, and tyrosine. Also, the ptmRS algorithm was added to the workflow, which scores phosphorylation sites with a site probability threshold set to 75. In the acetylation experiment, lysine and N-terminal protein acetylation (normal (d0) and heavy (d3)) were included as variable modifications. The analysis of SAAVs consisted of a two-step search. The non-assigned MS/MS spectra from the first search (as described above) were submitted to a second search using an in-house database of 57,134 entries (see paper V for details). Peptide variants identified with high confidence (FDR 1%) Peptide Spectrum Matches (PSMs) were subjected to verification using the bioinformatics tool SpectrumAI [193]. This resulted in the identification of 1015 unique missense somatic variants or mutations belonging to 828 proteins.

MaxQuant

The data generated in paper I were analysed with MaxQuant v1.6.0.1 using the Andromeda Search engine against the Homo sapiens revised database and against the Rattus norvegicus database excluding isoforms. The default contaminant protein database and the decoy database were used, and matches from these were excluded. In addition, similar settings used for the PD search were implemented, and the "match between runs" option was enabled.

Spectronaut X to search for phosphopeptides

The phosphoproteomic data was acquired by DIA and searched in Spectronaut X. First, the spectral library was generated from 45 DDA MS analyses using Pulsar against the UniProt Homo sapiens database, including isoforms with the same parameters as for the phosphopeptide search in Proteome Discoverer. The DIA files were searched using the generated spectral library, and the default factory settings were used. A maximum FDR of 1% was set for the precursors, and the peptides and proteins were quantified based on precursor MS1 intensity. The spiked-in iRT peptides were used for retention time alignment.

Pview

The analysis of lysine acetylation was performed in the Pview[194] software to complement the Proteome Discoverer analysis. For peptide identification, the mass tolerance was set to 10 ppm at the MS1 and 0.02 Da at the MS2 levels, and 1% FDR

was permitted. For the stoichiometry calculations, the isotopic tolerance was set to 3.5 ppm. Finally, only those peptides identified in Pview and Proteome Discoverer were considered for lysine acetylation stoichiometry calculations.

Pre-processing of the proteomic data in Perseus

The result files generated in Proteome Discoverer and Spectronaut were imported into Perseus[195]. Different valid value filtering was applied to each matrix. To correct for experimental variability, the protein intensities were log2 transformed and centred around zero by subtracting the median intensity in each sample. To correct batch effects in the TMT data, the pooled reference sample in channel 126 in each experiment was subtracted from each channel in the corresponding batch to obtain the final relative protein abundance values. In the phosphopeptide analysis, all phosphosites with more than 5% missing values were removed. For those phosphosites with less than 5% missing values, abundance values were imputed by applying the K Nearest Neighbour method. Additionally, in many biological comparisons, z-scoring of the data was performed, where the protein intensities were normalised to obtain a mean value of zero and a standard deviation of one.

Biological analyses and statistical methods for data evaluation

Throughout the studies, descriptive statistics were accompanied by several statistical tests. In papers I–III, mostly univariate analyses such as linear regression, frequency distribution, correlation analyses and analyses of variance were performed. In papers IV and V, univariate and multivariate analyses complemented each other to find features of interest, which were then subjected to functional enrichment analysis using various public databases such as KEGG, Reactome pathways and GSEA Hallmark gene set (see respective paper for details).

Results and discussion

Method development

A less laborious tissue processing protocol for proteomic studies

A sample preparation workflow for shotgun proteomics using fresh frozen tissues requires multiple processing steps often including tissue homogenisation and protein extraction, denaturation, alkylation, enzymatic digestion, peptide clean-up, enrichment for post-translational modifications and fractionation in one or multiple dimensions, followed by MS-based identification and quantification.

In the first paper, three instrumental platforms were evaluated and directly compared regarding experiment-to-experiment variation and the ability to increase the throughput of large-scale proteomic experiments using frozen sectioned tissues.

For tissue homogenisation and protein extraction, the Bioruptor plus sonicator model UCD-300 (Diagenode) and the Barocycler model 2320EXT (Pressure Biosience Inc.) were compared side by side, and their efficiency of extracting proteins from complex frozen tissue samples of melanoma, pancreatic cancer, and rat spleen was assessed. A buffer consisting of 4 M urea in 100 mM Ambic was used for all extraction comparisons.

First, the yield of the extracted proteins using the two instruments was compared by utilising a relatively homogenous rat spleen tissue. We concluded that for small amounts of tissue (2–3 mg or 3–5 sections with 10 µm thickness), the instruments performed equally well, yielding approximately 99–189 µg of proteins, corresponding to approximately 31–41 µg per section (Figure 13A). However, when larger tissue amounts were used, the Barocycler showed a limitation in extraction efficiency, most probably due to the limited amount of lysis buffer that can be added to the microtubes, resulting in a low buffer-to-tissue ratio. On the other hand, the Bioruptor could efficiently homogenise and extract larger amounts of proteins (20 sections with 10 µm thickness), yielding more than one milligram (47–51 µg per section). This amount is sufficient to perform multiple analyses, including global proteomics with extensive fractionation and to study PTMs such as phosphorylation and acetylation. Additionally, we found a very good correlation (Pearson, $r = 0.81$) between the section area and the protein yield in a more heterogeneous tissue type, examining ten patient-derived melanoma tumours (Figure 13B), suggesting that the

section area can be used to estimate the amount of extracted proteins for downstream analysis independently of the tissue composition and heterogeneity.

The instrument's capabilities to extract proteins from the tissues were comparable. As per gene ontology annotation, the quantified proteins from both approaches showed preserved diversity, and the reproducibility between replicates was very high. Furthermore, both instruments were robust in their ability to extract proteins, as confirmed by strong correlations in protein quantification and low intra- and inter-instrument coefficients of variation from downstream analyses (Figure 13C).

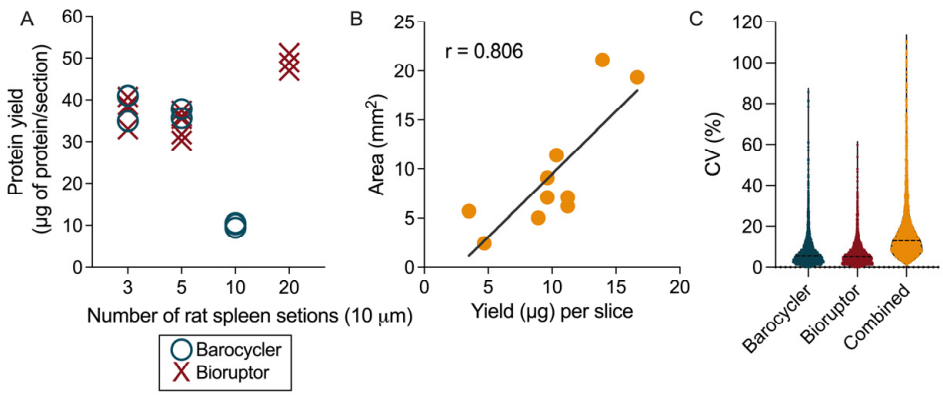

Figure 13. (A) Protein extraction comparison between the Bioruptor and the Barocycler. Various section numbers from fresh frozen rat spleen tissue (3, 5, 10, and 20) were used for protein extraction. The results are shown as each sample's protein yield (µg) per tissue section. The crosses and circles represent the samples processed in the Bioruptor and the Barocycler, respectively. (B) Correlation analysis between section area and protein yield for ten malignant melanoma tumours extracted in the Bioruptor. The correlation coefficient (r = 0.806) indicates that the section area can be used to estimate the amount of proteins. (C) The coefficient of variation of the proteins commonly quantified in three replicates for the two individual extraction methods and the methods combined. The dotted line indicates the median CV.

Next, the digestion efficiency using the Barocycler and AssayMAP Bravo platform (Agilent Technologies) was evaluated.

In the Barocycler, 30 and 50 µg of proteins extracted from rat spleen and melanoma tissues were digested. In the first digestion attempt, the protocol from the manufacturer was utilised, using a 1:50 enzyme-to-protein ratio (w/w), resulting in a high percentage (22.2%) of miscleaved peptides. Then, the digestion temperature and cycle numbers were adjusted, and we managed to decrease the rate of miscleaved peptides (19.8%). Finally, by increasing the trypsin-to-protein ratio to 1:25 (w/w), we further reduced the missed cleavages to 13.7%. Throughout the three digestion attempts, the number of quantified proteins was comparable; however, by decreasing the number of miscleaved peptides, the coefficient of variation of the quantified proteins was reduced from 33.7 to 11.5%, emphasising the importance of a thorough evaluation of the sample preparations steps for obtaining the most reliable protein quantification.

Our research group developed a urea in-solution digestion protocol where protein digestion was performed at room temperature (RT) [196]. In that study, we demonstrated a drop of carbamylated peptides by around 40% when performing digestion at RT. In addition, a decrease in the urea concentration, ranging from 1.5 M to 0.5 M, significantly improved the digestion efficiency and decreased the number of miscleaved peptides. At the same time, the number of identifications increased, and the variability between experimental replicates was reduced.

Therefore, this protocol was directly transferred to the 96-well plate format of the AssayMAP Bravo, where the robot performed all the pipetting steps of the in-solution digestion, resulting in minimal manual sample handling. Digestion and peptide clean-up was conducted in the AssayMAP Bravo and assessed using rat spleen tissue lysate in six experimental replicates processed in parallel. The average recovery of the desalted peptides was 83%, and the amount of miscleaved peptides was 8.9%. To evaluate the platform's stability over time, 100 µg of rat spleen lysate was digested four times over five weeks. The peptides were stored at -80°C and analysed sequentially by nLC-MS/MS. We found a high overlap of identified proteins between the four experiments (81.3%) and a median CV of 4.3% for the quantified proteins (Figure 14A).

Additionally, we observed a strong correlation between the quantified proteins processed with the two digestion platforms (Spearman correlation > 0.95), demonstrating good quantitative reproducibility (Figure 14B). In particular, the performance of the AssayMAP Bravo platform was outstanding, demonstrating its reliability to be used to process complex clinical samples at a large scale.

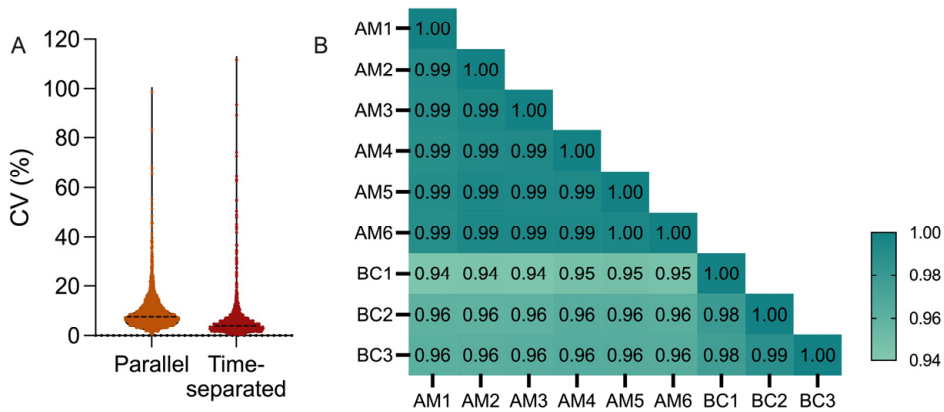

Figure 14. (A) The coefficients of variation (CV) for proteins commonly quantified in the six experimental replicates digested in parallel in the AssayMAP Bravo and for the proteins commonly quantified in the four experiments performed over time in separate batches. The dotted line indicates the median CV. (B) Spearman correlations between the proteins commonly quantified in the digestion experiment, using rat spleen lysates, performed in the Barocycler (BC) and the AssayMAP Bravo (AM), respectively, and for the two methods combined.

Lastly, we evaluated a high pH RP step-elution fractionation in the AssayMAP Bravo. Three 75 µg melanoma digests were used, and for each sample, seven fractions (including the flow-through) were collected and analysed by nLC-MS/MS. The MS analysis showed a two-fold increase in the number of identified proteins and a three to four-fold increase in the number of identified peptides compared to the unfractionated melanoma sample. In addition, the number of unique peptides per fraction varied from 57 to 84%, and the average percentage of shared peptides between the same fractions from different experiments was 84% (Figures 15A and B). These results indicate good resolution and reproducibility of the elution profiles within replicates and between experiments. The results also suggest that high pH RP fractionation could be an easier yet very efficient way of performing the prefractionation of peptides in clinical proteomic studies.

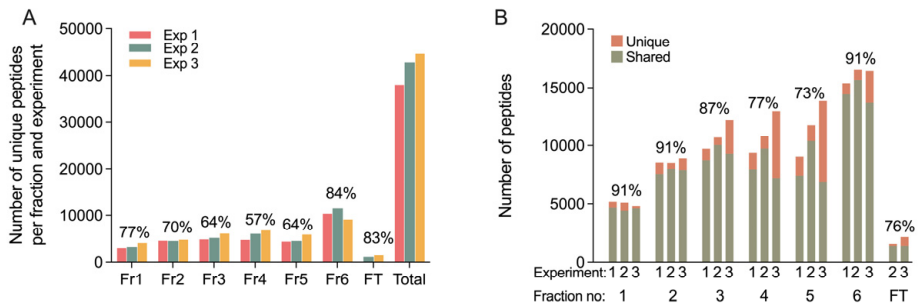

Figure 15. (A) The number of unique peptides per fraction and the average percentage of unique peptides in each fraction for the three separate experiments. The total number of quantified peptides in each experiment is also indicated. (B) The number of shared peptides between the same fractions from the three separate experiments (green), the total number of peptides per fraction (green + orange bars) and the percentage of shared peptides between fractions for the three experiments.

The three tested instruments showed high consistency overall. No process-specific bias was observed throughout the study. Furthermore, our optimised protocols can be used for studying proteomes of heterogeneous tissue samples without sacrificing the protein's diversity or quantitative nature.

Altogether, this work aimed at establishing the most automated workflow possible for the future preparation of large cohorts of sectioned frozen tissues in a robust and reproducible manner and to generate sufficient material to perform multi-omics analyses. For processing the 137 melanoma metastases, we selected the combination of tissue homogenisation and protein extraction in the Bioruptor with in-solution digestion, including peptide purification in the AssayMAP Bravo platform.

Automated phosphopeptide enrichment of small tissue amounts

As the next step of the method development, an automated phosphopeptide enrichment protocol was optimised for small tissue amounts. Usually, large quantities (1–2 mg) of starting material (tryptic peptides) are used for phosphoproteomic analyses due to the low occupancy of many phosphosites [197-199]. However, this can be hard to obtain when working with frozen clinical specimens from cancer patients since most of the tissue is often used for diagnostic purposes. Thereby the tissues are fixed in formalin and embedded in paraffin, and the leftovers, if any, are used for research purposes. Therefore, we evaluated and optimised a phosphopeptide enrichment protocol in the AssayMAP Bravo platform using Fe(III)-IMAC cartridges to meet our study requirements.

Proteins from melanoma tissues were extracted in the Bioruptor, digested, and desalted in the AssayMAP Bravo with the developed protocol described in paper I. Then phosphopeptides were enriched with our in-house optimised protocol. To assess the sensitivity and selectivity of the method, increasing amounts of peptides (12.5 µg to 200 µg) were used to enrich phosphopeptides from a pool of melanoma tissues (Figure 16A). The number of phosphopeptide identifications increased linearly with larger peptide amounts up to 100 µg. However, when loading 200 µg of peptides, there was a decrease in the number of peptides identified per microgram of starting material, indicating saturation of the cartridge. The selectivity (ratio between the identified phosphopeptides and all identified peptides) was above 90 % for all quantities. The enrichment of phosphorylated serine (pSer), threonine (pThr) and tyrosine (pTyr) followed the expected pattern where pSer > pThr > pTyr.

To evaluate the reproducibility of the enrichment, peptides from three melanoma samples were processed. Each sample was split in two, and 60 µg of peptides was processed in each cartridge in parallel. Despite the low amounts of starting material, good correlations between replicates and high overlap between the identified phosphoproteins were obtained (Figures 16B and C).

To increase the number of identified phosphopeptides, one melanoma peptide sample was subjected to high pH RP pre-fractionation before the phosphopeptide enrichment, according to the method developed in paper I. The seven fractions were then enriched using the optimised protocol. From 60 µg of starting material, we observed an increase of 49% in identified phosphopeptides (Figure 16D), suggesting that even low amounts of starting material can be fractionated before enrichment to increase the depth of the analysis substantially. However, larger peptide amounts would be necessary to obtain an even deeper analysis and improve the MS spectra quality of the low-abundant phosphopeptides.

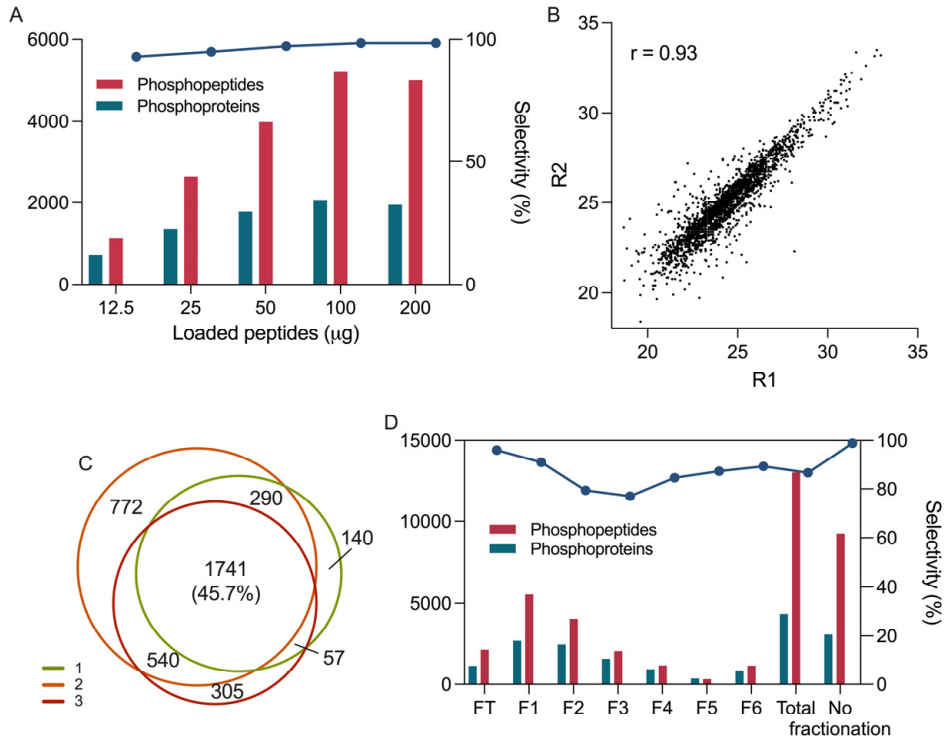

Figure 16. (A) Phosphopeptide enrichment of a pooled melanoma digest using 12.5 to 200 µg of material. The left axis represents the number of phosphopeptides and phosphoproteins in each experiment (from three separate enrichments). The right axis shows the enrichment selectivity of each experiment. (B) Pearson correlation between two independently-enriched samples from one melanoma patient. (C) Overlap between the phosphoproteomes of the three melanoma samples. (D) Phosphopeptide enrichment of the six fractions and the FT obtained from high pH RP prefractionation on the Bravo AssayMap platform using one melanoma sample. The graph includes the total number of enriched peptides and proteins compared with the sample enriched without prefractionation.

Altogether, the protocol showed remarkable sensitivity, and the results were in line with other phosphoproteomic analyses of individual samples or cell lines at that time [200-202]. Moreover, these results exceeded our expectations because our starting material was 12.5- to 100-fold less than the compared studies. Indeed, functional annotations of the differentially expressed phosphoproteins between the three melanoma samples showed enrichment in some of the most important regulators of melanoma development, such as the MAPK pathway, melanocyte development, integrin signalling and cytoskeleton structure.

Lastly, the protocol was successfully integrated into the workflow developed in paper I, and was used to perform phosphopeptide enrichment analysis of our large cohort of melanoma metastases as part of a multi-omics approach.

From frozen tissues to FPPE archives

Paper III aimed to explore the possibility of substituting frozen tissues with FFPE tissues in our proteomic experiments to expand beyond the difficult-to-store and often limited cohorts of fresh frozen tissues. Combined with clinical information and patient outcome, FFPE samples are enormous resources for retrospective studies [148,203-205]. However, although recent publications have shown promising and comparable results in terms of quality and quantity between frozen and FFPE samples in proteomics, it requires careful sample processing with well-established protocols. Therefore, in the third study, we developed different sample preparation protocols for processing FFPE tissues using suspension trapping (S-Trap). S-Trap has simplified and improved the sample preparation for MS-based proteomics by combining several preparation steps [154].

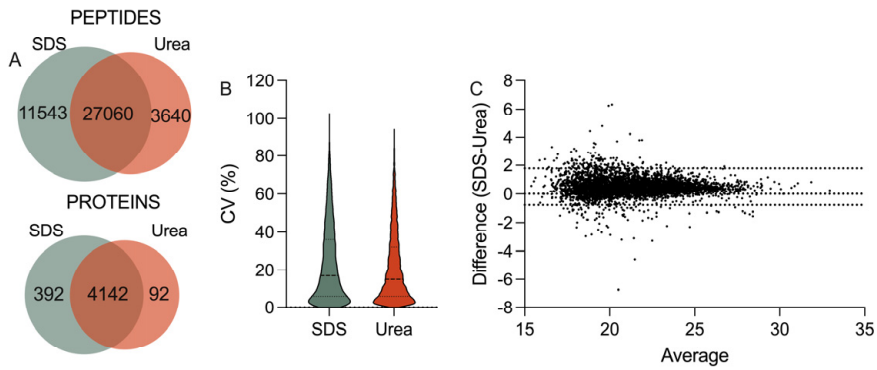

Figure 18. (A) Overlap of the identified peptides and proteins in three experimental replicates from each extraction method. (B) The sequence coverage for the proteins that were quantified in each extraction condition. The thicker dotted line indicates the median coverage, and the thin lines mark the quartiles. (C) Comparison of the protein expressions between the SDS and the urea extraction methods represented in a Bland−Altman plot. In total, 239 proteins (145 with higher and 94 with lower abundance in the SDS samples) were outside the limits of agreement (upper limit: 1.75 and lower limit: −0.77).

Before the samples were loaded onto the S-trap, a xylene-free method for deparaffinisation was applied, which was able to efficiently remove large pieces of paraffin without any substantial protein loss. Then two protein extraction protocols using 1) 100 mM Ambic containing 8M urea and 2) 100 mM TEAB containing 25 mM DTT and 10% SDS were compared. For protein digestion, the protocol provided by the manufacturer of the S-Trap was modified to decrease miscleaved peptides by adding a two-hour Lys-C digestion step before digestion with trypsin overnight, as demonstrated in paper I and by Betancourt et al.[196]. We found an increase of 26% in identified peptides and a slight increase in protein sequence coverage when using the SDS buffer (Figures 18A and B).

When comparing the two methods regarding digestion efficiency, the urea buffer performed slightly better than the SDS buffer (91.9% vs 87.5% fully cleaved peptides). Also, a good quantitative agreement (94.8%) was observed between the methods, although, the proteins extracted using the SDS buffer showed slightly higher intensities (Figure 18C).

Finally, the cellular component distribution and physicochemical properties of the peptides identified by the two methods did not show any noteworthy differences. They showed similar distribution patterns when compared to each other and the theoretical human proteome. Altogether, the results indicate that both methods retain the proteome integrity. Nevertheless, the SDS-containing buffer was selected for all further experiments due to the increased sequence coverage and the higher number of quantified peptides and proteins.

Next, we looked at the protein-to-peptide recovery of the S-Trap 96-well plate (nominal capacity 100–300 µg) by digesting different amounts of proteins (50–150 µg) from FFPE lung adenocarcinoma (LADC) patient tissues. Recoveries of 61–100% were obtained, and the two-enzyme digestion protocol (Lys-C and trypsin) resulted in more than 90% fully cleaved peptides in all samples. The quantitative reproducibility of the common proteins between the experimental replicates, within and between the different digestion amounts, was very high (Pearson correlation, $r > 0.98$).

To investigate whether the peptides eluted from the S-Trap are compatible with isobaric labelling using TMTpro 16 plex, we performed a "model experiment". The peptides obtained from LADC samples were pooled, split into four different amounts, and labelled (Table 3). The labelling efficiency was above 98%, and, despite the known ratio compression of TMT-data [206,207], we could regain good ratios, confirming the compatibility.

Table 3. TMTpro 16-plex experiment showing the different labelling amounts of each channel. Also, the expected ratios and the obtained ratios are displayed.

Group (amount (µg))	TMT channels				Lung tissue amount (µg)	Expected ratio (mean)	Obtained ratio (mean)
A	126	128C	130C	132C	29	-	-
B	127N	129N	131N	133N	26	A/B = 1.12	1.12
C	127C	129C	131C	133C	21.5	A/C = 1.35	1.38
D	128N	130N	132N	134N	14.75	A/D = 1.97	1.91

Finally, but most interestingly, we developed a fast S-Trap-based protocol to study endogenous lysine acetylation, based on a protocol developed by Gil et al. [208]. The method makes it possible to assign the exact localisation of the acetylation site and the relative quantification of the acetylation rate. In the first step of the protocol, the protein's free amino groups were chemically acetylated using deuterated N-acetoxisuccinimide (NAS-d3), which enables the differentiation between the heavy-labelled acetylation from endogenous acetylation in the MS analysis. The protocol of Gil et al. includes overnight ethanol precipitation and ethyl acetate extraction, resulting in considerable sample manipulation and loss. Therefore, we adapted the protocol to the S-trap and performed on-filter acetylation. This resulted in a shortening of the protocol by more than a day by eliminating the precipitation and increasing the throughput substantially by removing the ethyl acetate extraction, which takes about one hour per sample and is performed one sample at a time. As a result, we obtained very low variability in the peptide and protein quantifications between the experimental replicates (Figure 19A).

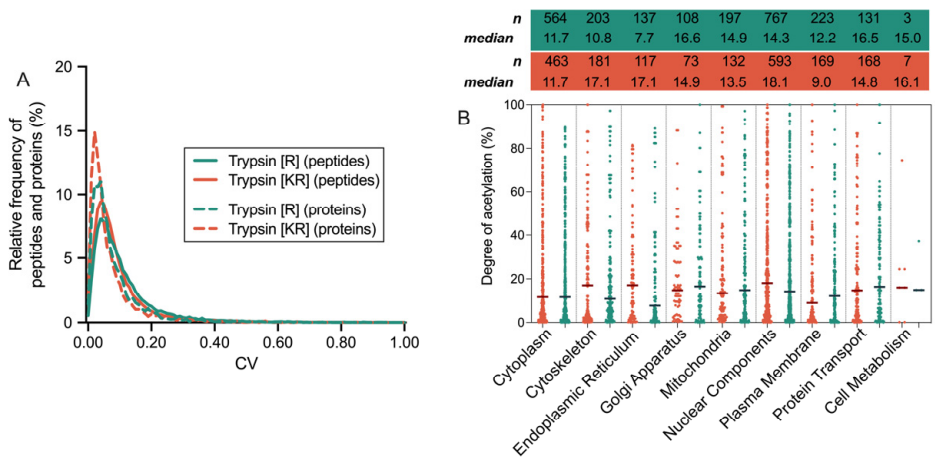

Figure 19. (A) Coefficients of variation calculated at peptide (continuous) and protein levels (dashed) between the experimental replicates for the acetylation method and the classical trypsin digestion method. (B) The subcellular compartment distribution of the endogenous acetylation sites, including their corresponding acetylation stoichiometry for the FFPE (orange) and frozen (green) tissue samples, for one of the melanoma patients. The black lines represent the median acetylation rate.

After establishing the protocol, as a next step, we wanted to assess to which extent acetylation stoichiometry can be studied in FFPE tissue. Therefore, paired FFPE and frozen tissue samples from three melanoma patients were compared. From 48,064 and 50,026 peptides, 6,602 and 6,625 proteins were identified in total in the three pairs of FFPE and frozen patient samples.

This resulted in the identification of 2,336 and 2,665 endogenously acetylated peptides, corresponding to 1,698 and 1,884 proteins in the FFPE and frozen tissues, respectively (Table 4). Noticeably, more than 70% of the proteins were previously reported to be acetylated, confirming the validity of our approach. Furthermore, functional enrichment of the acetylated proteins showed that most acetylation sites originated from the nucleus, cytoplasm and plasma membrane in all three patients (Figure 19B).

Table 4. The number of peptides and proteins identified in total, peptides containing lysine residues, acetylated peptides and proteins identified in each sample individually and in total from the three paired melanoma FFPE and frozen tissue samples.

Patients	Peptides		Proteins		Peptides (K)		Peptides (Ac)		Proteins (Ac)	
	FFPE	Frozen	FFPE	Frozen	FFPE	Frozen	FFPE	Frozen	FFPE	Frozen
1	44,228	46,326	6,460	6,478	23,054	25,800	1,138	1,219	972	1,015
2	38,602	45,142	6,333	6,452	20,111	24,166	1,033	1,247	878	1,018
3	44,841	46,173	6,463	6,441	24,016	25,581	1,159	1,334	952	1,086
Total	48,064	50,026	6,602	6,625	26,890	29,050	2,336	2,665	1,698	1,884

As an example, a histone H3 peptide [10KSTGGKAPR18] containing two lysine residues was selected to compare and demonstrate the degree of endogenous acetylation between frozen and FFPE tissues. The tandem mass spectra of the H3 peptide with 2, 1, and no endogenously acetylated lysine residues were assessed (Figure 20). The relative proportions of each acetylation state showed comparable results with only a slight increase of the acetylation degree obtained in the FFPE sample compared to the frozen. The calculation was based on unmodified peptides, and since the formalin fixation process can increase the degree of monomethylation [209], as was observed in our data (4% higher in FFPE compared to frozen tissue) (Table 5), and consequently change the relative distribution between the modified and unmodified peptides. As a result, the acetylation rate of H3, an endogenously methylated peptide, might be slightly increased in the FFPE tissue compared to the frozen.

In summary, the S-Trap protocol for proteomic analysis of FFPE and frozen tissues is robust and generates reproducible results. It also offers flexibility regarding the choice of extraction buffer as the S-Trap effectively removes nonprotein products from the sample before digestion. This might allow harsher extraction conditions, such as 10 % SDS or 8 M urea in harder-to-extract tissue types. Furthermore, the workflow is easy to scale up using the S-Trap 96-well plate, making it applicable for analysing large patient cohorts.

Additionally, we can conclude that the quantitative analysis of endogenous lysine acetylation in FFPE tissues is as valid as in frozen tissue samples, which has not been shown before to the best of our knowledge. Also, the sample preparation protocol offers a simple and fast way of studying endogenous lysine acetylation and complements other types of multi-omics data obtained from clinical samples.

Adding an additional omics layer provides a more comprehensive presentation of disease pathology and, thus, a better understanding of the underlying mechanisms.

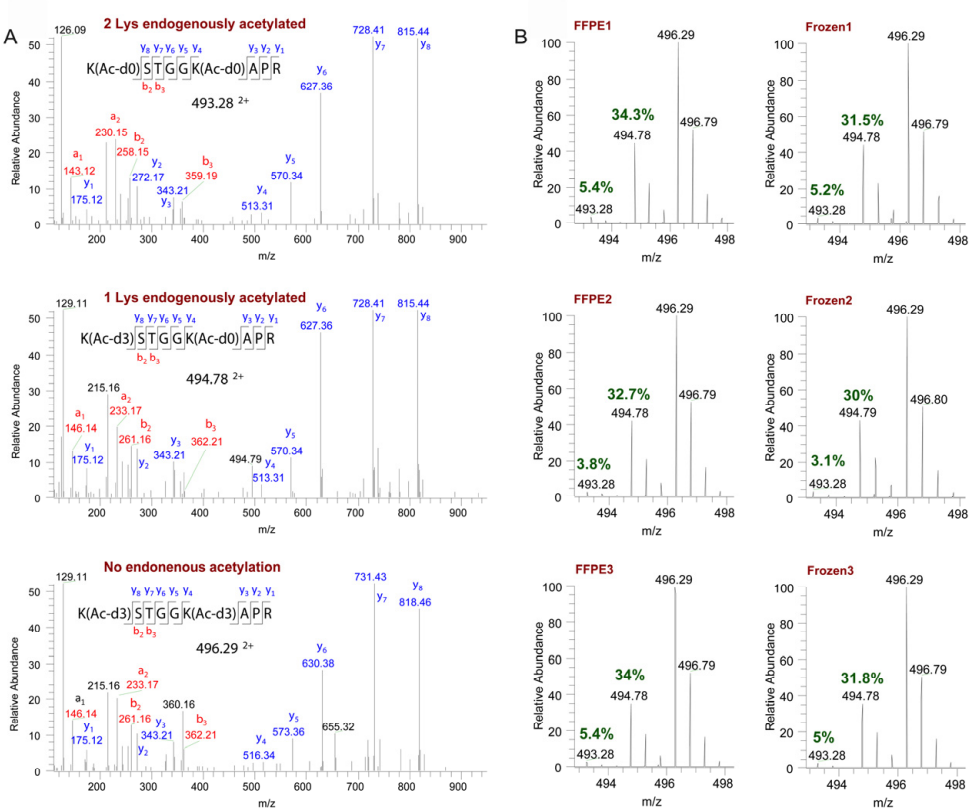

Figure 20. MS/MS and MS spectra of the peptide 10KSTGGKAPR18 from histone H3, identified in the three melanoma patient's FFPE and frozen tissue samples that underwent chemical acetylation. (A) Representative MS/MS spectra of the peptide with different degrees of endogenous acetylation, including the doubly acetylated form (2 × Ac-d0), the singly acetylated form (1 × Ac-d03 and 1 × Ac-d0) and the nonacetylated form (2 × Ac-d3) (from top to bottom). (B) MS spectra showing the isotopic distribution and relative degree of acetylation (green) of the peptide with two endogenously acetylated lysine (493.28), one endogenously acetylated lysine (494.78), and without endogenous acetylation (496.29), in the FFPE and frozen tissue samples, from the three melanoma patients.

Table 5. The average percentage of mono methylation at lysine residues, O-acetylation, and labelling efficiency in all FFPE and frozen tissue samples.

Samples (average)	Methylation (K)	Acetylation (S, T, Y)	Labelling efficiency
FFPE	4.9 %	0.39 %	98.4 %
Frozen	0.8 %	0.35 %	98.9 %

Biological interpretations and clinical implications

The understanding of melanoma biology has increased profoundly over the last two decades. Important scientific milestones include the identification of the oncogenic driver genes BRAF[210], NRAS[47], NF1[211] and KIT[53] in melanoma and the introduction of immune checkpoint and targeted therapies, with the approval of CTLA4 and BRAF targeted therapy in 2011. However, many melanoma patients do not respond to immunotherapy, and patients on targeted therapy eventually progress [212]. Additional challenges that appear ahead include the continuous increase in melanoma diagnoses worldwide. Attempts to classify melanoma based on molecular signatures, such as mutations and gene expression (transcriptomics), have been proposed to predict prognosis and improve therapy response and clinical management [42,80,109,110,112,213,214]. However, proteomic-based molecular classification with proximity to histopathology is lacking. Therefore, to complement the present classifications of melanoma, we propose several ways of stratifying melanoma metastases based on protein expression coupled with histopathology and patient outcome.

In papers IV and V, 142 treatment-naïve metastases from 137 melanoma patients were analysed (Table 1). The cohort was collected before the era of immunotherapy and targeted therapy. Therefore, we hypothesised that the proteogenomic and histopathological analysis of these samples allow us to study the natural course of melanoma biology and disease progression.

The melanoma metastases, mainly lymph nodes, were analysed by global proteomics and phosphoproteomics. These analyses were complemented with previously published transcriptomic data [214] from matched tumours. Of 12,695 proteins and 45,356 phosphosites, 8,124 proteins and 4,644 phosphosites were commonly quantified in every sample.

Proteomic classification of melanoma metastases

Unsupervised-consensus hierarchical clustering analysis using the 3000 proteins with the most variant expression levels (coefficient of variation > 0.36) was performed, and by visually examining the hierarchical tree, five subgroups were identified. They were classified according to their enriched characteristics based on GO terms and KEGG pathways into extracellular (EC, n = 23), extracellular-immune (EC-Im, n = 26), mitochondrial (Mit, n = 30), mitochondrial-immune (Mit-Im, n = 23), and extracellular-mitochondrial (EC-Mit, n = 16) (Figure 21). One-way ANOVA was performed on each omics dataset to identify proteins, phosphosites, and transcripts differentially expressed between each molecular subtype. In the EC, EC-Im and EC-Mit, we observed an upregulation of proteins and phosphorylation of proteins in pathways associated with ECM organisation and the complement and

coagulation pathways, suggesting a more invasive phenotype [42,72,77,80]. In contrast, the Mit, Mit-Im, and EC-Mit, to some extent, showed upregulation of oxidative phosphorylation, ribosomal activity, metabolism, and RNA-related pathways. As expected, the EC-Im and Mit-Im subtypes displayed enrichment in immune signalling, upregulation of antigen processing and presentation, and T cell receptor signalling pathways, including higher expression of PD-L1. At the transcript level, the EC-Mit, Mit and Mit-Im subtypes showed increased RNA activity, and T cell receptor signalling was strongly enriched in both immune subtypes.

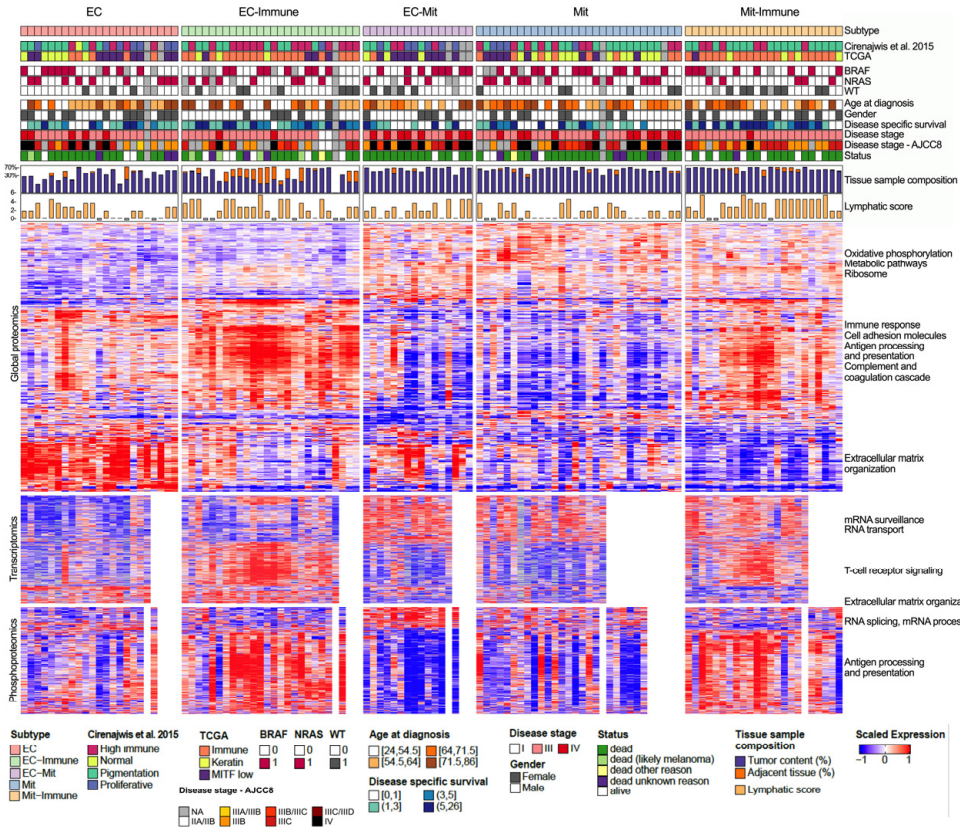

Figure 21. The tumour samples are grouped according to the proteomic subtypes and annotated with the transcriptomic classifications[110,214] and clinical and histological data. The heatmap displays the most significant proteins (top 500, FDR < 0.005), phosphosites (top 1000, FDR < 0.05), and transcripts (top 500, FDR < 0.05) and the enriched pathways, based on ANOVA across the five proteomic subtypes.

Next, we used Independent Component Analysis (ICA) to identify proteomic signatures for each subtype. The top ten ranked proteins from the independent component (IC) most significantly associated with each subtype were selected (Figure 22). In the EC-Im signature, we found an upregulation of the antigen

receptor-mediated signalling pathway, emphasising the immune system's involvement in this subtype. Furthermore, upregulated cell-cell and cell-matrix adhesion regulation was seen, contributing to the extracellular matrix component of this subtype. The protein signature of the EC subtype was enriched for ECM proteins and neutrophil degranulation, suggestive of poor prognosis and short overall survival in melanoma [215]. Additionally, several proteins from the S100 family (S100P, S100A12, S100A8, and S1009) were identified, advocating their potential as markers of this subtype.

The EC-Mit signature differed from the others in that no pathways were enriched. Instead, the signature included the downregulation of CHL1, a cell adhesion protein, which could contribute to cancer growth [216]. In the protein signature associated with the Mit subtype, we found enrichment in proteins essential to mitochondrial function, including OAT[217], VDAC2[218], and SHMT2[219]. Additionally, high expression of S100A1 was evident, indicating a strong link to the Mit subtype.

The top ten signature proteins in the Mit-Im subtype were associated with a downregulation of the complement and coagulation cascade rather than enrichment in a mitochondria-related signature or an upregulation of protective immune mechanisms. When upregulated in the tumour microenvironment, the complement and coagulation cascade may enhance tumour growth and increase metastasis and is implied in the contribution to EMT [220,221]. Interestingly, we could see an upregulation of these proteins in the EC subtype, highlighting the molecular differences between these two subtypes.

When our proteomic subtypes were aligned with two transcriptomic classifications performed on the same set of samples (109 overlapping samples)[110,214], several significant associations were obtained (Figure 23A). Samples classified as immune by TCGA [110] were mainly divided into the EC-Im and Mit-Im subtypes and the proliferative [214] and MITF-low[110] were separated into the EC and the EC-Mit subtypes.

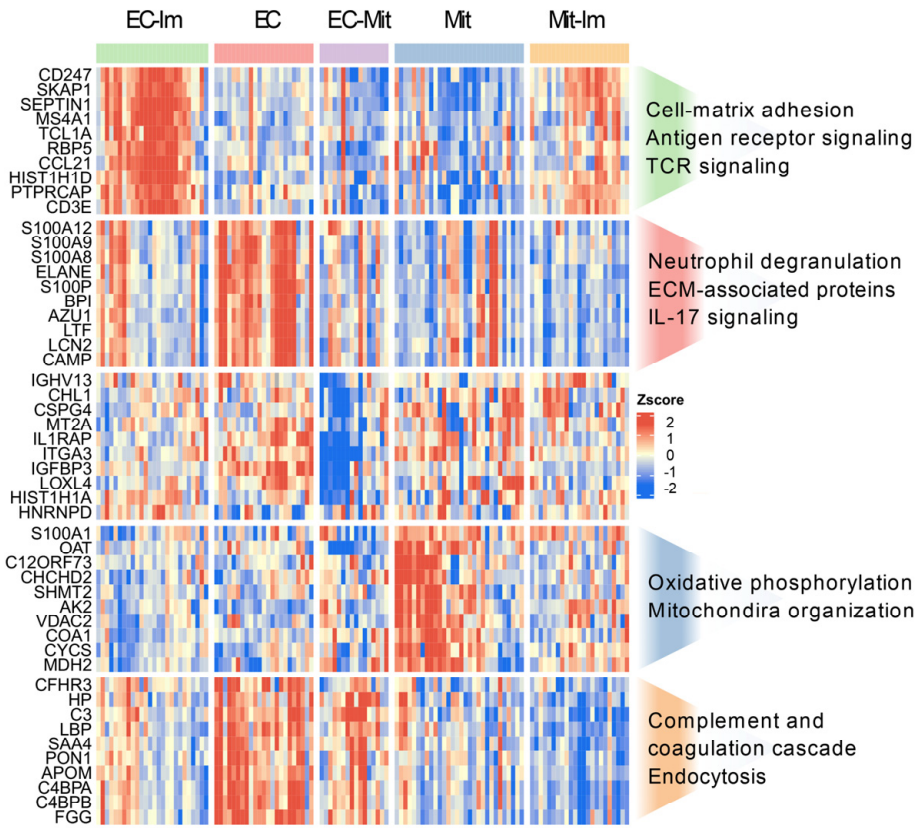

Figure 22. Proteomic signatures with enriched pathways of each proteomic subtype obtain by ICA.

Clinical parameters associated with the five subtypes

Among the clinical features associated with the five subtypes, we found that patients with tumours in the EC, EC-Mit, and Mit groups had an increased risk of developing distant metastases and displayed shorter survival times from the detection of the first metastasis. In addition, they were associated with an overall survival (OS) of less than five years compared to the patients with metastases belonging to the Mit-Im and EC-Im subtypes. As expected, the Kaplan-Meier analysis showed that patients within the immune subtypes (Mit-Im + EC-Im) had a significantly better prognosis than patients with metastases belonging to the other subtypes (EC + EC-Mit + Mit) (Figure 23B).

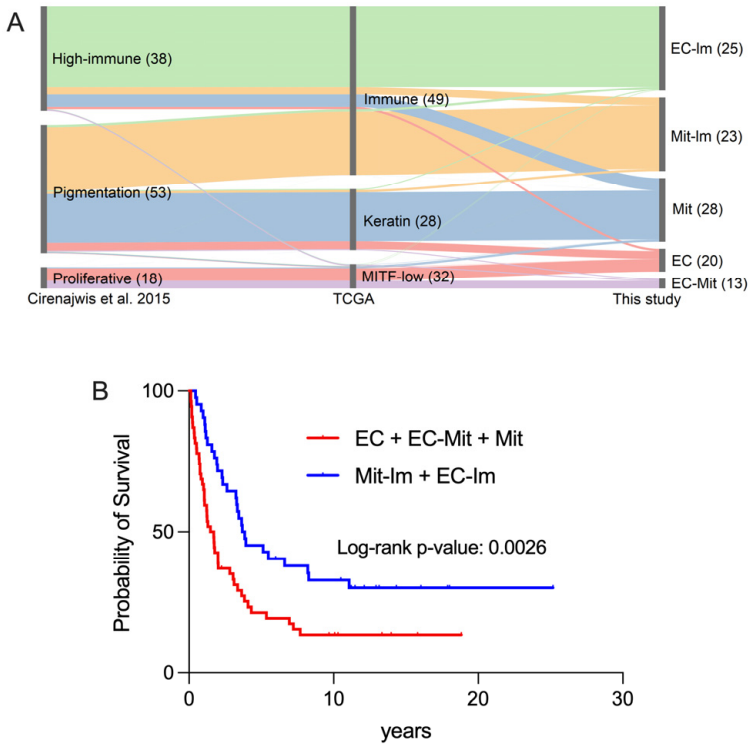

Figure 23. (A) The associations between proteomic (this study) and published transcriptomic subtypes[110,214]. The EC-Im subtype was significantly associated with the high-immune (FDR = 0.021) and immune (FDR = 0.0095) groups. The Mit-Im subtype was significantly linked to the pigmentation (FDR = 0.021) and the immune (FDR = 0.0021) groups. In comparison, the EC-Mit was significantly associated with the proliferative (p-value = 0.014) and the MITF-low (FDR = 0.026) groups. In addition, the Mit proteomic subtype was significantly linked to the keratin class (FDR = 0.040) from the TCGA classification, and the EC subtype was associated with the proliferative (p-value = 0.0244) and the MITF-low (p-value = 0.032) groups. (B) Survival (from surgical intervention to death or censoring) probability for patients with tumours in subtypes associated with long and short survival.

Moreover, there were no significant associations between the proteomic subtypes and BRAF V600E or NRAS Q61K/R mutations, which indicates that the subtypes are not driven by any of these gene mutations, similar to what was shown on transcriptomic level by TCGA[110] (Table 6). Furthermore, we observed that metastases from patients in disease stage III clustered with metastases from patients in stage IV across the more aggressive subtypes (EC, EC-Mit and Mit) (Figure 21). Thus, indicating that the proteomic subtypes stratify melanoma metastases beyond the level of clinical staging and genomic driver mutations and with a connection to patient outcome.

Table 6. Association between the proteomic subtypes and mutational status.

Mutation	Subtype	Enrichment factor	P-value	Benj. Hoch. FDR
BRAF	EC	1.06	0.18	0.25
	EC-Im	0.80	0.12	0.25
	EC-Mit	1.20	0.17	0.25
	Mit	1.11	0.15	0.25
	Mit-Im	0.90	0.18	0.25
NRAS	EC	1.26	0.14	0.24
	EC-Im	0.93	0.14	0.24
	EC-Mit	0.69	0.19	0.24
	Mit	1.23	0.12	0.24
	Mit-Im	0.75	0.15	0.24
Double wt	EC	0.58	0.11	0.27
	EC-Im	1.14	0.18	0.27
	EC-Mit	1.13	0.24	0.28
	Mit	0.75	0.15	0.27
	Mit-Im	1.47	0.08	0.27

Association between molecular subtypes and histological features

A thorough histological evaluation was performed on the sections adjacent to the ones used for proteomic and phosphoproteomic analysis (Figure 12 and Table 2). The assessed features were then correlated to the proteomic subtypes. Several significant differences in the tissue composition were observed, where tumours in the EC and EC-Im groups showed a lower tumour content (Figure 24A). The immune subtypes displayed higher lymphatic scores (sum of lymphocyte infiltration and density within the tumour), and adjacent lymph node and necrosis content were higher in the EC-Im and EC subtypes, respectively. The morphological differences spotted when examining the histological images showed interesting features (Figure 24B). Samples within the Mit subtype showed solid nests of aggressive tumour cells with eosinophilic-stained cytoplasm and atypical nuclear features, resembling the cells they originate from. In contrast, the EC subtype displayed an abundance of an intercellular matrix as desmoplastic stroma with fewer tumour cells, a typical characteristic of phenotype switching in melanoma.

Mit-Im and EC-Im appear to be subclasses of the highly aggressive Mit and EC subtypes, respectively, where the presence of adaptive immune cells indicates a more favourable clinical behaviour, pointing towards a possible antitumour effect of the adjacent lymphatic tissue [222]. Histologically, the EC-Mit group also represents a more dedifferentiated phenotype with features of epithelioid and stromal-rich areas within the tumour. The EC-Mit subtype may represent an intermediate or transitory state in-between the more differentiated Mit groups and dedifferentiated EC groups.

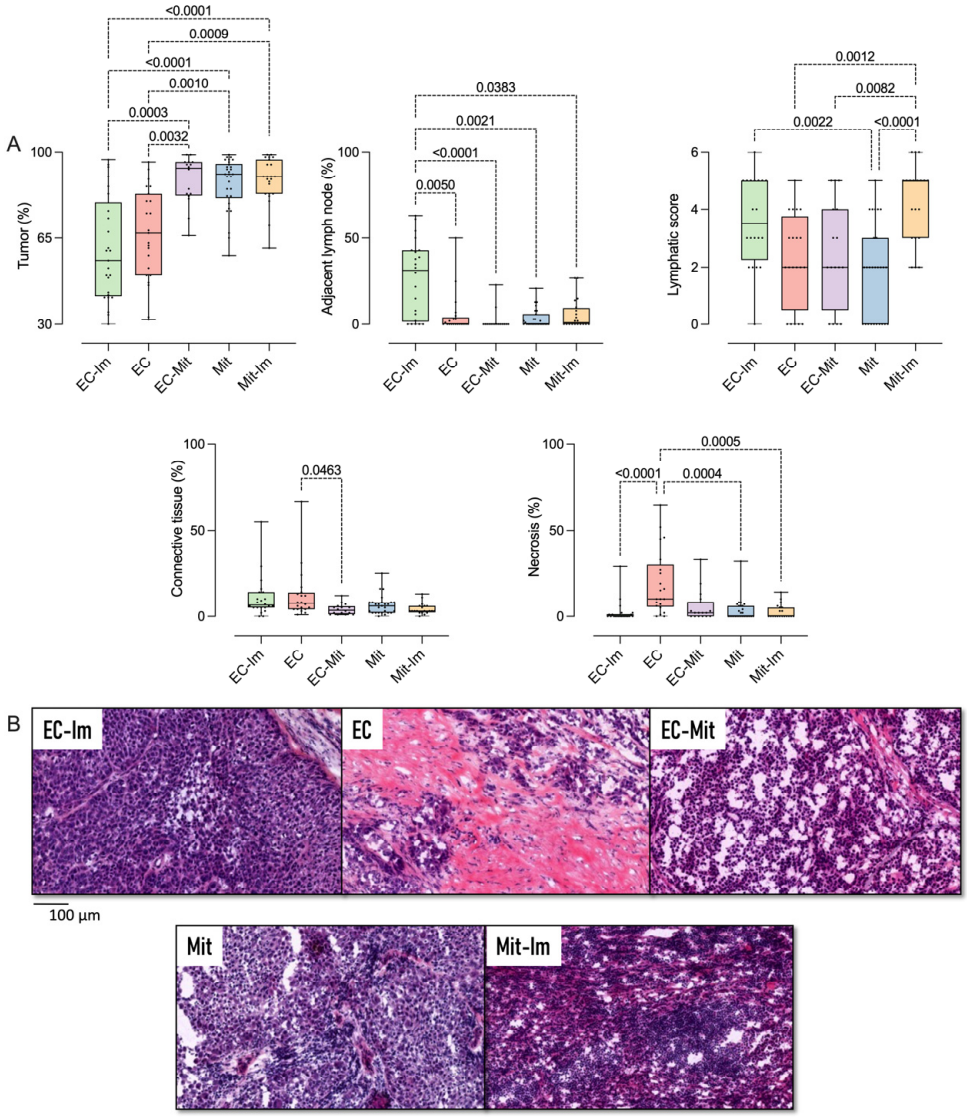

Figure 24. Distribution of the annotated histological parameters; tumour content; adjacent lymph node; lymphatic score; connective tissue, and necrosis among the five proteomic subtypes (Kruskal-Wallis and Dunn's multiple comparisons test). (B) Histological images from tomours within the five subtypes representing their distinct features.

Melanoma phenotype markers across the five subtypes

Phenotype switching of melanoma cells is an essential feature of progression, and several markers have been identified (Figure 7)[42,72,80,81]. The melanocytic linage markers MLANA, PMEL, TYR, and SOX10, used in the clinic for diagnosis, are often expressed at higher levels in more differentiated tumours and displayed a significantly higher protein and transcript expression in the Mit and Mit-Im subtypes when compared to EC, EC-Im and EC-Mit (Figures 25A and B).

MITF is considered one of the most important regulators of melanoma and is involved in several aspects of the disease, such as survival, cell cycle control, invasion, senescence, DNA damage repair, differentiation, and dedifferentiation[73,223]. The role of MITF depends on its expression levels, where generally, low MITF activity promotes invasion and cell cycle arrest, while high activity favours proliferation and differentiation by upregulation of melanocytic lineage genes[41,42]. We found a significant upregulation of MIFT in the Mit and Mit-Im subtypes at transcript and protein levels, although many missing values were observed in the proteomic data. The receptor tyrosine kinase AXL, the counterpart of MITF[42,80,81], was upregulated, on protein and transcript levels, in the EC and EC-Im compared to the Mit and Mit-Im subtypes. The tumours within the EC-Mit group displayed a mixed expression, highlighting the contribution of both EC and Mit-like features in this subtype.

Furthermore, a switched gene expression from CDH1 to CDH2, coding for E- and N-Cadherin, is known to have a profound role in melanoma phenotype switching, resulting in a more invasive phenotype[77]. Indeed, we found an upregulation of CDH1 protein expression in the Mit and Mit-Im subtypes. On the contrary, an upregulation of CDH2 was observed in the EC, EC-Im and EC-Mit subtypes, again emphasising the different phenotypes observed in these subgroups. Furthermore, other proteins that characterise a melanocytic phenotype, such as CAPN3, IRF4, MBP, and GPR143, were upregulated in the Mit and Mit-Im subtypes at protein and/or transcript levels. In contrast, proteins that are known to be expressed in a more undifferentiated phenotype (e.g. including the neural-crest-like phenotype[72]), including FAP, SERPINE1, TWIST1, NGFR, JUN, WNT5A, FN1, TCF4, among others, were upregulated in the EC, EC-Im and EC-Mit subtypes [78,79]. Remarkably, there was no significant difference for some of the well-known markers of melanoma phenotype switching, including VIM, SNAI1/2, and ZEB1/2 transcription factors among the metastatic subtypes, which might reflect the often-simultaneous presence of various differentiation patterns within melanoma, including the intermediate, transitory and neural-crest-like states[72].

Moreover, there was no significant difference in the expression of the proliferation marker Ki67 in the EC and EC-Im compared to the more differentiated Mit and Mit-Im subtypes. This somewhat challenges the assumed association between invasiveness and proliferation unless there is a co-existence of multiple phenotypes

within the tumour[224]. The EC-Mit metastases, on the other hand, showed significantly lower expression of Ki67 than the others. Slower proliferation might indicate aggressiveness and invasiveness, often counteracting proliferation, which other studies have demonstrated in cell cultures and mouse models[225,226].

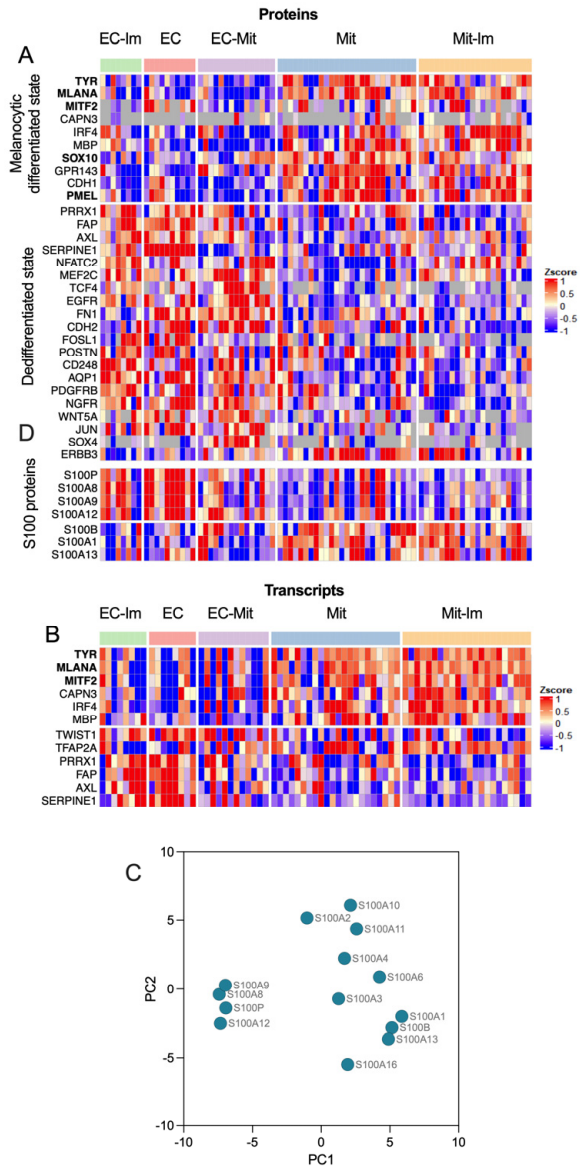

Figure 25. (A–B) Protein (top) and transcript (bottom) expression of melanoma markers and markers of EMT across each subtype. In bold are the melanoma markers frequently used in clinical practice for diagnosis by immunohistochemistry. (C) Principal component analysis of the S100 protein expression across all samples. (D) Expression of selected S100 proteins across the proteomic subtypes.

Expression of S100 protein family members across the five subtypes

Diagnosing melanoma can be challenging due to the absent expression of common melanoma markers, which can be observed in highly dedifferentiated melanomas [5,10,11,227]. In these cases, antibodies directed towards proteins from the S100 family can be used. Several proteins from this family have been implicated in cell proliferation, metastasis, angiogenesis, invasion, and inflammation in different types of cancer [10,228-230]. Seven of the sixteen identified proteins formed two distinct groups among our samples (Figure 25C). The first group, consisting of S100P, S100A8, S100A9, and S100A12[231], was significantly upregulated in the EC subtypes. In the second group, S100B[232], S100A1 and S100A13[233] were significantly upregulated in both mitochondrial subtypes compared to the EC subtypes (Figure 25D)[234]. This result can be interpreted as a coordinated expression of selected proteins from the S100 family across the proteomic subtypes.

The heterogeneous disease presentation often seen in melanoma was emphasised by the proteomic subtypes[1,106]. They were characterised by different levels of differentiation, where the Mit and Mit-Im subtypes displayed a higher expression of melanocytic markers. In contrast, the EC, EC-Im, and EC-Mit subtypes showed increased expression of markers related to a more invasive and undifferentiated state. The results were supported by protein and transcript abundances and histological features observed in nearby sections of each tumour. Furthermore, the proposed proteomic subtypes integrate the microenvironment, including the immune and stroma components, enabling refined subtyping of melanoma. Additionally, EC-Im and Mit-Im subtypes seem to be associated with slower metastatic spread and better prognoses.

On the other hand, the EC, EC-Mit, and Mit subtypes appear to escape immune control and are accompanied by a more aggressive disease presentation. Additionally, our results suggest that the subtypes can be distinguished based on the abundance of routinely used immunohistochemical markers such as MITF, TYR, PMEL (HMB45), MLANA, and members from the S100 protein family. Moreover, a proteomic signature was assigned to each subtype, enriched in features closely related to the overall characteristics of that particular subtype.

The role of BRAF V600 mutations in melanoma

About 50% of melanoma tumours harbour mutations in the BRAF gene, specifically a V600E amino acid substitution (~ 90 % of all BRAF mutations)[226,235]. BRAF V600E encodes a serine/threonine kinase and has been implicated in different mechanisms of melanoma progression due to the deregulated activation of its downstream effectors, MEK and ERK[235]. In clinical settings, PCR-based DNA methods that amplify the mutant BRAF gene are often used to assign the presence or absence of a BRAF V600E mutation[236]. However, verifying a BRAF mutation

does not mean that the BRAF gene is transcribed and translated. Also, in most studies, the detection of a BRAF mutation at the genomic level has failed to show a relationship with survival[110,237,238]. On the other hand, immunohistochemistry staining of the BRAF V600E protein has displayed correlations between semi-quantitative expression levels and survival[237]. However, it comes with some disadvantages in interpreting the staining pattern, which can vary among pathologists[238]. Therefore, it was of great interest to investigate the BRAF V600E protein expression by MS.

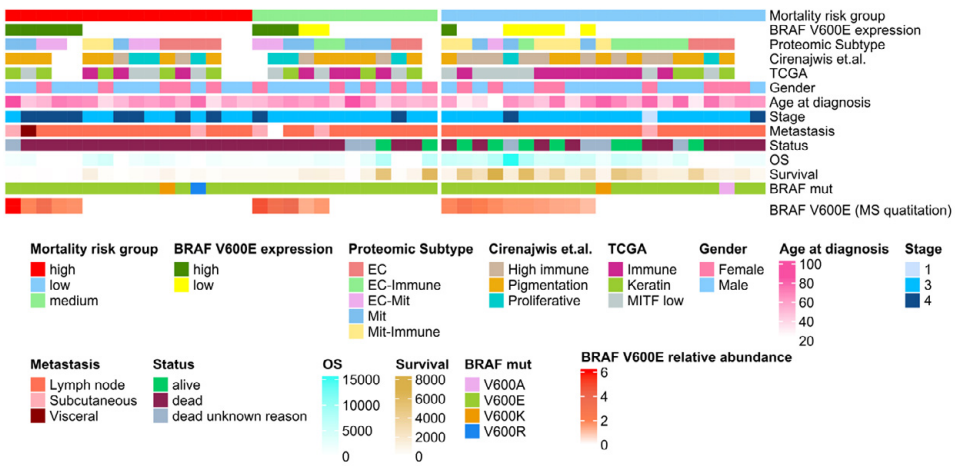

Figure 26. Clinical data of a subgroup of 49 patients harbouring a BRAF V600 mutation confirmed at DNA and/or RNA levels. The relative abundance of the BRAF V600E mutated protein is depicted at the bottom and was used to divide the patients into low and high-expression groups (yellow and green).

In papers IV and V, a subgroup of 49 metastases from the main cohort, with an established BRAF V600E mutation on RNA and/or DNA levels, were assessed on protein level (Figure 26). In 22 of the 49 samples, we could identify the mutated BRAF V600E peptide (IGDFGLATEK) by MS (Figure 27), where 20 agreed with the mRNA analysis and were therefore used for further investigations. A method seldom exhibits 100% sensitivity and specificity[238], meaning the tumour samples that showed disagreement between DNA, RNA, and protein might still harbour a BRAF V600E mutation. Additionally, the tumour piece used for the clinical DNA-based evaluation differed from the piece analysed by transcriptomics and proteomics, which might contribute to the diverging results due to the heterogeneous nature of melanoma tumours[238]. When we compared the relative abundance of the BRAF V600E protein across the 20 samples, we found an additional layer of heterogeneity among the patients, where the tumour samples showed a variable expression level of the mutated protein. To investigate whether the protein level influenced the patient outcome, we correlated the abundance with survival for patients above 40 years of age at the time of diagnosis of the metastasis.

Patients below 40 years of age displayed a trend of more prolonged survival and were omitted, as several studies have indicated previously[239,240]. ROC curve analysis followed by Kaplan-Meier analysis showed that high levels of the mutated BRAF V600E protein correlated negatively with patient survival, and strikingly all patients expressing high levels of the BRAF V600E protein died within 18 months of diagnosis. This suggests that higher expression levels of the BRAF V600E protein can serve as a risk- and prognostic factor in melanoma patients in stages III and IV who are above 40 years of age at the time of diagnosis.

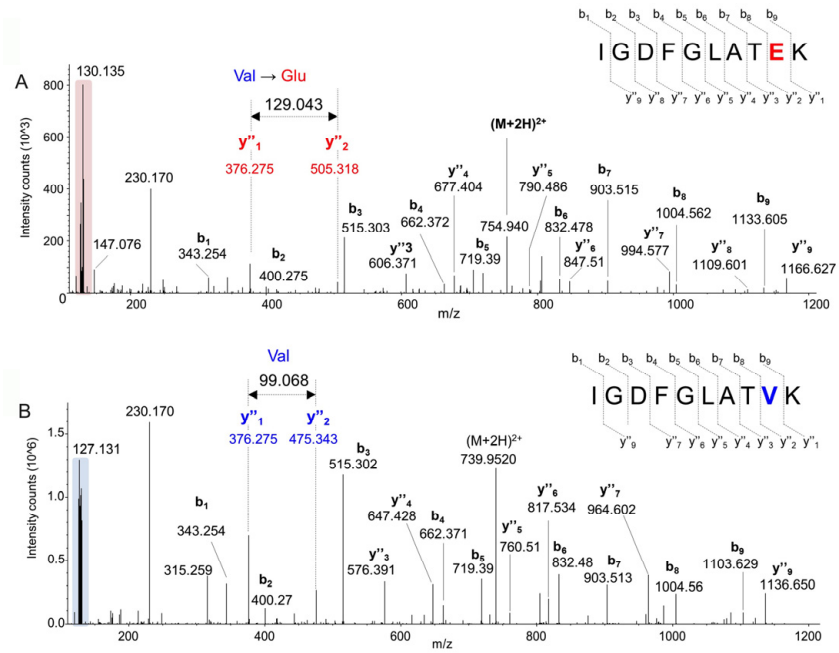

Figure 27. (A) Assigned MS/MS spectrum of the TMT-labelled peptide IGDFGLATEK from BRAF V600E. Interpretation of the data showed the substitution of valine residue for glutamic acid (Glu, m/ztheo = 129.0425) that corresponds to the mutation. (B) Assigned MS/MS spectrum of the TMT-labelled peptide IGDFGLATVK from wt BRAF. Interpretation of the data showed the presence of the expected valine residue (Val, m/ztheo = 99.0684). The low m/z region is highlighted in both MS/MS spectra to indicate the presence of TMT 11-plex reporter ions used for relative protein quantification.

The histological images were examined to see whether any apparent morphological differences between the high and low BRAF V600E expression groups could be observed. Indeed, for the tumours expressing high protein levels, we found an increased vascularisation together with smaller but more heterogeneous cells with a non-cohesive pattern. On the contrary, the cells from tumours expressing low levels of the mutated protein were bigger and displayed a deeper cytoplasmic colour, more frequent multinucleation and increased cell grouping. Based on this analysis, a

heterogeneity-based scoring system was set up (0–4) comprising tumour cell size variation, vascularisation, decohesion and multinucleation.

For positivity, a minimum of 55% of the samples in the respective group had to display the feature. As expected, we observed a higher heterogeneity score in the group expressing high levels of the mutated BRAF V600E protein (Table 7).

Table 7. Heterogeneity assessment of the high and low BRAF V600E protein expression

Group	Cell size variation (> 7 µm)	Neo-vascularisation	Discohesive pattern	Multi-nucleation	Heterogeneity score (0–4)
BRAF V600E high	5/9 (56%)	7/9 (77%)	6/9 (66%)	3/9 (33%)	3
BRAF V600E low	3/7 (43%)	1/7 (14%)	2/7 (29%)	5/7 (71%)	1

As a next step, we extended the analysis, including all 49 patients with a BRAF V600 mutation confirmed by RNA analysis. We hypothesised that patients with a BRAF V600 mutation might present different mortality risks. Therefore, the 697 differentially expressed proteins between the BRAF V600E high and low-expressing groups from paper IV were subjected to pathway enrichment. These pathways were then matched with the protein matrix from the 49 samples and further subjected to Integrative Genomics Robust iDentification of cancer subgroups (InGRiD) analysis [241]. Simplified, InGRiD is a statistical approach that integrates biological pathways with omics data to identify molecularly defined subgroups of cancer patients. Each protein from the matched matrix belonging to the identified biological pathways is first subjected to Cox regression and given a score depending on its association with survival. The protein scores of each patient are then summed, and the patients are categorised into three subgroups based on mortality risk (Figure 28A). The patient's survival information was used as the outcome variable.

Based on the results, three groups with different mortality risks were created, supporting the hypothesis that patients with a BRAF mutation might have different outcomes related to different BRAF V600 mutated protein levels. Notably, eight out of nine patients with high expression levels of the mutated protein ended up in the high and medium-risk groups, while most patients with low levels ended up in the low-risk group. Furthermore, pathway enrichment of the differentially expressed proteins between the low and medium-high mortality risk groups showed that neutrophil degranulation, the complement cascade, transcription, TGF-beta signalling and DNA repair pathways were positively related to mortality risk. In contrast, signal transduction, vesicle-mediate transport, mitochondrial fatty acid beta-oxidation, fatty acid metabolism and nucleotide metabolism pathways were found to be negatively related to mortality risk.

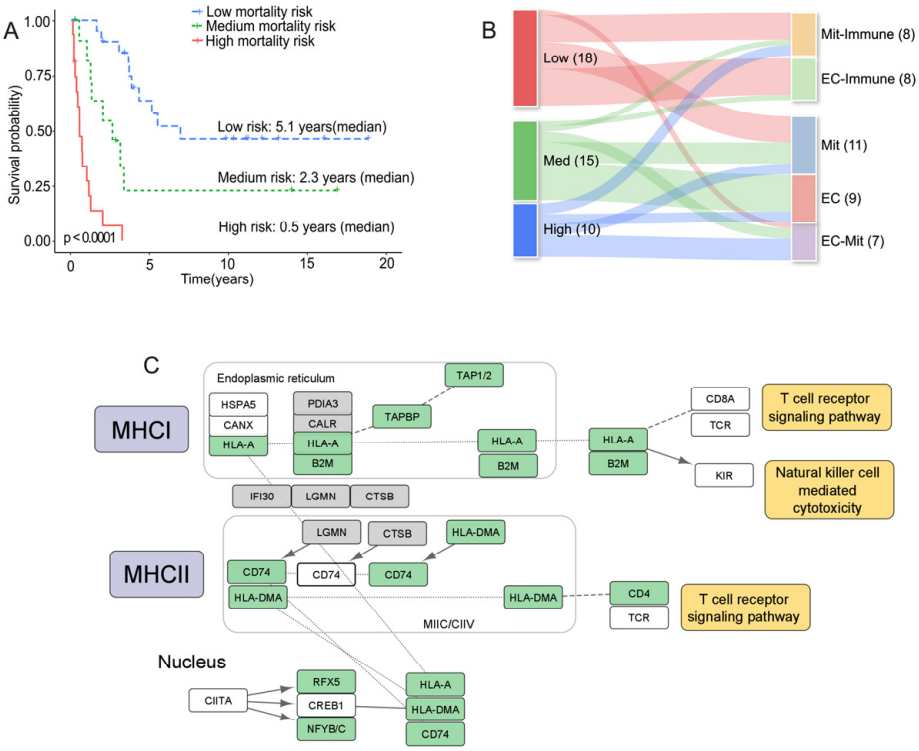

Figure 28. (A) Survival probability based on mortality risk among the BRAF V600 subgroups of patients, coloured by survival probabilities: red (high risk of mortality, n = 16), green (medium risk, n = 12), and blue (low risk, n = 21). Median survival times for the three groups are shown. (B) Association between BRAF mortality groups and the five proteomic subtypes. A significant association was found between the low-risk mortality subgroup and the proteomic subtypes with better prognosis (EC-Im and Mit-Im) (Fisher exact test, FDR=0.002). In comparison, the medium and high-risk BRAF subgroups were significantly associated (Fisher exact test FDR=0.002) with the subtypes having worse prognoses (EC, Mit, and EC-Mit). (C) Significantly upregulated proteins (green) of the antigen processing and presentation pathway in the low-mortality risk group compared to the med-high. Identified proteins are shown in (grey).

The proposed BRAF V600-based mortality risk groups displayed associations with the proteomic subtypes, whereas the low mortality risk group was significantly associated with the immune subtypes. In contrast, the med-high mortality risk group was significantly associated with the subtypes displaying worse prognoses (Figure 28B).

After a comprehensive investigation of the patient samples belonging to the low-risk group and from our previous knowledge of the patients expressing lower levels of the BRAF V600E protein, a hypothesis of an oncogene-induced senescence-like (OIS-like) phenotype emerged. The presence of such a phenotype might act as a tumour suppressor and consequently lead to a better outcome in these patients. The patients in the low-risk group were characterised by higher lymphatic scores and more adjacent lymph node tissue, as well as an upregulation of MHC II molecules (Figure 28C).

Additionally, upregulation of interferon-gamma signalling was observed on protein- and phosphoprotein levels, another hallmark of senescence and an activator of MHC I antigen presentation[242]. This indicates an increased susceptibility to cell-mediated cytotoxicity and possibly a contribution to the OIS-like phenotype[243].

Additionally, several proteins and phosphoproteins from the cellular senescence pathway were dysregulated in favour of a senescent phenotype in the low-risk group, including two JmjC demethylases (KDM5B and KDM4A) known to trigger senescence were downregulated [244] (Figure 29A). Downregulation of KDM5B activates p53 and thereby inhibits cell proliferation. It also contributes to the silencing of E2F target gene promoters through direct interaction with Rb [137,245-248]. Downregulation of KDM4A also activates the p53 pathway and contributes to the accumulation of promyelocytic leukaemia (PML) nuclear bodies. The PML protein is a known tumour suppressor[249]. We found an upregulation of several phosphosites in the protein, responsible for its accumulation and degradation, suggesting an increased turnover of the PML protein (Figure 29B). KDM4A and KDM5B can be considered proto-oncogenes, and targeting these demethylases could potentially result in tumour suppression, which makes them attractive therapeutic targets in melanoma.

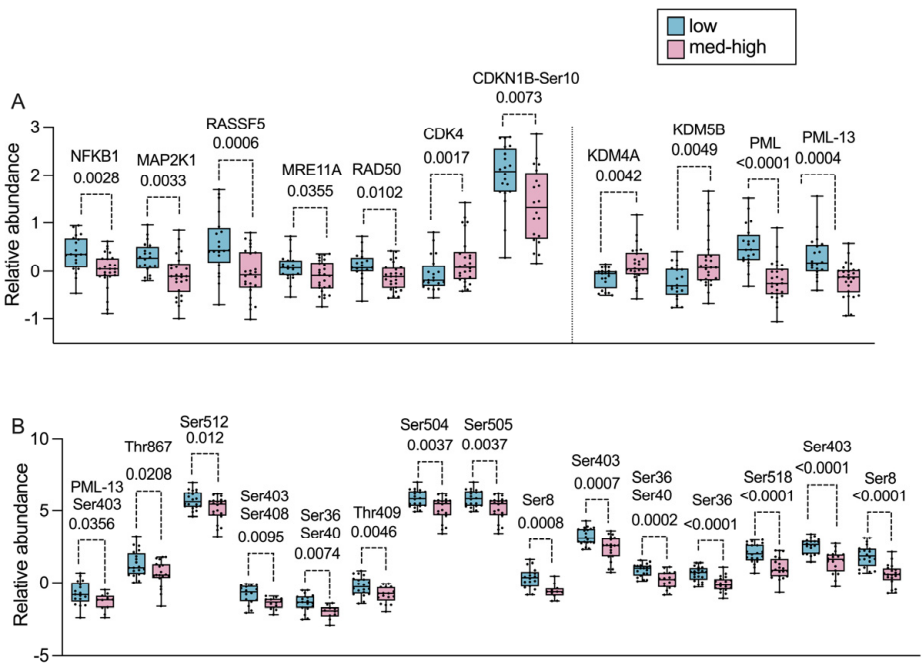

Figure 29. (A) Proteins and phosphoproteins linked to cellular senescence and their expression patterns between the low- and med-high mortality risk groups. (B) Expression differences of the identified phosphosites in the PML protein and the PML-13 isoform between the low and medium-high mortality risk groups.

The differences in protein profiles, biological pathway enrichments, and histology assessment support the hypothesis of a heterogeneous mutated BRAF protein expression. This is defined by two major groups of BRAF V600E positive metastases (low and medium-high), linked to the escape from, or exposure to immune surveillance. These facts pose challenges and opportunities from diagnostic and therapeutic perspectives, such as whether all patients harbouring BRAF V600 mutations benefit equally from targeted therapy. Our results indicate that a BRAF V600 protein expression-based metastasis stratification could help the patients and contribute to more informed clinical decisions, as these tumours do not display the same biology. Additionally, due to the higher presence of TILs in the low-risk mortality group, these patients likely respond better to immunotherapy. In future studies, it would be interesting to associate the BRAF V600 mutated protein levels with response durations of targeted therapy.

The landscape of single amino acid variants in melanoma

Despite melanoma being the cancer type with the highest mutational burden [1], the literature is scarce when addressing the expression of mutated proteins within melanoma. Therefore, we wanted to explore the single amino acid variants (SAAVs) in the melanoma proteome. A custom protein sequence database was built using protein mutations from the Cancer Mutant Proteome Database [250]. This included the skin cutaneous melanoma data from TCGA (369 cases) and seven melanoma cell lines from the NCI-60 panel. We identified 1015 SAAVs in 828 proteins, where 81 of the SAAVs have been linked directly or indirectly to cancer or have been predicted to be cancer-promoting. Functional annotations of the proteins affected by the SAAVs, showed enrichment in pathways commonly dysregulated in melanoma. This included the PI3K/AKT and MAPK signalling pathways as well as ECM-related processes, cellular metabolism and the complement and coagulation cascade (Figure 30A). Most of the SAAV of the PI3K/AKT pathway were structurally or functionally associated with the ECM (Figure 30B). Less than 2%, corresponding to 19 SAAVs, originated from samples with < 50% tumour content, indicating that the ECM-related protein variants, such as MMP2, are likely produced by the melanoma cells. This finding is in line with a recent Pan-Cancer genomic study, which revealed that a higher copy number and more missense mutational alterations are present in the ECM genes compared with the rest of the genome[251].

Quantitative analysis of the SAAV expression resulted in 52 differentially expressed variants across the proteomic subtypes, where the highest number of overexpressed SAAVs was found in the EC subtype (Figure 31A). This further emphasises the important role of ECM-remodelling and dysregulation of the TME in melanoma progression, and these events are possibly related to phenotype switching of melanoma cells.

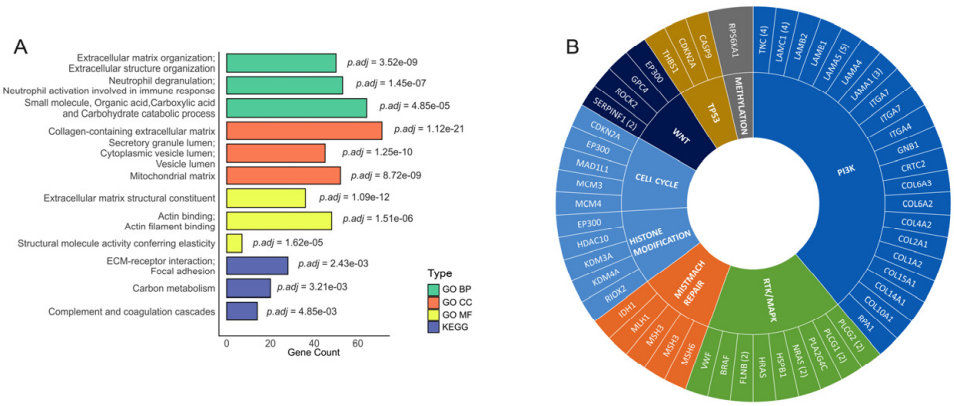

Figure 30. (A) KEGG and GO enrichment analysis of the 828 proteins with SAAVs. (B) Identified Genes with SAAVs belonging to signalling pathways frequently dysregulated in melanoma. In brackets are the number of SAAVs within that gene.

To predict which SAAVs are expressed at a higher frequency in melanoma tissue, we searched the dbSNP Short Genetic Variations database[252] for the European population's corresponding variant allele frequencies (VAf) to acquire an understanding of the expected contributions of these SAAVs in the population. The variants with a frequency in our melanoma cohort greatly different from the VAf in the population were used to generate a signature of 167 SAAVs likely associated with melanoma. These SAAVs were classified into three levels. Level 1 included the SAAVs with frequency differences outside the limits of agreement of the VAf and were considered under and over-represented in our cohort (Figure 31B). This included the melanoma driver mutations NRAS Q61K/R, BRAF V600E, CDKN2A P114L, and HRAS G13. The SAAVs belonging to level 2 fulfilled three criteria, namely, 1) a VAf in the population of below 30%, 2) no wild-type peptide detected in our data, although it is present at a high frequency in the population (~70%) and lastly, 3) there is evidence of the wild-type peptide in the Peptide Atlas database, meaning that the wt peptide has been identified by proteomics previously, and consequently should not be missing in our data due to technical aspects (Figure 31C). Thus, we believe these SAAVs to be over-represented in melanoma tissue. Level 3 comprised the SAAVs, where VAfs were absent. The absence of VAf data can indicate a low occurrence of these SAAVs in the population while being identified at different levels in our cohort and potentially associated with melanoma. In eight cases, the wt-peptide was not detected despite being previously identified in proteomic studies reported in the Peptide Atlas database.

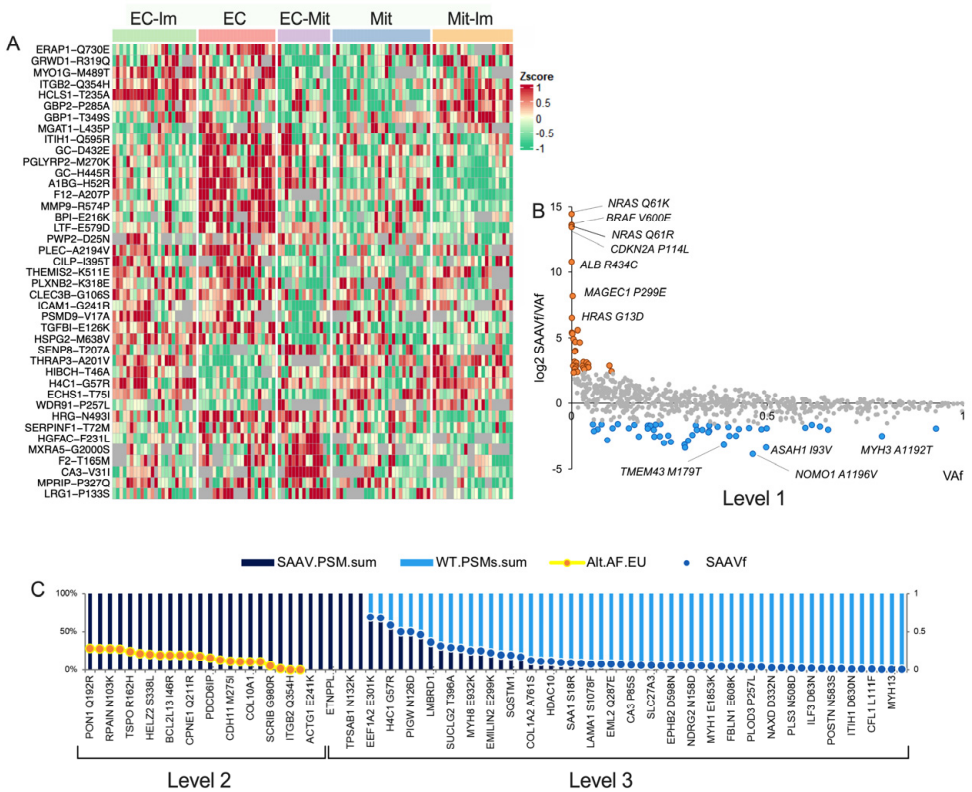

Figure 31. (A) Differentially expressed SAAVs across the proteomic subtypes. (B) Level 1 of the melanoma-associated SAAV signature, with 34 over- (orange) and 49 under- (blue) represented SAAVs, from the expected frequency in the population, based on a SAAVf and Vaf ratio. (C) SAAVs categorised as level 2 (22) and level 3 (62) from the melanoma-associated signature.

The melanoma SAAV signature was enriched in pathways closely related to melanoma development and progression (Figure 32A). Interestingly, across the three levels, we found five SAAVs in the proteins of the heavy chains of muscle myosin II complex (MYH1 E1853K, MYH2 E486K, MYH4 N1627I, MYH8 E932K, and MYH13 D1765N), which originate from the loci 17p13.1, the same loci of TP53, a frequently mutated tumour suppressor in melanoma and other cancers[33,54]. Myosin II is required for cell contractility, cytoskeleton reorganisation, and cytokinesis. Different reports have associated mutations and polymorphism in heavy chains of muscle myosin II with cancer predisposition[253] and non-cancer-related diseases[254,255]. We hypothesise that these variants are reactivated by melanoma cells as part of cytoskeletal remodelling, where myosin II might contribute to the survival of melanoma cells with reduced MAPK activity[256].

Furthermore, the tumour mutational burden can predict response to immunotherapy in melanoma[257], which suggests that mutated peptides binding to MHC I molecules can be the targets of an anti-tumoural immune response. To investigate neoantigens

with the potential to express identified SAAVs, we aligned the amino acid sequence of the SAAV-bearing peptides to a large experimental dataset of a melanoma-associated immunopeptidome[258]. This resulted in 56 SAAVs that could be presented as variant peptide ligands by an HLA I complex. To compare the MHC I binding prediction of the 56 matched peptides with our SAAV counterparts, we used the NetMH prediction tool[259]. The tool uses different peptide lengths (8–12), which are matched against several HLA types, summing up to 140 SAAV-altered peptide combinations ranking better as HLA class I neoepitopes than their wt counterparts. This included 19 cases where the wt was outside the specified threshold (%Rank_EL < 2) in the binding prediction (Figure 32B). The variant peptide ligands CYB5R1 N44S, CD300LF Q218R, GCA S80A, and QARS N285S were the best candidates for the HLA allotypes HLA-A26:01, HLA-B07:02, HLA-B15:01, and HLA-B58:01, respectively. Among the significant HLA I peptide ligand variants, we found CDKN2A P114L, ARL6IP6 R56L, GCA S80A, LOXL1 R141L, CFL1 L111F, HSPB1 I179N, and TGFBI E126K, which were included in the melanoma-associated SAAV signature defined in this study. These results indicate that knowledge of variant expression, supported by the melanoma-associated immunopeptidome and MHC I binding prediction tools, may lead to the discovery of neoantigen candidates as targets of anti-tumour immune responses.

In the landscape of SAAVs, we found a mixture of commonly dysregulated pathways and less explored SAAVs and pathways. Many of them are enriched in genes related to different functions of the ECM, suggesting a contribution of these SAAVs to the formation of a pro-tumourigenic TME, as further emphasised by their higher abundance in the EC subtype. Additionally, we created a signature of over and under-represented SAAVs in melanoma, which included the most important driver mutations, supporting our approach and strengthening the link to melanoma. Furthermore, we identified several SAAVs with higher peptide-MHC I binding prediction than corresponding wild-type peptide ligands. This highlights the potential of identifying SAAV expression as a valuable source of antigens eliciting tumour-specific immune responses. In the future, additional studies are required to address the function of these SAAVs and their role in melanoma development and progression.

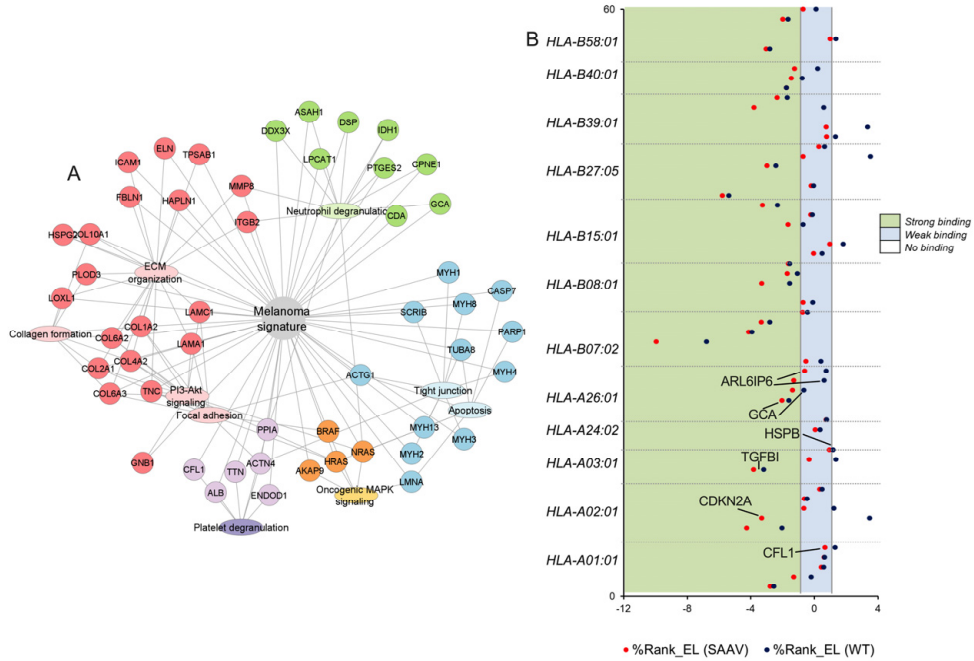

Figure 32. (A) Using KEGG and the Reactome databases, the corresponding proteins and enriched pathways of the melanoma-associated SAAV signature. (B) The predicted affinity of the top 5 SAAV-neoantigen candidates for each HLA, ranking better than their wt counterparts using NetMHC. The peptide ligand variants that were a part of the melanoma-associated SAAVs signature are displayed.

Tumour microenvironment composition as a prognostic factor

The TME is essential in melanoma progression and metastatic spread [56]. Throughout this study, the recurrence of differences in TME properties observed among the proteomic subtypes, within the BRAF mortality risk groups, and among the signature of melanoma-associated SAAVs pointed towards an association with patient outcome. A subset of 29 samples exhibited a tumour content of less than 50% and was used to analyse the TME composition in more detail. First, ROC curve analysis was used to separate the samples based on three-years survival from sample collection (Figure 33A). The two groups were named high and low lymph node (HLN or LLN) and high and low connective tissue (HCT or LCT), reflecting the tissue content based on the histological assessment (Figure 33B). The sample overlap between the groups was nearly 100 % (Figure 33C). When performing the Kaplan-Meier analysis, it was clear that patients in the HLN and LCT groups had a much better prognosis compared to the LLN and HCT groups (Figure 33D).

Interestingly, a Cox regression analysis showed that LN (Cox coefficient = -1.661, p-value = 0.001) and CT (Cox coefficient = 1.718, p-value = 0.001) content were better indicators of prognosis than disease stage (III versus IV) (Cox

coefficient = 1.265, p-value = 0.008). Furthermore, a multivariate Cox regression analysis adjusted for age, gender, and disease stage showed an increased risk of developing distant metastasis and a shorter overall survival for the LLN group compared to the HLN group (Table 8).

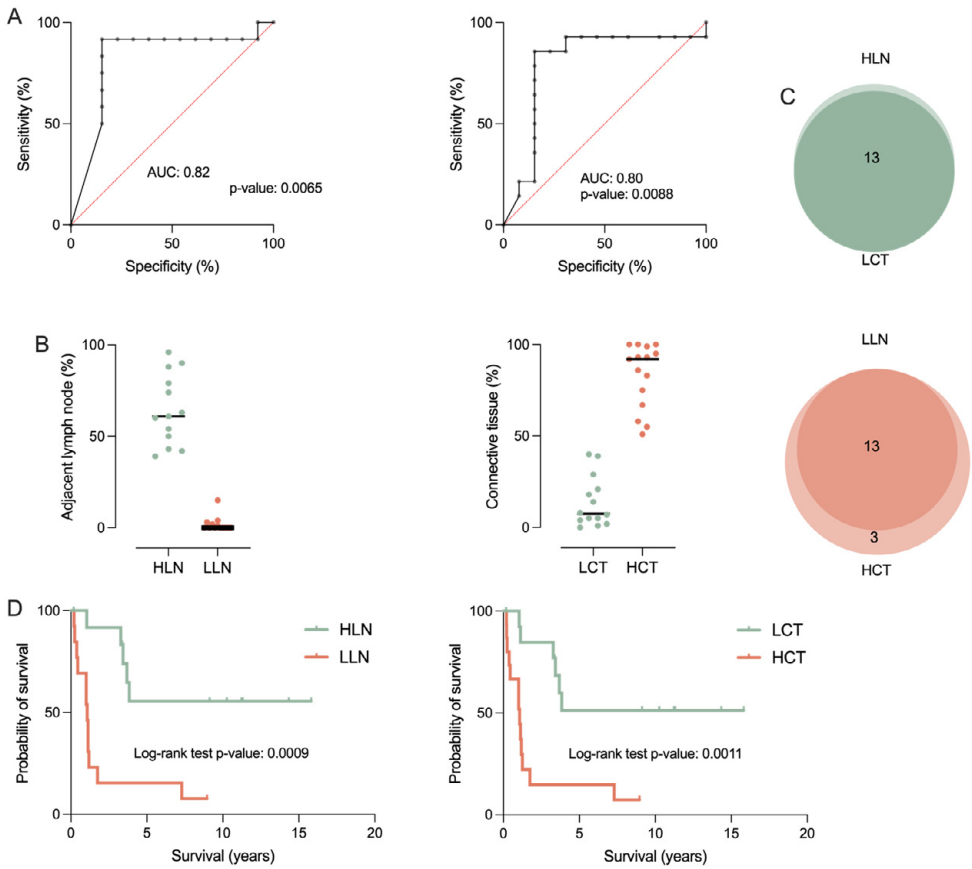

Figure 33. (A) ROCs of adjacent lymph node (left) and connective tissue (right) based on three years of survival. (B) Adjacent lymph node (left, cut-off = 27%) and connective tissue (right, cut-off = 45.5%) contents in the TME for the subgroups of samples generated from the ROC analysis. (C) The patient overlaps between the HLN and LCT groups and between the LLN and HCT groups. (D) Survival probability for patients with tumours grouped based on their tissue content, HLN and LLN (left) or HCT and LCT (right).

Table 8. Multivariate Cox regression comparing the LLN and HLN groups.

Variables (age, gender, stage adj.)	**Distant metastasis**			**Overall survival**		
	HR	95% CI	p-value	HR	95% CI	p-value
LLN vs. HLN	5.96	1.63–28.96	0.021	19.91	3.35–173.4	0.0023

Histological images from the different groups showed distinctly different features. The HLN/LCT tumours mainly displayed a TME consisting of TILs surrounding and infiltrating the tumour. On the contrary, the LLN/HCT group displayed large areas of stroma and fatty tissue mixed with tumour cells (Figure 33E).

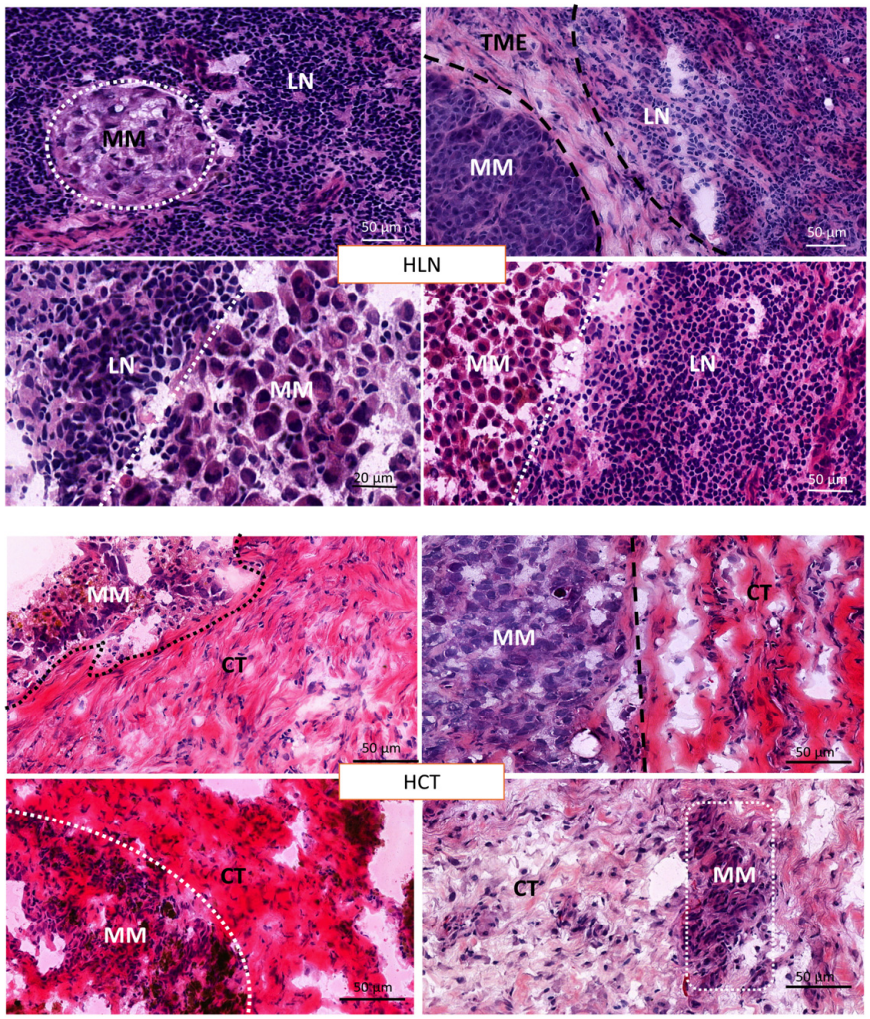

Figure 34. Histological images from different tumours in the HLN (top) and HCT groups (bottom).

To see whether these observations could be complemented with quantitated cell-specific data. We applied the cell-specific transcriptomic signatures of melanoma from Tirosh et al.[66] to our proteomic and transcriptomic data. Indeed, the HLN group was enriched in proteins and transcripts mainly expressed by B and T lymphocytes,

macrophages, and endothelial cells. Two-dimension pathway enrichment of the upregulated proteins and transcripts in the HLN group were related to antigen processing and presentation, ribosome activity, and B and T cell receptor signalling (Figure 34). The LLN group displayed enrichment in markers of cancer-associated fibroblasts (CAFs), macrophages, and endothelial cells. Specific markers of CAFs, including collagens, complement components, and growth factor proteins, were upregulated. This group was also enriched in pathways related to the complement and coagulation cascades, EMT, ECM organisation, and collagen turnover. Among the upregulated proteins in the LLN group, we found LOX (lysyl oxidase enzymes), which catalyse the crosslinking of collagens and elastin, increasing tissue stiffness. This protein has been shown to promote tumour progression through increased integrin signalling and EMT [67]. Additionally, upregulation of the fibroblast activation protein (FAP), known to enhance migration and invasion capabilities [260,261] was observed in the LLN group. Based on the results from these analyses, it is not surprising that the patient outcome greatly differs with respect to the TME composition.

These results align with previous breast and colon cancer studies, where the stroma-to-tumour ratio in lymph node tissue was linked to prognosis. Just as in study (paper V), it was found that a high stromal content (> 50%) was associated with a more aggressive tumour progression [69,70,262]. The stroma-tumour and lymphocyte-tumour ratio can be assessed in routine pathology on HE-stained slides. It might be helpful as a selection criterion for therapy, as suggested for colorectal cancer and breast cancer [58,69,262-264]. Consequently, these results emphasise the need to explore this phenomenon in larger cohorts, combining different analysis strategies. The translation of such histopathological assessments could be readily implemented in clinical practice and used for better-informed medical decisions. Thus, our study (paper V) underscores the importance of further investigating the relationship between the tumour and its microenvironment and its association with clinical outcomes.

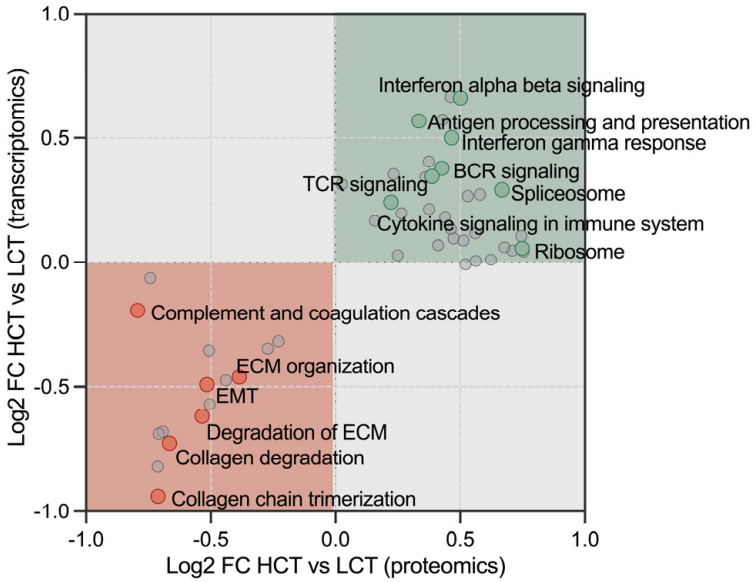

Figure 34. Enrichment analysis in two dimensions displaying significant pathways (FDR < 0.001) commonly dysregulated on the proteomic and transcriptomic levels between the HLN and LLN groups.

To sum up, the presented results (papers IV and V) provide insights into melanoma biology, emphasising comprehensive patient stratification within three main areas. Firstly, the proteomic subtypes provide a foundation for an in-depth molecular classification of the disease. Secondly, identifying BRAF V600E mortality-based risk groups allows for a more individualised treatment approach. Lastly, classifying patients into subgroups based on the surrounding microenvironment in lymph node tissue can foresee prognosis. And finally, our study provides a detailed and well-integrated multi-omics dataset that can generate new hypotheses and set the foundation for several follow-up studies to verify the results.

Conclusions and future perspectives

Melanoma and many other cancer forms represent major public health problems. Disease management of melanoma is challenging due to its heterogeneous nature and unpredictable progression pattern[265,266]. The emergence of immunotherapy and targeted therapy has prolonged numerous lives, but many patients relapse or do not respond. We believe the key to successful therapy is selecting the right molecular target leading to immune activation, whether?? an approved drug or a newly found potential drug target.

Clinical proteomics is continuously evolving, mainly due to improvements in MS technology and the availability of new bioinformatics tools, enabling researchers to advance and gain further insight into disease biology, thereby improving patient care. In addition, as new therapies are continuously being developed, there is a prominent need for patient stratification and prognostic and predictive biomarkers.

Due to the complexity of the proteome, no standard method for sample preparation in bottom-up proteomics exists. Protocols differ depending on sample type, experimental goals and analytical method used. The most important factors to consider were discussed in **papers I–III** and included minimal sample handling, optimised cellular lysis and protein extraction, generation of fully cleaved peptides and throughput. Additionally, the results in **paper III** provided evidence of the interchangeability between frozen and FFPE tissues for studying the proteome of melanoma tumours. This is a valuable finding due to many existing FFPE archives with accompanying clinical information available worldwide.

Several disease classifications have emphasised melanoma complexity at genomic and transcriptomic levels – and now at the proteomic level, as outlined in **paper V**. The proposed proteomic subtypes and previously identified transcriptomic subtypes show associative features characterised by the presence of phenotypes with different capabilities to proliferate and invade, named in broad terms as $MITF^{high}/AXL^{low}$ and $MIFT^{low}/AXL^{high}$. Although the identified proteomic subtypes were linked to several markers of phenotype switching and displayed distinct histological features, multiple phenotypes seem to coexist within a tumour. These results partly explain the challenges in finding the proper treatment regime for each patient. A successful validation followed by alignment of protein expression to the phenotypic characteristics observed in each subtype would enable the potential translation into clinical practices. Thus subtype-specific treatment approaches may be applied.

Furthermore, the proteomic subtypes were significantly linked to the proposed BRAF V600 mortality risk groups, with the patients in the low-risk group being associated with the immune subtypes and, consequently, better survival. Several features directly or indirectly related to oncogene-induced senescence were enriched in the BRAF V600 low-risk mortality group. This might explain the underlying molecular mechanism supporting a better clinical outcome among these patients. The additional layer of patient stratification based on the BRAF V600E protein expression, discovered in **paper IV**, might contribute to the understanding of the variable treatment responses to BRAF inhibitors and thus gives rise to a more individualised therapeutic strategy, as the simple "presence" or "absence" of a BRAF mutation is not enough.

The well-known mutational burden of melanoma directed us towards identifying a melanoma-associated SAAV signature. Among the genes generating the highest frequency of SAAVs compared with non-melanoma tissue, we found known melanoma drivers, including BRAF, NRAS and CDKN2A. Furthermore, the largest proportion of SAAV-containing proteins was associated with functions of the ECM, suggesting their involvement in forming a pro-tumourigenic microenvironment. Additionally, the potential role of particular SAAVs as neoantigen candidates with stronger binding affinity to MHC I compared to their wt counterparts was elucidated. Future studies should aim at decoding the role of these SAAVs in terms of protein function, melanoma predisposition and progression, and their relation to patient outcome.

In papers **IV and V,** the recurrent difference in tumour microenvironment properties observed among the proteomic subtypes, within the BRAF mortality risk groups, and among the signature of melanoma-associated SAAVs led to the discovery of the tumour microenvironment composition as a strong predictor of prognosis. The assessment of stroma-tumour and lymph node-tumour ratios in lymph node metastases of melanoma patients bears the potential to be implemented in clinical practice and used for more comprehensive patient evaluations. Thus, our studies underscore the importance of further investigating the relationship between the tumour and its microenvironment in larger melanoma lymph node metastases cohorts.

In every aspect of melanoma biology investigated throughout these studies, the immune system was the key determinant of prognosis and outcome. Melanoma is one of the cancer types with the highest response rate to immune checkpoint inhibitors. Although resistance to immunotherapies may manifest at different times, similar or overlapping mechanisms are often seen, enabling tumour cells to evade anti-tumour immune responses. Revealing these underlying mechanisms in melanoma might benefit patients with other cancer types as well.

Although progress in understanding melanoma biology and development has improved significantly over the past two decades, new challenges are emerging,

such as the continuously increasing incidence of melanoma worldwide. Moreover, we are only beginning to understand how the complex constellation of mutations relates to and affects the signalling between the tumour and its microenvironment, giving rise to particular melanoma phenotypes that are determinants of disease progression. As we move forward, our rapidly growing knowledge will allow us to bring melanoma to the level of a chronic, manageable disease, and a cure for most patients with disseminated melanoma may be close behind.

Populärvetenskaplig sammanfattning

Malignt melanom är den mest aggressiva hudcancerformen och incidensen har ökat kraftigt de senaste decennierna – med omkring fyra procent per år. I Sverige insjuknar mer än 4 000 personer årligen. Malignt melanom förekommer i alla åldrar, men är mycket sällsynt hos barn. Genomsnittsåldern för diagnos var år 2019, 66 år för kvinnor och 70 år för män. Melanom kan förekomma var som helst på kroppen men är vanligast på underbenen hos kvinnor och bålen hos män.

Melanom utvecklas ur en celltyp som kallas melanocyt. Melanocyter har till uppgift att producera pigmentet melanin som skyddar kroppen mot solens ultravioletta strålar. Hög exponering av ultraviolett strålning kan ge upphov till skador i melanocyternas DNA, vilket i sin tur kan leda till att de börjar dela sig okontrollerat – och då kan malignt melanom utvecklas. Det vanligaste symtomet vid melanom i huden är att ett födelsemärke har vuxit, ändrat färg eller form och börjat klia eller blöda. Förutom ultraviolett strålning utgör färg- och storleksförändrade födelsemärken, stort antal födelsemärken, benägenhet att bli bränd av solen, hög ålder, blond eller röd hårfärg samt blå eller grön ögonfärg betydande riskfaktorer i sammanhanget.

Melanom diagnostiseras genom att en läkare inspekterar huden med ett dermatoskop; ett förstoringsglas med stark lampa. Om misstanke om malignt melanom uppstår opereras förändringen bort och undersöks i mikroskop. Därefter ställs diagnos. Om melanomet växer på bredden och är väldigt tunt är risken för spridning till andra delar av kroppen minimal och avlägsnande av förändringen anses vara botande. Växer det däremot vertikalt, ner i underhuden, kan tumörcellerna få kontakt med blod- och lymfkärlssystemen och på så sätt sprida sig och bilda metastaser i andra organ. Om en patient bedöms ha metastaser görs en helkroppsundersökning. En sådan undersökning inkluderar oftast datortomografi eller motsvarande röntgen och provtagning för att lokalisera och bekräfta utbredningen av metastaserna.

År 2011 godkändes immunterapi och målinriktad terapi för behandling av malignt melanom. Det var en vändpunkt i behandlingsväg för patienter med metastaser. Immunterapi med så kallade PD1-hämmare är oftast förstahandsalternativ vid spridd sjukdom. PD1-hämmare kan också kombineras med en annan typ av läkemedel med immunmodulerande effekt (CTLA4) för att ytterligare förbättra behandlingsresultaten. Dessa läkemedel fungerar genom att aktivera en viss typ av

vita blodkroppar så att de angriper tumörcellerna. Medianöverlevnaden för melanompatienter med spridd sjukdom har förbättrats avsevärt sedan införandet av immunterapi, från cirka 9 månader till nyligen rapporterade 72 månader, det vill säga 6 år i en lång studie där en kombination av PD1 och CTLA4 användes.

Ungefär hälften av alla melanomtumörer har en förvärvad BRAF-mutation vilket gör att BRAF-proteinet signalerar kontinuerligt och det leder till att cellerna delar sig okontrollerat. Det finns målinriktad behandling mot det muterade BRAF-proteinet (så kallade BRAF-hämmare) och därför utförs alltid en genetisk analys för att fastställa mutation inför eventuell systemisk behandling. Alla patienter med BRAF-genmutationer uttrycker inte samma mängd av det muterade proteinet i tumörcellerna och eftersom måltavlorna som de flesta läkemedlen riktar sig mot är proteiner så är det särskilt intressant att studera uttrycket av proteiner i tumörceller och den omkringliggande vävnaden, tumörmikromiljön.

I takt med att allt fler läkemedel introduceras för behandling av melanom, och med hänsyn till de biverkningar som ofta uppstår och den betydande samhällskostnad som är förenad med varje behandling, är det viktigare än någonsin att få kunskap om vilka faktorer som kan förutsäga hur olika patientgrupper kommer att svara på respektive behandling. I den här avhandlingen undersöks skillnader i tumörcellernas och deras omkringliggande vävnaders proteinuttryck med målet att kunna dela in patienter i grupper och sedan koppla grupperna till prognos och överlevnad. Målet framöver är att använda uttrycket av några specifika proteiner som skiljer sig åt mellan melanompatienter som proteinmarkörer och på ett bättre sätt skräddarsy behandlingsstrategi och förutsäga prognos.

I avhandlingens tre första studier var huvudfokuset metodutveckling. Närmare bestämt syftade artikel ett till att etablera ett arbetsflöde för att möjliggöra provupparbetning av ett stort antal frysta tumörvävnader på ett reproducerbart och effektivt sätt med målet att erhålla tillförlitliga data. Som nästa steg i metodutvecklingen optimerades i artikel två ett arbetsflöde för att studera viktiga proteinmodifieringar anpassat för små vävnadsmängder. För den här typen av analys används normalt stora mängder fryst vävnad, men det kan vara svårt att få fram när man arbetar med kliniska prover från cancerpatienter eftersom det mesta av vävnaden används för diagnostik och endast eventuella rester används för forskningsändamål. I artikel tre undersöktes och bekräftades möjligheten att ersätta frysta vävnader med formalin-fixerade och paraffin inbäddade (FFPE) vävnader i våra experiment. Frysta vävnader är ofta svåra att få tag på och dyra att förvara medan FFPE-vävnader, som används i rutindiagnostik, kan förvaras i rumstemperatur. Dessutom finns det stora arkiv med FFPE-vävnader på flera sjukhus som kan användas för forskningsändamål och som i kombination med klinisk information utgör enorma möjligheter att bedriva preklinisk och klinisk forskning.

I avhandlingens två sista arbeten applicerades de utvecklade protokollen på en grupp av 137 frysta metastaser från patienter med malignt melanom. Tumörproverna insamlades mellan år 1993 och 2012 från patienter som opererats för spridd melanomsjukdom, oftast till lymfkörtlar, där en liten tumörbit frysts ner för att kunna användas i forskningssyfte. Tumörproverna analyserades för att avgöra vilka förändringar i proteinuttryck som förekom i tumörcellerna och den omkringliggande tumörmikromiljön mellan patienter. Resultaten visade att patienterna kunde delas in i fem grupper. Den grupp där tumören uttryckte många proteiner kopplade till immunförsvaret hade den bästa prognosen, medan gruppen med uppreglering av proteiner kopplade till tumörmikromiljön och extracellulärmatrix, en typ av proteinnätverk som omger de flesta cellerna i kroppen, uppvisade sämst prognos.

Närvaro eller frånvaro av en BRAF-genmutation säger inte mycket om en patients prognos, men vad vi kunde konstatera var att om man tittar på det specifika uttrycket av det muterade BRAF-proteinet så kunde vi koppla ett högre uttryck till en sämre överlevnad. Dessutom kunde vi dela in patienter med BRAF mutationer i tre riskgrupper för dödlighet (låg, medium och hög), vilket skulle kunna bidra till att bättre skräddarsy deras behandling. Vår hypotes är att patienter i lågriskgruppen kan tänkas svara bättre på immunterapi jämfört med de andra grupperna.

Att mikromiljön omkring tumören spelar en viktig roll för huruvida patienter svarar på behandling och deras prognos börjar bli mer vedertaget. Studier av tumörmikromiljön börjar få en alltmer framträdande roll i forskningen. I vår studie kunde vi klassificera melanompatienter i grupper baserat på de celltyper och proteiner som uttrycktes i tumörmikromiljön i lymfkörtelvävnad och på så sätt förutse prognos.

Sammantaget ger resultaten i den här avhandlingen en detaljerad beskrivning av malignt melanom ur flera olika aspekter vilket kan generera nya hypoteser och lägga grunden för flera uppföljningsstudier att verifiera våra resultat. De olika proteinprofilerna vi identifierade har betydelse för prognos och även chansen att svara på behandling. Vidare studier krävs för att säkrare kunna avgöra vilka patienter som bör få respektive behandling, hur man ska undvika att resistens uppstår och att hitta nya sätt att göra melanomtumörer mer känsliga för behandling med immunterapi.

Acknowledgements

This thesis is a product of many, and I would like to express my deepest gratitude to everyone who helped me along the way. I have greatly enjoyed this PhD journey, mainly because of all the competent and supportive people around me. I feel privileged to have such amazing co-workers.

First and foremost, I want to thank my supervisors for all the help and endless support during my PhD studies. My main supervisor *Johan Malm*, thank you for always finding the time to support and guide me and convincing me of my independence as a researcher. My co-supervisor *György Marko-Varga*, for believing in me and giving me the opportunity to pursue my career within academia as a PhD student. Thank you for introducing me to melanoma research and transmitting your enthusiasm. My co-supervisor *Melinda Rezeli*, I would not be where I am today without your endless guidance and encouragement. I want to express my deepest gratitude and appreciation to you, and I look forward to continuing the research path together. *Lazaro Betancourt*, my unofficial supervisor, thank you for your constructive criticisms and infinite passion for science. You are remarkably impartial, and your honesty is something I truly cherish.

Throughout my PhD studies, I have relied on the help and support of many people. *Roger*, few people are as kind and easy to talk to as you. *Jeovanis*, thank you for always challenging me and ensuring I stay competitive. *Aniel* & *Indira*, your warmth and kindness are out of the ordinary. You always offer to help both professionally and personally. *Zsolt*, thank you for all the help with my not-always-so-cooperative computer (until you helped me select a better one) and for sharing my sense of humour. *Henriett, Henrik* and *Tilly*, for all the assistance with the biobank and for ensuring that we have high sample quality to pursue top-quality research. Your work is indispensable. *Lotta* and *Elisabet*, your mentorship and numerous discussions over the years have genuinely impacted my thesis. *Leticia*, thank you for your clinical expertise and willingness to always help. *Barbara*, for welcoming me into the "student gang" and for your support during my early encounters with science. *Bea*, thank you for your patience and continued programming support in all my projects.

Yutaka, Jonatan, Kim and *Boram*, for all the work we have done together over the years – you are missed.

I want to give a special shout-out to my roommates *Nicole* and *Natalia* and my new roommate *Jessica*. I could not wish for better PhD-friends. *Nicole*, your generosity and inner calm make me a better person and a much more organised scientist. Your and *Jessica's* creativity taught me the importance of visualising science. Thank you for always supporting me with the most excellent scientific figures. *Natalia*, we are very alike, and your motivation has been a true inspiration.

I would also like to thank my foreign colleagues and collaborators, *Krzysztof, Marcell, Istvan, Peter, Runyu, David* and *Bartek*, for always sharing your knowledge and for everything you taught me throughout the years.

To all my past and present colleagues at BMC D13, thank you for your friendship, valuable input, and exciting discussions in the coffee room.

To the medical doctors, professors and research nurses, *Henrik, Christian, Lotta, Håkan, Bo, Marie* and *Carina*, for your clinical expertise, valuable input and sample collection.

I also want to express my gratitude to my closest friends who have supported me during my PhD studies and throughout my life. *Ida, Malin, Mariel* and *Matilda*, thank you for always having my back and standing by me.

To all my friends and coaches I have had the pleasure of encountering from years of competitive swimming, with who I forever will share beautiful memories. A special thank you to the girls in MSG for being the best training buddies when I needed to take my mind off science.

To my family:
Thank you for your never-ending support and encouragement and for understanding how much this PhD journey means to me. *My parents*, for your unwavering support and unlimited love. Especially my *mother* for all your sacrifices to enable my life goals. My partner *Patrik* and our son *Wilhelm* – you fill my life with love, joy and laughter. Thank you for all the wonderful moments we have shared. Thank you for supporting me at my worst and inspiring me to be my best. My two cats, *Lilly* and *Munchie*, thank you for choosing us as your family.

This work would not have been possible without the support from the Fru Berta Kamprad Foundation, Thermo Fisher Scientific, LiCONiC UK and the Swedish Pharmaceutical Society. I also want to thank the Royal Physiographic Society of Lund for supporting me throughout my PhD studies. This work was carried out with the encouragement of the U.S. National Cancer Institute's International Cancer Proteogenome Consortium.

References

1 Grzywa, T. M., Paskal, W. & Wlodarski, P. K. Intratumor and Intertumor Heterogeneity in Melanoma. *Translational oncology* **10**, 956-975 (2017). https://doi.org:10.1016/j.tranon.2017.09.007

2 Coricovac, D., Dehelean, C., Moaca, E. A., Pinzaru, I., Bratu, T., Navolan, D. & Boruga, O. Cutaneous Melanoma-A Long Road from Experimental Models to Clinical Outcome: A Review. *International journal of molecular sciences* **19** (2018). https://doi.org:10.3390/ijms19061566

3 Naik, P. P. Cutaneous Malignant Melanoma: A Review of Early Diagnosis and Management. *World journal of oncology* **12**, 7-19 (2021). https://doi.org:10.14740/wjon1349

4 Brenner, M. & Hearing, V. J. The protective role of melanin against UV damage in human skin. *Photochemistry and photobiology* **84**, 539-549 (2008). https://doi.org:10.1111/j.1751-1097.2007.00226.x

5 Garbe, C., Amaral, T., Peris, K., Hauschild, A., Arenberger, P., Basset-Seguin, N., . . . Lorigan, P. European consensus-based interdisciplinary guideline for melanoma. Part 1: Diagnostics: Update 2022. *European journal of cancer (Oxford, England : 1990)* **170**, 236-255 (2022). https://doi.org:10.1016/j.ejca.2022.03.008

6 Situm, M., Buljan, M., Kolić, M. & Vučić, M. Melanoma--clinical, dermatoscopical, and histopathological morphological characteristics. *Acta Dermatovenerol Croat* **22**, 1-12 (2014).

7 Duncan, L. M. The classification of cutaneous melanoma. *Hematology/oncology clinics of North America* **23**, 501-513, ix (2009). https://doi.org:10.1016/j.hoc.2009.03.013

8 Pavri, S. N., Clune, J., Ariyan, S. & Narayan, D. Malignant Melanoma: Beyond the Basics. *Plast Reconstr Surg* **138**, 330e-340e (2016). https://doi.org:10.1097/prs.0000000000002367

9 Lopes, J., Rodrigues, C. M. P., Gaspar, M. M. & Reis, C. P. Melanoma Management: From Epidemiology to Treatment and Latest Advances. *Cancers* **14** (2022). https://doi.org:10.3390/cancers14194652

10 Weinstein, D., Leininger, J., Hamby, C. & Safai, B. Diagnostic and prognostic biomarkers in melanoma. *The Journal of clinical and aesthetic dermatology* **7**, 13-24 (2014).

11 Banerjee, S. S. & Harris, M. Morphological and immunophenotypic variations in malignant melanoma. *Histopathology* **36**, 387-402 (2000). https://doi.org:10.1046/j.1365-2559.2000.00894.x

12 Lam, G. T., Prabhakaran, S., Sorvina, A., Martini, C., Ung, B. S., Karageorgos, L., . . . Logan, J. M. Pitfalls in Cutaneous Melanoma Diagnosis and the Need for New Reliable Markers. *Mol Diagn Ther* **27**, 49-60 (2023). https://doi.org:10.1007/s40291-022-00628-9

13 Lallier, T. E. Cell lineage and cell migration in the neural crest. *Annals of the New York Academy of Sciences* **615**, 158-171 (1991). https://doi.org:10.1111/j.1749-6632.1991.tb37758.x

14 Raposo, G. & Marks, M. S. Melanosomes--dark organelles enlighten endosomal membrane transport. *Nature reviews. Molecular cell biology* **8**, 786-797 (2007). https://doi.org:10.1038/nrm2258

15 Kollias, N., Sayre, R. M., Zeise, L. & Chedekel, M. R. Photoprotection by melanin. *Journal of photochemistry and photobiology. B, Biology* **9**, 135-160 (1991). https://doi.org:10.1016/1011-1344(91)80147-a

16 Kippenberger, S., Bernd, A., Bereiter-Hahn, J., Ramirez-Bosca, A. & Kaufmann, R. The mechanism of melanocyte dendrite formation: the impact of differentiating keratinocytes. *Pigment cell research* **11**, 34-37 (1998). https://doi.org:10.1111/j.1600-0749.1998.tb00708.x

17 Miller, A. J. & Mihm, M. C. Melanoma. *New England Journal of Medicine* **355**, 51-65 (2006). https://doi.org:10.1056/NEJMra052166

18 Hida, T., Kamiya, T., Kawakami, A., Ogino, J., Sohma, H., Uhara, H. & Jimbow, K. Elucidation of Melanogenesis Cascade for Identifying Pathophysiology and Therapeutic Approach of Pigmentary Disorders and Melanoma. *International journal of molecular sciences* **21** (2020). https://doi.org:10.3390/ijms21176129

19 Young, A. R., Potten, C. S., Nikaido, O., Parsons, P. G., Boenders, J., Ramsden, J. M. & Chadwick, C. A. Human melanocytes and keratinocytes exposed to UVB or UVA in vivo show comparable levels of thymine dimers. *The Journal of investigative dermatology* **111**, 936-940 (1998). https://doi.org:10.1046/j.1523-1747.1998.00435.x

20 Fadadu, R. P. & Wei, M. L. Ultraviolet A radiation exposure and melanoma: a review. *Melanoma research* **32**, 405-410 (2022). https://doi.org:10.1097/cmr.0000000000000857

21 Adams, J. M., Kelly, P. N., Dakic, A., Carotta, S., Nutt, S. L. & Strasser, A. Role of "cancer stem cells" and cell survival in tumor development and maintenance. *Cold Spring Harb Symp Quant Biol* **73**, 451-459 (2008). https://doi.org:10.1101/sqb.2008.73.004

22 Liu, J., Fukunaga-Kalabis, M., Li, L. & Herlyn, M. Developmental pathways activated in melanocytes and melanoma. *Arch Biochem Biophys* **563**, 13-21 (2014). https://doi.org:10.1016/j.abb.2014.07.023

23 Paluncic, J., Kovacevic, Z., Jansson, P. J., Kalinowski, D., Merlot, A. M., Huang, M. L., . . . Richardson, D. R. Roads to melanoma: Key pathways and emerging players in melanoma progression and oncogenic signaling. *Biochimica et biophysica acta* **1863**, 770-784 (2016). https://doi.org:10.1016/j.bbamcr.2016.01.025

24 Leonardi, G. C., Falzone, L., Salemi, R., Zanghi, A., Spandidos, D. A., McCubrey, J. A., . . . Libra, M. Cutaneous melanoma: From pathogenesis to therapy (Review). *International journal of oncology* **52**, 1071-1080 (2018). https://doi.org:10.3892/ijo.2018.4287

25 Lu, Y., Ek, W. E., Whiteman, D., Vaughan, T. L., Spurdle, A. B., Easton, D. F., . . . Macgregor, S. Most common 'sporadic' cancers have a significant germline genetic component. *Human molecular genetics* **23**, 6112-6118 (2014). https://doi.org:10.1093/hmg/ddu312

26 Read, J., Wadt, K. A. & Hayward, N. K. Melanoma genetics. *Journal of medical genetics* **53**, 1-14 (2016). https://doi.org:10.1136/jmedgenet-2015-103150

27 Soura, E., Eliades, P. J., Shannon, K., Stratigos, A. J. & Tsao, H. Hereditary melanoma: Update on syndromes and management: Genetics of familial atypical multiple mole melanoma syndrome. *Journal of the American Academy of Dermatology* **74**, 395-407; quiz 408-310 (2016). https://doi.org:10.1016/j.jaad.2015.08.038

28 Mukherjee, B., Delancey, J. O., Raskin, L., Everett, J., Jeter, J., Begg, C. B., . . . Gruber, S. B. Risk of non-melanoma cancers in first-degree relatives of CDKN2A mutation carriers. *Journal of the National Cancer Institute* **104**, 953-956 (2012). https://doi.org:10.1093/jnci/djs221

29 Bandarchi, B., Ma, L., Navab, R., Seth, A. & Rasty, G. From melanocyte to metastatic malignant melanoma. *Dermatology research and practice* **2010** (2010). https://doi.org:10.1155/2010/583748

30 Tagliabue, E., Gandini, S., Bellocco, R., Maisonneuve, P., Newton-Bishop, J., Polsky, D., . . . Raimondi, S. MC1R variants as melanoma risk factors independent of at-risk phenotypic characteristics: a pooled analysis from the M-SKIP project. *Cancer management and research* **10**, 1143-1154 (2018). https://doi.org:10.2147/cmar.S155283

31 Fargnoli, M. C., Gandini, S., Peris, K., Maisonneuve, P. & Raimondi, S. MC1R variants increase melanoma risk in families with CDKN2A mutations: a meta-analysis. *European journal of cancer (Oxford, England : 1990)* **46**, 1413-1420 (2010). https://doi.org:10.1016/j.ejca.2010.01.027

32 Cao, J., Wan, L., Hacker, E., Dai, X., Lenna, S., Jimenez-Cervantes, C., . . . Cui, R. MC1R is a potent regulator of PTEN after UV exposure in melanocytes. *Molecular cell* **51**, 409-422 (2013). https://doi.org:10.1016/j.molcel.2013.08.010

33 Shtivelman, E., Davies, M. Q., Hwu, P., Yang, J., Lotem, M., Oren, M., . . . Fisher, D. E. Pathways and therapeutic targets in melanoma. *Oncotarget* **5**, 1701-1752 (2014). https://doi.org:10.18632/oncotarget.1892

34 Courtois-Cox, S., Jones, S. L. & Cichowski, K. Many roads lead to oncogene-induced senescence. *Oncogene* **27**, 2801-2809 (2008). https://doi.org:10.1038/sj.onc.1210950

35 van Tuyn, J., Jaber-Hijazi, F., MacKenzie, D., Cole, J. J., Mann, E., Pawlikowski, J. S., . . . Adams, P. D. Oncogene-Expressing Senescent Melanocytes Up-Regulate MHC Class II, a Candidate Melanoma Suppressor Function. *The Journal of investigative dermatology* **137**, 2197-2207 (2017). https://doi.org:10.1016/j.jid.2017.05.030

36 Bartek, J. & Lukas, J. Cyclin D1 multitasks. *Nature* **474**, 171-172 (2011). https://doi.org:10.1038/474171a

37 Michaloglou, C., Vredeveld, L. C., Soengas, M. S., Denoyelle, C., Kuilman, T., van der Horst, C. M., . . . Peeper, D. S. BRAFE600-associated senescence-like cell cycle arrest of human naevi. *Nature* **436**, 720-724 (2005). https://doi.org:10.1038/nature03890

38 Zuber, J., Tchernitsa, O. I., Hinzmann, B., Schmitz, A. C., Grips, M., Hellriegel, M., . . . Schäfer, R. A genome-wide survey of RAS transformation targets. *Nature genetics* **24**, 144-152 (2000). https://doi.org:10.1038/72799

39 Dhillon, A. S., Hagan, S., Rath, O. & Kolch, W. MAP kinase signalling pathways in cancer. *Oncogene* **26**, 3279-3290 (2007). https://doi.org:10.1038/sj.onc.1210421

40 Guo, W., Wang, H. & Li, C. Signal pathways of melanoma and targeted therapy. *Signal Transduction and Targeted Therapy* **6**, 424 (2021). https://doi.org:10.1038/s41392-021-00827-6

41 Li, F. Z., Dhillon, A. S., Anderson, R. L., McArthur, G. & Ferrao, P. T. Phenotype switching in melanoma: implications for progression and therapy. *Frontiers in oncology* **5**, 31 (2015). https://doi.org:10.3389/fonc.2015.00031

42 Tsoi, J., Robert, L., Paraiso, K., Galvan, C., Sheu, K. M., Lay, J., . . . Graeber, T. G. Multi-stage Differentiation Defines Melanoma Subtypes with Differential Vulnerability to Drug-Induced Iron-Dependent Oxidative Stress. *Cancer Cell* **33**, 890-904.e895 (2018). https://doi.org:10.1016/j.ccell.2018.03.017

43 Garraway, L. A., Widlund, H. R., Rubin, M. A., Getz, G., Berger, A. J., Ramaswamy, S., . . . Sellers, W. R. Integrative genomic analyses identify MITF as a lineage survival oncogene amplified in malignant melanoma. *Nature* **436**, 117-122 (2005). https://doi.org:10.1038/nature03664

44 Campbell, P. M. & Der, C. J. Oncogenic Ras and its role in tumor cell invasion and metastasis. *Seminars in cancer biology* **14**, 105-114 (2004). https://doi.org:10.1016/j.semcancer.2003.09.015

45 Burotto, M., Chiou, V. L., Lee, J. M. & Kohn, E. C. The MAPK pathway across different malignancies: a new perspective. *Cancer* **120**, 3446-3456 (2014). https://doi.org:10.1002/cncr.28864

46 De Luca, A., Maiello, M. R., D'Alessio, A., Pergameno, M. & Normanno, N. The RAS/RAF/MEK/ERK and the PI3K/AKT signalling pathways: role in cancer pathogenesis and implications for therapeutic approaches. *Expert Opin Ther Targets* **16 Suppl 2**, S17-27 (2012). https://doi.org:10.1517/14728222.2011.639361

47 Randic, T., Kozar, I., Margue, C., Utikal, J. & Kreis, S. NRAS mutant melanoma: Towards better therapies. *Cancer Treat Rev* **99**, 102238 (2021). https://doi.org:10.1016/j.ctrv.2021.102238

48 Cheung, M., Sharma, A., Madhunapantula, S. V. & Robertson, G. P. Akt3 and mutant V600E B-Raf cooperate to promote early melanoma development. *Cancer research* **68**, 3429-3439 (2008). https://doi.org:10.1158/0008-5472.Can-07-5867

49 Dankort, D., Curley, D. P., Cartlidge, R. A., Nelson, B., Karnezis, A. N., Damsky, W. E., Jr., . . . Bosenberg, M. Braf(V600E) cooperates with Pten loss to induce metastatic melanoma. *Nature genetics* **41**, 544-552 (2009). https://doi.org:10.1038/ng.356

50 Vredeveld, L. C., Possik, P. A., Smit, M. A., Meissl, K., Michaloglou, C., Horlings, H. M., . . . Peeper, D. S. Abrogation of BRAFV600E-induced senescence by PI3K pathway activation contributes to melanomagenesis. *Genes Dev* **26**, 1055-1069 (2012). https://doi.org:10.1101/gad.187252.112

51 Delmas, V., Beermann, F., Martinozzi, S., Carreira, S., Ackermann, J., Kumasaka, M., . . . Larue, L. Beta-catenin induces immortalization of melanocytes by suppressing p16INK4a expression and cooperates with N-Ras in melanoma development. *Genes Dev* **21**, 2923-2935 (2007). https://doi.org:10.1101/gad.450107

52 Cai, J., Guan, H., Fang, L., Yang, Y., Zhu, X., Yuan, J., . . . Li, M. MicroRNA-374a activates Wnt/β-catenin signaling to promote breast cancer metastasis. *The Journal of clinical investigation* **123**, 566-579 (2013). https://doi.org:10.1172/jci65871

53 Pham, D. D. M., Guhan, S. & Tsao, H. KIT and Melanoma: Biological Insights and Clinical Implications. *Yonsei medical journal* **61**, 562-571 (2020). https://doi.org:10.3349/ymj.2020.61.7.562

54 Hodis, E., Watson, I. R., Kryukov, G. V., Arold, S. T., Imielinski, M., Theurillat, J. P., . . . Chin, L. A landscape of driver mutations in melanoma. *Cell* **150**, 251-263 (2012). https://doi.org:10.1016/j.cell.2012.06.024

55 Horn, S., Figl, A., Rachakonda, P. S., Fischer, C., Sucker, A., Gast, A., . . . Kumar, R. TERT promoter mutations in familial and sporadic melanoma. *Science* **339**, 959-961 (2013). https://doi.org:10.1126/science.1230062

56 Yuan, Y., Jiang, Y. C., Sun, C. K. & Chen, Q. M. Role of the tumor microenvironment in tumor progression and the clinical applications (Review). *Oncology reports* **35**, 2499-2515 (2016). https://doi.org:10.3892/or.2016.4660

57 Kimm, M. A., Klenk, C., Alunni-Fabbroni, M., Kästle, S., Stechele, M., Ricke, J., . . . Wildgruber, M. Tumor-Associated Macrophages-Implications for Molecular Oncology and Imaging. *Biomedicines* **9** (2021). https://doi.org:10.3390/biomedicines9040374

58 van Pelt, G. W., Sandberg, T. P., Morreau, H., Gelderblom, H., van Krieken, J., Tollenaar, R. & Mesker, W. E. The tumour-stroma ratio in colon cancer: the biological role and its prognostic impact. *Histopathology* **73**, 197-206 (2018). https://doi.org:10.1111/his.13489

59 Neagu, M. Metabolic Traits in Cutaneous Melanoma. *Frontiers in oncology* **10**, 851 (2020). https://doi.org:10.3389/fonc.2020.00851

60 Trotta, A. P., Gelles, J. D., Serasinghe, M. N., Loi, P., Arbiser, J. L. & Chipuk, J. E. Disruption of mitochondrial electron transport chain function potentiates the pro-apoptotic effects of MAPK inhibition. *The Journal of biological chemistry* **292**, 11727-11739 (2017). https://doi.org:10.1074/jbc.M117.786442

61 Hanahan, D. & Weinberg, R. A. Hallmarks of cancer: the next generation. *Cell* **144**, 646-674 (2011). https://doi.org:10.1016/j.cell.2011.02.013

62 Danhier, P., Bański, P., Payen, V. L., Grasso, D., Ippolito, L., Sonveaux, P. & Porporato, P. E. Cancer metabolism in space and time: Beyond the Warburg effect. *Biochim Biophys Acta Bioenerg* **1858**, 556-572 (2017). https://doi.org:10.1016/j.bbabio.2017.02.001

63 Porporato, P. E., Filigheddu, N., Pedro, J. M. B., Kroemer, G. & Galluzzi, L. Mitochondrial metabolism and cancer. *Cell Res* **28**, 265-280 (2018). https://doi.org:10.1038/cr.2017.155

64 Roberts, E. R. & Thomas, K. J. The role of mitochondria in the development and progression of lung cancer. *Comput Struct Biotechnol J* **6**, e201303019 (2013). https://doi.org:10.5936/csbj.201303019

65 Ping, Q., Yan, R., Cheng, X., Wang, W., Zhong, Y., Hou, Z., . . . Li, R. Cancer-associated fibroblasts: overview, progress, challenges, and directions. *Cancer Gene Therapy* **28**, 984-999 (2021). https://doi.org:10.1038/s41417-021-00318-4

66 Tirosh, I., Izar, B., Prakadan, S. M., Wadsworth, M. H., 2nd, Treacy, D., Trombetta, J. J., . . . Garraway, L. A. Dissecting the multicellular ecosystem of metastatic melanoma by single-cell RNA-seq. *Science* **352**, 189-196 (2016). https://doi.org:10.1126/science.aad0501

67 Venning, F. A., Wullkopf, L. & Erler, J. T. Targeting ECM Disrupts Cancer Progression. *Frontiers in oncology* **5**, 224 (2015). https://doi.org:10.3389/fonc.2015.00224

68 Martinez-Vidal, L., Murdica, V., Venegoni, C., Pederzoli, F., Bandini, M., Necchi, A., . . . Alfano, M. Causal contributors to tissue stiffness and clinical relevance in urology. *Commun Biol* **4**, 1011 (2021). https://doi.org:10.1038/s42003-021-02539-7

69 Mesker, W. E., van Pelt, G. W. & Tollenaar, R. Tumor stroma as contributing factor in the lymph node metastases process? *Oncotarget* **10**, 922-923 (2019). https://doi.org:10.18632/oncotarget.26644

70 van Pelt, G. W., Kjær-Frifeldt, S., van Krieken, J., Al Dieri, R., Morreau, H., Tollenaar, R., . . . Mesker, W. E. Scoring the tumor-stroma ratio in colon cancer: procedure and recommendations. *Virchows Archiv : an international journal of pathology* **473**, 405-412 (2018). https://doi.org:10.1007/s00428-018-2408-z

71 Denko, N. C. Hypoxia, HIF1 and glucose metabolism in the solid tumour. *Nature reviews. Cancer* **8**, 705-713 (2008). https://doi.org:10.1038/nrc2468

72 Pedri, D., Karras, P., Landeloos, E., Marine, J. C. & Rambow, F. Epithelial-to-mesenchymal-like transition events in melanoma. *The FEBS journal* **289**, 1352-1368 (2022). https://doi.org:10.1111/febs.16021

73 Hoek, K. S. & Goding, C. R. Cancer stem cells versus phenotype-switching in melanoma. *Pigment cell & melanoma research* **23**, 746-759 (2010). https://doi.org:10.1111/j.1755-148X.2010.00757.x

74 Rambow, F., Marine, J. C. & Goding, C. R. Melanoma plasticity and phenotypic diversity: therapeutic barriers and opportunities. *Genes Dev* **33**, 1295-1318 (2019). https://doi.org:10.1101/gad.329771.119

75 Verfaillie, A., Imrichova, H., Atak, Z. K., Dewaele, M., Rambow, F., Hulselmans, G., . . . Aerts, S. Decoding the regulatory landscape of melanoma reveals TEADS as regulators of the invasive cell state. *Nature communications* **6**, 6683 (2015). https://doi.org:10.1038/ncomms7683

76 Mort, R. L., Jackson, I. J. & Patton, E. E. The melanocyte lineage in development and disease. *Development* **142**, 1387 (2015). https://doi.org:10.1242/dev.123729

77 Hoek, K., Rimm, D. L., Williams, K. R., Zhao, H., Ariyan, S., Lin, A., . . . Halaban, R. Expression profiling reveals novel pathways in the transformation of melanocytes to melanomas. *Cancer research* **64**, 5270-5282 (2004). https://doi.org:10.1158/0008-5472.Can-04-0731

78 Pearlman, R. L., Montes de Oca, M. K., Pal, H. C. & Afaq, F. Potential therapeutic targets of epithelial-mesenchymal transition in melanoma. *Cancer Lett* **391**, 125-140 (2017). https://doi.org:10.1016/j.canlet.2017.01.029

79 Hodorogea, A., Calinescu, A., Antohe, M., Balaban, M., Nedelcu, R. I., Turcu, G., . . . Brinzea, A. Epithelial-Mesenchymal Transition in Skin Cancers: A Review. *Anal Cell Pathol (Amst)* **2019**, 3851576 (2019). https://doi.org:10.1155/2019/3851576

80 Hoek, K. S., Schlegel, N. C., Brafford, P., Sucker, A., Ugurel, S., Kumar, R., . . . Dummer, R. Metastatic potential of melanomas defined by specific gene expression profiles with no BRAF signature. *Pigment cell research* **19**, 290-302 (2006). https://doi.org:10.1111/j.1600-0749.2006.00322.x

81 Rodriguez, M., Aladowicz, E., Lanfrancone, L. & Goding, C. R. Tbx3 represses E-cadherin expression and enhances melanoma invasiveness. *Cancer research* **68**, 7872-7881 (2008). https://doi.org:10.1158/0008-5472.Can-08-0301

82 Carlino, M. S., Larkin, J. & Long, G. V. Immune checkpoint inhibitors in melanoma. *The Lancet* **398**, 1002-1014 (2021). https://doi.org:10.1016/S0140-6736(21)01206-X

83 Kalaora, S., Nagler, A., Wargo, J. A. & Samuels, Y. Mechanisms of immune activation and regulation: lessons from melanoma. *Nature reviews. Cancer* **22**, 195-207 (2022). https://doi.org:10.1038/s41568-022-00442-9

84 Leach, D. R., Krummel, M. F. & Allison, J. P. Enhancement of antitumor immunity by CTLA-4 blockade. *Science* **271**, 1734-1736 (1996). https://doi.org:10.1126/science.271.5256.1734

85 Okazaki, T. & Honjo, T. The PD-1-PD-L pathway in immunological tolerance. *Trends in immunology* **27**, 195-201 (2006). https://doi.org:10.1016/j.it.2006.02.001

86 Marzagalli, M., Ebelt, N. D. & Manuel, E. R. Unraveling the crosstalk between melanoma and immune cells in the tumor microenvironment. *Seminars in cancer biology* **59**, 236-250 (2019). https://doi.org:10.1016/j.semcancer.2019.08.002

87 Vesely, M. D., Kershaw, M. H., Schreiber, R. D. & Smyth, M. J. Natural innate and adaptive immunity to cancer. *Annu Rev Immunol* **29**, 235-271 (2011). https://doi.org:10.1146/annurev-immunol-031210-101324

88 Lee, N., Zakka, L. R., Mihm, M. C., Jr. & Schatton, T. Tumour-infiltrating lymphocytes in melanoma prognosis and cancer immunotherapy. *Pathology* **48**, 177-187 (2016). https://doi.org:10.1016/j.pathol.2015.12.006

89 Ohue, Y. & Nishikawa, H. Regulatory T (Treg) cells in cancer: Can Treg cells be a new therapeutic target? *Cancer science* **110**, 2080-2089 (2019). https://doi.org:10.1111/cas.14069

90 Fridman, W. H., Pagès, F., Sautès-Fridman, C. & Galon, J. The immune contexture in human tumours: impact on clinical outcome. *Nature reviews. Cancer* **12**, 298-306 (2012). https://doi.org:10.1038/nrc3245

91 Cabrita, R., Lauss, M., Sanna, A., Donia, M., Skaarup Larsen, M., Mitra, S., . . . Jonsson, G. Tertiary lymphoid structures improve immunotherapy and survival in melanoma. *Nature* **577**, 561-565 (2020). https://doi.org:10.1038/s41586-019-1914-8

92 Garbe, C., Amaral, T., Peris, K., Hauschild, A., Arenberger, P., Basset-Seguin, N., . . . Lorigan, P. European consensus-based interdisciplinary guideline for melanoma. Part 2: Treatment - Update 2022. *European journal of cancer (Oxford, England : 1990)* **170**, 256-284 (2022). https://doi.org:10.1016/j.ejca.2022.04.018

93 Wolchok, J. D., Chiarion-Sileni, V., Gonzalez, R., Grob, J. J., Rutkowski, P., Lao, C. D., . . . Hodi, F. S. Long-Term Outcomes With Nivolumab Plus Ipilimumab or Nivolumab Alone Versus Ipilimumab in Patients With Advanced Melanoma. *Journal of clinical oncology : official journal of the American Society of Clinical Oncology* **40**, 127-137 (2022). https://doi.org:10.1200/jco.21.02229

94 Atkins, M. B., Lee, S. J., Chmielowski, B., Tarhini, A. A., Cohen, G. I., Truong, T.-G., . . . Kirkwood, J. M. Combination Dabrafenib and Trametinib Versus Combination Nivolumab and Ipilimumab for Patients With Advanced BRAF-Mutant Melanoma: The DREAMseq Trial—ECOG-ACRIN EA6134. *Journal of Clinical Oncology* **41**, 186-197 (2023). https://doi.org:10.1200/jco.22.01763

95 Kozar, I., Margue, C., Rothengatter, S., Haan, C. & Kreis, S. Many ways to resistance: How melanoma cells evade targeted therapies. *Biochim Biophys Acta Rev Cancer* **1871**, 313-322 (2019). https://doi.org:10.1016/j.bbcan.2019.02.002

96 Raigani, S., Cohen, S. & Boland, G. M. The Role of Surgery for Melanoma in an Era of Effective Systemic Therapy. *Current oncology reports* **19**, 17 (2017). https://doi.org:10.1007/s11912-017-0575-8

97 Queirolo, P., Boutros, A., Tanda, E., Spagnolo, F. & Quaglino, P. Immune-checkpoint inhibitors for the treatment of metastatic melanoma: a model of cancer immunotherapy. *Seminars in cancer biology* **59**, 290-297 (2019). https://doi.org:10.1016/j.semcancer.2019.08.001

98 Ni, J.-j., Zhang, Z.-z., Ge, M.-j., Chen, J.-y. & Zhuo, W. Immune-based combination therapy to convert immunologically cold tumors into hot tumors: an update and new insights. *Acta Pharmacologica Sinica* (2022). https://doi.org:10.1038/s41401-022-00953-z

99 Lee, K. A. & Nathan, P. Cutaneous Melanoma - A Review of Systemic Therapies. *Acta dermato-venereologica* **100**, adv00141 (2020). https://doi.org:10.2340/00015555-3496

100 Beiu, C., Giurcaneanu, C., Grumezescu, A. M., Holban, A. M., Popa, L. G. & Mihai, M. M. Nanosystems for Improved Targeted Therapies in Melanoma. *J Clin Med* **9** (2020). https://doi.org:10.3390/jcm9020318

101 Zamarin, D., Holmgaard, R. B., Subudhi, S. K., Park, J. S., Mansour, M., Palese, P., . . . Allison, J. P. Localized oncolytic virotherapy overcomes systemic tumor resistance to immune checkpoint blockade immunotherapy. *Sci Transl Med* **6**, 226ra232 (2014). https://doi.org:10.1126/scitranslmed.3008095

102 Ott, P. A., Hu, Z., Keskin, D. B., Shukla, S. A., Sun, J., Bozym, D. J., . . . Wu, C. J. An immunogenic personal neoantigen vaccine for patients with melanoma. *Nature* **547**, 217-221 (2017). https://doi.org:10.1038/nature22991

103 Hong, D. S., Van Tine, B. A., Biswas, S., McAlpine, C., Johnson, M. L., Olszanski, A. J., . . . Butler, M. O. Autologous T cell therapy for MAGE-A4(+) solid cancers in HLA-A*02(+) patients: a phase 1 trial. *Nature medicine* (2023). https://doi.org:10.1038/s41591-022-02128-z

104 Rosenberg, S. A. & Restifo, N. P. Adoptive cell transfer as personalized immunotherapy for human cancer. *Science* **348**, 62-68 (2015). https://doi.org:10.1126/science.aaa4967

105 Rezaei, R., Esmaeili Gouvarchin Ghaleh, H., Farzanehpour, M., Dorostkar, R., Ranjbar, R., Bolandian, M., . . . Ghorbani Alvanegh, A. Combination therapy with CAR T cells and oncolytic viruses: a new era in cancer immunotherapy. *Cancer Gene Therapy* **29**, 647-660 (2022). https://doi.org:10.1038/s41417-021-00359-9

106 Kasakovski, D., Skrygan, M., Gambichler, T. & Susok, L. Advances in Targeting Cutaneous Melanoma. *Cancers* **13** (2021). https://doi.org:10.3390/cancers13092090

107 Das, S. & Johnson, D. B. Immune-related adverse events and anti-tumor efficacy of immune checkpoint inhibitors. *Journal for ImmunoTherapy of Cancer* **7**, 306 (2019). https://doi.org:10.1186/s40425-019-0805-8

108 Jönsson, G., Busch, C., Knappskog, S., Geisler, J., Miletic, H., Ringnér, M., . . . Lønning, P. E. Gene expression profiling-based identification of molecular subtypes in stage IV melanomas with different clinical outcome. *Clinical cancer research : an official journal of the American Association for Cancer Research* **16**, 3356-3367 (2010). https://doi.org:10.1158/1078-0432.Ccr-09-2509

109 Harbst, K., Staaf, J., Lauss, M., Karlsson, A., Måsbäck, A., Johansson, I., . . . Jönsson, G. Molecular profiling reveals low- and high-grade forms of primary melanoma. *Clinical cancer research : an official journal of the American Association for Cancer Research* **18**, 4026-4036 (2012). https://doi.org:10.1158/1078-0432.Ccr-12-0343

110 Cancer Genome Atlas, N. Genomic Classification of Cutaneous Melanoma. *Cell* **161**, 1681-1696 (2015). https://doi.org:10.1016/j.cell.2015.05.044

111 Rambow, F., Rogiers, A., Marin-Bejar, O., Aibar, S., Femel, J., Dewaele, M., . . . Marine, J. C. Toward Minimal Residual Disease-Directed Therapy in Melanoma. *Cell* **174**, 843-855.e819 (2018). https://doi.org:10.1016/j.cell.2018.06.025

112 Konieczkowski, D. J., Johannessen, C. M., Abudayyeh, O., Kim, J. W., Cooper, Z. A., Piris, A., . . . Garraway, L. A. A melanoma cell state distinction influences sensitivity to MAPK pathway inhibitors. *Cancer discovery* **4**, 816-827 (2014). https://doi.org:10.1158/2159-8290.Cd-13-0424

113 Zhang, H., Liu, T., Zhang, Z., Payne, S. H., Zhang, B., McDermott, J. E., . . . Investigators, C. Integrated Proteogenomic Characterization of Human High-Grade Serous Ovarian Cancer. *Cell* **166**, 755-765 (2016). https://doi.org:10.1016/j.cell.2016.05.069

114 Vasaikar, S., Huang, C., Wang, X., Petyuk, V. A., Savage, S. R., Wen, B., . . . Zhang, B. Proteogenomic Analysis of Human Colon Cancer Reveals New Therapeutic Opportunities. *Cell* **177**, 1035-1049.e1019 (2019). https://doi.org:10.1016/j.cell.2019.03.030

115 Gillette, M. A., Satpathy, S., Cao, S., Dhanasekaran, S. M., Vasaikar, S. V., Krug, K., . . . Carr, S. A. Proteogenomic Characterization Reveals Therapeutic Vulnerabilities in Lung Adenocarcinoma. *Cell* **182**, 200-225.e235 (2020). https://doi.org:10.1016/j.cell.2020.06.013

116 Dou, Y., Kawaler, E. A., Cui Zhou, D., Gritsenko, M. A., Huang, C., Blumenberg, L., . . . Clinical Proteomic Tumor Analysis, C. Proteogenomic Characterization of Endometrial Carcinoma. *Cell* **180**, 729-748 e726 (2020). https://doi.org:10.1016/j.cell.2020.01.026

117 Cao, L., Huang, C., Cui Zhou, D., Hu, Y., Lih, T. M., Savage, S. R., . . . Zhang, H. Proteogenomic characterization of pancreatic ductal adenocarcinoma. *Cell* **184**, 5031-5052.e5026 (2021). https://doi.org:10.1016/j.cell.2021.08.023

118 Wilkins, M. R., Sanchez, J. C., Gooley, A. A., Appel, R. D., Humphery-Smith, I., Hochstrasser, D. F. & Williams, K. L. Progress with proteome projects: why all proteins expressed by a genome should be identified and how to do it. *Biotechnol Genet Eng Rev* **13**, 19-50 (1996). https://doi.org:10.1080/02648725.1996.10647923

119 Shah, T. R. & Misra, A. in *Challenges in Delivery of Therapeutic Genomics and Proteomics* (ed Ambikanandan Misra) 387-427 (Elsevier, 2011).

120 Marc R. Wilkins, K. L. W., Ron D. Appel, Denis F. Hochstrasser. *Proteome Research: New Frontiers in Functional Genomics*. Vol. 1 (Springer-Verlag Berlin Heidelberg, 1997).

121 Burnum-Johnson, K. E., Conrads, T. P., Drake, R. R., Herr, A. E., Iyengar, R., Kelly, R. T., . . . Kelleher, N. L. New Views of Old Proteins: Clarifying the Enigmatic Proteome. *Molecular & cellular proteomics : MCP* **21**, 100254 (2022). https://doi.org:10.1016/j.mcpro.2022.100254

122 Blackstock, W. P. & Weir, M. P. Proteomics: quantitative and physical mapping of cellular proteins. *Trends in biotechnology* **17**, 121-127 (1999). https://doi.org:10.1016/s0167-7799(98)01245-1

123 Anderson, N. L. & Anderson, N. G. Proteome and proteomics: new technologies, new concepts, and new words. *Electrophoresis* **19**, 1853-1861 (1998). https://doi.org:10.1002/elps.1150191103

124 Verrills, N. M. Clinical proteomics: present and future prospects. *Clin Biochem Rev* **27**, 99-116 (2006).

125 Paik, Y. K., Kim, H., Lee, E. Y., Kwon, M. S. & Cho, S. Y. Overview and introduction to clinical proteomics. *Methods in molecular biology (Clifton, N.J.)* **428**, 1-31 (2008). https://doi.org:10.1007/978-1-59745-117-8_1

126 Hacohen, N., Fritsch, E. F., Carter, T. A., Lander, E. S. & Wu, C. J. Getting personal with neoantigen-based therapeutic cancer vaccines. *Cancer immunology research* **1**, 11-15 (2013). https://doi.org:10.1158/2326-6066.Cir-13-0022

127 Heemskerk, B., Kvistborg, P. & Schumacher, T. N. The cancer antigenome. *The EMBO journal* **32**, 194-203 (2013). https://doi.org:10.1038/emboj.2012.333

128 Sensi, M. & Anichini, A. Unique tumor antigens: evidence for immune control of genome integrity and immunogenic targets for T cell-mediated patient-specific immunotherapy. *Clinical cancer research : an official journal of the American Association for Cancer Research* **12**, 5023-5032 (2006). https://doi.org:10.1158/1078-0432.Ccr-05-2682

129 Del Giudice, I., Chiaretti, S., Tavolaro, S., De Propris, M. S., Maggio, R., Mancini, F., . . . Foà, R. Spontaneous regression of chronic lymphocytic leukemia: clinical and biologic features of 9 cases. *Blood* **114**, 638-646 (2009). https://doi.org:10.1182/blood-2008-12-196568

130 Rajasagi, M., Shukla, S. A., Fritsch, E. F., Keskin, D. B., DeLuca, D., Carmona, E., . . . Wu, C. J. Systematic identification of personal tumor-specific neoantigens in chronic lymphocytic leukemia. *Blood* **124**, 453-462 (2014). https://doi.org:10.1182/blood-2014-04-567933

131 Olsen, J. V. & Mann, M. Status of large-scale analysis of post-translational modifications by mass spectrometry. *Molecular & cellular proteomics : MCP* **12**, 3444-3452 (2013). https://doi.org:10.1074/mcp.O113.034181

132 Pawson, T. & Scott, J. D. Protein phosphorylation in signaling--50 years and counting. *Trends in biochemical sciences* **30**, 286-290 (2005). https://doi.org:10.1016/j.tibs.2005.04.013

133 Brognard, J. & Hunter, T. Protein kinase signaling networks in cancer. *Current opinion in genetics & development* **21**, 4-11 (2011). https://doi.org:10.1016/j.gde.2010.10.012

134 Harsha, H. C. & Pandey, A. Phosphoproteomics in cancer. *Molecular oncology* **4**, 482-495 (2010). https://doi.org:10.1016/j.molonc.2010.09.004

135 Olsen, J. V., Blagoev, B., Gnad, F., Macek, B., Kumar, C., Mortensen, P. & Mann, M. Global, in vivo, and site-specific phosphorylation dynamics in signaling networks. *Cell* **127**, 635-648 (2006). https://doi.org:10.1016/j.cell.2006.09.026

136 Ashton, A. W., Dhanjal, H. K., Rossner, B., Mahmood, H., Patel, V. I., Nadim, M., . . . Pestell, R. G. Acetylation of nuclear receptors in health and disease: an update. *The FEBS journal* (2022). https://doi.org:10.1111/febs.16695

137 Li, X., Liu, L., Yang, S., Song, N., Zhou, X., Gao, J., . . . Shi, L. Histone demethylase KDM5B is a key regulator of genome stability. *Proceedings of the National Academy of Sciences of the United States of America* **111**, 7096-7101 (2014). https://doi.org:10.1073/pnas.1324036111

138 Choudhary, C., Kumar, C., Gnad, F., Nielsen, M. L., Rehman, M., Walther, T. C., . . . Mann, M. Lysine acetylation targets protein complexes and co-regulates major cellular functions. *Science* **325**, 834-840 (2009). https://doi.org:10.1126/science.1175371

139 Gil, J., Ramirez-Torres, A. & Encarnacion-Guevara, S. Lysine acetylation and cancer: A proteomics perspective. *J Proteomics* **150**, 297-309 (2017). https://doi.org:10.1016/j.jprot.2016.10.003

140 Eckschlager, T., Plch, J., Stiborova, M. & Hrabeta, J. Histone Deacetylase Inhibitors as Anticancer Drugs. *International journal of molecular sciences* **18** (2017). https://doi.org:10.3390/ijms18071414

141 Aebersold, R. & Mann, M. Mass spectrometry-based proteomics. *Nature* **422**, 198-207 (2003). https://doi.org:10.1038/nature01511

142 Steen, H. & Mann, M. The ABC's (and XYZ's) of peptide sequencing. *Nature reviews. Molecular cell biology* **5**, 699-711 (2004). https://doi.org:10.1038/nrm1468

143 Zubarev, R. A. The challenge of the proteome dynamic range and its implications for in-depth proteomics. *Proteomics* **13**, 723-726 (2013). https://doi.org:10.1002/pmic.201200451

144 Craven, R. A., Cairns, D. A., Zougman, A., Harnden, P., Selby, P. J. & Banks, R. E. Proteomic analysis of formalin-fixed paraffin-embedded renal tissue samples by label-free MS: assessment of overall technical variability and the impact of block age. *Proteomics. Clinical applications* **7**, 273-282 (2013). https://doi.org:10.1002/prca.201200065

145 Piehowski, P. D., Petyuk, V. A., Sontag, R. L., Gritsenko, M. A., Weitz, K. K., Fillmore, T. L., . . . Rodland, K. D. Residual tissue repositories as a resource for population-based cancer proteomic studies. *Clinical proteomics* **15**, 26 (2018). https://doi.org:10.1186/s12014-018-9202-4

146 Coscia, F., Doll, S., Bech, J. M., Schweizer, L., Mund, A., Lengyel, E., . . . Mann, M. A streamlined mass spectrometry-based proteomics workflow for large-scale FFPE tissue analysis. *The Journal of pathology* **251**, 100-112 (2020). https://doi.org:10.1002/path.5420

147 Dapic, I., Uwugiaren, N., Jansen, P. J. & Corthals, G. L. Fast and Simple Protocols for Mass Spectrometry-Based Proteomics of Small Fresh Frozen Uterine Tissue Sections. *Analytical chemistry* **89**, 10769-10775 (2017). https://doi.org:10.1021/acs.analchem.7b01937

148 Friedrich, C., Schallenberg, S., Kirchner, M., Ziehm, M., Niquet, S., Haji, M., . . . Mertins, P. Comprehensive micro-scaled proteome and phosphoproteome characterization of archived retrospective cancer repositories. *Nature communications* **12**, 3576 (2021). https://doi.org:10.1038/s41467-021-23855-w

149 Wisniewski, J. R. Proteomic sample preparation from formalin fixed and paraffin embedded tissue. *Journal of visualized experiments : JoVE* (2013). https://doi.org:10.3791/50589

150 Kandyala, R., Raghavendra, S. P. & Rajasekharan, S. T. Xylene: An overview of its health hazards and preventive measures. *Journal of oral and maxillofacial pathology : JOMFP* **14**, 1-5 (2010). https://doi.org:10.4103/0973-029X.64299

151 Hu, D., Ansari, D., Pawlowski, K., Zhou, Q., Sasor, A., Welinder, C., . . . Andersson, R. Proteomic analyses identify prognostic biomarkers for pancreatic ductal adenocarcinoma. *Oncotarget* **9**, 9789-9807 (2018). https://doi.org:10.18632/oncotarget.23929

152 Danenberg, E., Bardwell, H., Zanotelli, V. R. T., Provenzano, E., Chin, S. F., Rueda, O. M., . . . Ali, H. R. Breast tumor microenvironment structures are associated with genomic features and clinical outcome. *Nature genetics* **54**, 660-669 (2022). https://doi.org:10.1038/s41588-022-01041-y

153 Alfonso-Garrido, J., Garcia-Calvo, E. & Luque-Garcia, J. L. Sample preparation strategies for improving the identification of membrane proteins by mass spectrometry. *Analytical and bioanalytical chemistry* **407**, 4893-4905 (2015). https://doi.org:10.1007/s00216-015-8732-0

154 Marchione, D. M., Ilieva, I., Devins, K., Sharpe, D., Pappin, D. J., Garcia, B. A., . . . Wojcik, J. B. HYPERsol: High-Quality Data from Archival FFPE Tissue for Clinical Proteomics. *Journal of proteome research* **19**, 973-983 (2020). https://doi.org:10.1021/acs.jproteome.9b00686

155 Stepanova, E., Gygi, S. P. & Paulo, J. A. Filter-Based Protein Digestion (FPD): A Detergent-Free and Scaffold-Based Strategy for TMT Workflows. *Journal of proteome research* **17**, 1227-1234 (2018). https://doi.org:10.1021/acs.jproteome.7b00840

156 Giansanti, P., Tsiatsiani, L., Low, T. Y. & Heck, A. J. Six alternative proteases for mass spectrometry-based proteomics beyond trypsin. *Nature protocols* **11**, 993-1006 (2016). https://doi.org:10.1038/nprot.2016.057

157 Yang, F., Shen, Y., Camp, D. G., 2nd & Smith, R. D. High-pH reversed-phase chromatography with fraction concatenation for 2D proteomic analysis. *Expert review of proteomics* **9**, 129-134 (2012). https://doi.org:10.1586/epr.12.15

158 Gilar, M., Olivova, P., Daly, A. E. & Gebler, J. C. Orthogonality of separation in two-dimensional liquid chromatography. *Analytical chemistry* **77**, 6426-6434 (2005). https://doi.org:10.1021/ac050923i

159 Pinkse, M. W., Mohammed, S., Gouw, J. W., van Breukelen, B., Vos, H. R. & Heck, A. J. Highly robust, automated, and sensitive online TiO2-based phosphoproteomics applied to study endogenous phosphorylation in Drosophila melanogaster. *Journal of proteome research* **7**, 687-697 (2008). https://doi.org:10.1021/pr700605z

160 Karpievitch, Y. V., Dabney, A. R. & Smith, R. D. Normalization and missing value imputation for label-free LC-MS analysis. *BMC Bioinformatics* **13**, S5 (2012). https://doi.org:10.1186/1471-2105-13-S16-S5

161 Tyanova, S., Temu, T. & Cox, J. The MaxQuant computational platform for mass spectrometry-based shotgun proteomics. *Nature protocols* **11**, 2301-2319 (2016). https://doi.org:10.1038/nprot.2016.136

162 Wang, X., Shen, S., Rasam, S. S. & Qu, J. MS1 ion current-based quantitative proteomics: A promising solution for reliable analysis of large biological cohorts. *Mass spectrometry reviews* **38**, 461-482 (2019). https://doi.org:10.1002/mas.21595

163 Zubarev, R. A. & Makarov, A. Orbitrap mass spectrometry. *Analytical chemistry* **85**, 5288-5296 (2013). https://doi.org:10.1021/ac4001223

164 Aebersold, R. & Mann, M. Mass-spectrometric exploration of proteome structure and function. *Nature* **537**, 347-355 (2016). https://doi.org:10.1038/nature19949

165 Kelstrup, C. D., Aizikov, K., Batth, T. S., Kreutzman, A., Grinfeld, D., Lange, O., . . . Olsen, J. V. Limits for Resolving Isobaric Tandem Mass Tag Reporter Ions Using Phase-Constrained Spectrum Deconvolution. *Journal of proteome research* **17**, 4008-4016 (2018). https://doi.org:10.1021/acs.jproteome.8b00381

166 Zecha, J., Satpathy, S., Kanashova, T., Avanessian, S. C., Kane, M. H., Clauser, K. R., . . . Kuster, B. TMT Labeling for the Masses: A Robust and Cost-efficient, In-solution Labeling Approach. *Molecular & cellular proteomics : MCP* **18**, 1468-1478 (2019). https://doi.org:10.1074/mcp.TIR119.001385

167 Zecha, J., Meng, C., Zolg, D. P., Samaras, P., Wilhelm, M. & Kuster, B. Peptide Level Turnover Measurements Enable the Study of Proteoform Dynamics. *Molecular & cellular proteomics : MCP* **17**, 974-992 (2018). https://doi.org:10.1074/mcp.RA118.000583

168 Ross, P. L., Huang, Y. N., Marchese, J. N., Williamson, B., Parker, K., Hattan, S., . . . Pappin, D. J. Multiplexed protein quantitation in Saccharomyces cerevisiae using amine-reactive isobaric tagging reagents. *Molecular & cellular proteomics : MCP* **3**, 1154-1169 (2004). https://doi.org:10.1074/mcp.M400129-MCP200

169 Ong, S. E., Blagoev, B., Kratchmarova, I., Kristensen, D. B., Steen, H., Pandey, A. & Mann, M. Stable isotope labeling by amino acids in cell culture, SILAC, as a simple and accurate approach to expression proteomics. *Molecular & cellular proteomics : MCP* **1**, 376-386 (2002). https://doi.org:10.1074/mcp.m200025-mcp200

170 Tabb, D. L. The SEQUEST family tree. *Journal of the American Society for Mass Spectrometry* **26**, 1814-1819 (2015). https://doi.org:10.1007/s13361-015-1201-3

171 Cox, J., Neuhauser, N., Michalski, A., Scheltema, R. A., Olsen, J. V. & Mann, M. Andromeda: a peptide search engine integrated into the MaxQuant environment. *Journal of proteome research* **10**, 1794-1805 (2011). https://doi.org:10.1021/pr101065j

172 Martinez-Val, A., Bekker-Jensen, D. B., Hogrebe, A. & Olsen, J. V. Data Processing and Analysis for DIA-Based Phosphoproteomics Using Spectronaut. *Methods in molecular biology (Clifton, N.J.)* **2361**, 95-107 (2021). https://doi.org:10.1007/978-1-0716-1641-3_6

173 Yang, Y., Liu, X., Shen, C., Lin, Y., Yang, P. & Qiao, L. In silico spectral libraries by deep learning facilitate data-independent acquisition proteomics. *Nature communications* **11**, 146 (2020). https://doi.org:10.1038/s41467-019-13866-z

174 Sinitcyn, P., Hamzeiy, H., Salinas Soto, F., Itzhak, D., McCarthy, F., Wichmann, C., . . . Cox, J. MaxDIA enables library-based and library-free data-independent acquisition proteomics. *Nat Biotechnol* **39**, 1563-1573 (2021). https://doi.org:10.1038/s41587-021-00968-7

175 Demichev, V., Messner, C. B., Vernardis, S. I., Lilley, K. S. & Ralser, M. DIA-NN: neural networks and interference correction enable deep proteome coverage in high throughput. *Nature methods* **17**, 41-44 (2020). https://doi.org:10.1038/s41592-019-0638-x

176 Steger, M., Demichev, V., Backman, M., Ohmayer, U., Ihmor, P., Muller, S., . . . Daub, H. Time-resolved in vivo ubiquitinome profiling by DIA-MS reveals USP7 targets on a proteome-wide scale. *Nature communications* **12**, 5399 (2021). https://doi.org:10.1038/s41467-021-25454-1

177 Elias, J. E. & Gygi, S. P. Target-decoy search strategy for increased confidence in large-scale protein identifications by mass spectrometry. *Nature methods* **4**, 207-214 (2007). https://doi.org:10.1038/nmeth1019

178 Gupta, N., Bandeira, N., Keich, U. & Pevzner, P. A. Target-decoy approach and false discovery rate: when things may go wrong. *Journal of the American Society for Mass Spectrometry* **22**, 1111-1120 (2011). https://doi.org:10.1007/s13361-011-0139-3

179 Kim, S. & Pevzner, P. A. MS-GF+ makes progress towards a universal database search tool for proteomics. *Nature communications* **5**, 5277 (2014). https://doi.org:10.1038/ncomms6277

180 Lualdi, M. & Fasano, M. Statistical analysis of proteomics data: A review on feature selection. *J Proteomics* **198**, 18-26 (2019). https://doi.org:10.1016/j.jprot.2018.12.004

181 Lualdi, M. & Fasano, M. Features Selection and Extraction in Statistical Analysis of Proteomics Datasets. *Methods in molecular biology (Clifton, N.J.)* **2361**, 143-159 (2021). https://doi.org:10.1007/978-1-0716-1641-3_9

182 Kaimal, V., Bardes, E. E., Tabar, S. C., Jegga, A. G. & Aronow, B. J. ToppCluster: a multiple gene list feature analyzer for comparative enrichment clustering and network-based dissection of biological systems. *Nucleic acids research* **38**, W96-102 (2010). https://doi.org:10.1093/nar/gkq418

183 Franceschini, A., Szklarczyk, D., Frankild, S., Kuhn, M., Simonovic, M., Roth, A., . . . Jensen, L. J. STRING v9.1: protein-protein interaction networks, with increased coverage and integration. *Nucleic acids research* **41**, D808-815 (2013). https://doi.org:10.1093/nar/gks1094

184 Mi, H., Ebert, D., Muruganujan, A., Mills, C., Albou, L. P., Mushayamaha, T. & Thomas, P. D. PANTHER version 16: a revised family classification, tree-based classification tool, enhancer regions and extensive API. *Nucleic acids research* **49**, D394-d403 (2021). https://doi.org:10.1093/nar/gkaa1106

185 Huang, D. W., Sherman, B. T., Tan, Q., Collins, J. R., Alvord, W. G., Roayaei, J., . . . Lempicki, R. A. The DAVID Gene Functional Classification Tool: a novel biological module-centric algorithm to functionally analyze large gene lists. *Genome biology* **8**, R183 (2007). https://doi.org:10.1186/gb-2007-8-9-r183

186 Kanehisa, M., Furumichi, M., Sato, Y., Kawashima, M. & Ishiguro-Watanabe, M. KEGG for taxonomy-based analysis of pathways and genomes. *Nucleic acids research* (2022). https://doi.org:10.1093/nar/gkac963

187 Mi, H., Muruganujan, A., Ebert, D., Huang, X. & Thomas, P. D. PANTHER version 14: more genomes, a new PANTHER GO-slim and improvements in enrichment analysis tools. *Nucleic acids research* **47**, D419-d426 (2019). https://doi.org:10.1093/nar/gky1038

188 Gillespie, M., Jassal, B., Stephan, R., Milacic, M., Rothfels, K., Senff-Ribeiro, A., . . . D'Eustachio, P. The reactome pathway knowledgebase 2022. *Nucleic acids research* **50**, D687-d692 (2022). https://doi.org:10.1093/nar/gkab1028

189 Liberzon, A., Birger, C., Thorvaldsdóttir, H., Ghandi, M., Mesirov, J. P. & Tamayo, P. The Molecular Signatures Database (MSigDB) hallmark gene set collection. *Cell systems* **1**, 417-425 (2015). https://doi.org:10.1016/j.cels.2015.12.004

190 Welinder, C., Pawlowski, K., Szasz, A. M., Yakovleva, M., Sugihara, Y., Malm, J., . . . Marko-Varga, G. Correlation of histopathologic characteristics to protein expression and function in malignant melanoma. *PLoS One* **12**, e0176167 (2017). https://doi.org:10.1371/journal.pone.0176167

191 Feldman, A. T. & Wolfe, D. Tissue processing and hematoxylin and eosin staining. *Methods in molecular biology (Clifton, N.J.)* **1180**, 31-43 (2014). https://doi.org:10.1007/978-1-4939-1050-2_3

192 Wick, M. R. The hematoxylin and eosin stain in anatomic pathology-An often-neglected focus of quality assurance in the laboratory. *Semin Diagn Pathol* **36**, 303-311 (2019). https://doi.org:10.1053/j.semdp.2019.06.003

193 Zhu, Y., Orre, L. M., Johansson, H. J., Huss, M., Boekel, J., Vesterlund, M., . . . Lehtiö, J. Discovery of coding regions in the human genome by integrated proteogenomics analysis workflow. *Nature communications* **9**, 903 (2018). https://doi.org:10.1038/s41467-018-03311-y

194 Baeza, J., Dowell, J. A., Smallegan, M. J., Fan, J., Amador-Noguez, D., Khan, Z. & Denu, J. M. Stoichiometry of site-specific lysine acetylation in an entire proteome. *The Journal of biological chemistry* **289**, 21326-21338 (2014). https://doi.org:10.1074/jbc.M114.581843

195 Tyanova, S., Temu, T., Sinitcyn, P., Carlson, A., Hein, M. Y., Geiger, T., . . . Cox, J. The Perseus computational platform for comprehensive analysis of (prote)omics data. *Nature methods* **13**, 731-740 (2016). https://doi.org:10.1038/nmeth.3901

196 Betancourt, L. H., Sanchez, A., Pla, I., Kuras, M., Zhou, Q., Andersson, R. & Marko-Varga, G. Quantitative Assessment of Urea In-Solution Lys-C/Trypsin Digestions Reveals Superior Performance at Room Temperature over Traditional Proteolysis at 37 degrees C. *Journal of proteome research* **17**, 2556-2561 (2018). https://doi.org:10.1021/acs.jproteome.8b00228

197 Tan, C. S. & Bader, G. D. Phosphorylation sites of higher stoichiometry are more conserved. *Nature methods* **9**, 317; author reply 318 (2012). https://doi.org:10.1038/nmeth.1941

198 Zhou, H., Ye, M., Dong, J., Corradini, E., Cristobal, A., Heck, A. J., . . . Mohammed, S. Robust phosphoproteome enrichment using monodisperse microsphere-based immobilized titanium (IV) ion affinity chromatography. *Nature protocols* **8**, 461-480 (2013). https://doi.org:10.1038/nprot.2013.010

199 Post, H., Penning, R., Fitzpatrick, M. A., Garrigues, L. B., Wu, W., MacGillavry, H. D., . . . Altelaar, A. F. Robust, Sensitive, and Automated Phosphopeptide Enrichment Optimized for Low Sample Amounts Applied to Primary Hippocampal Neurons. *Journal of proteome research* **16**, 728-737 (2017). https://doi.org:10.1021/acs.jproteome.6b00753

200 Galan, J. A., Geraghty, K. M., Lavoie, G., Kanshin, E., Tcherkezian, J., Calabrese, V., . . . Roux, P. P. Phosphoproteomic analysis identifies the tumor suppressor PDCD4 as a RSK substrate negatively regulated by 14-3-3. *Proceedings of the National Academy of Sciences of the United States of America* **111**, E2918-2927 (2014). https://doi.org:10.1073/pnas.1405601111

201 Smit, M. A., Maddalo, G., Greig, K., Raaijmakers, L. M., Possik, P. A., van Breukelen, B., . . . Peeper, D. S. ROCK1 is a potential combinatorial drug target for BRAF mutant melanoma. *Molecular systems biology* **10**, 772 (2014). https://doi.org:10.15252/msb.20145450

202 Basken, J., Stuart, S. A., Kavran, A. J., Lee, T., Ebmeier, C. C., Old, W. M. & Ahn, N. G. Specificity of Phosphorylation Responses to Mitogen Activated Protein (MAP) Kinase Pathway Inhibitors in Melanoma Cells. *Molecular & cellular proteomics : MCP* **17**, 550-564 (2018). https://doi.org:10.1074/mcp.RA117.000335

203 Kokkat, T. J., Patel, M. S., McGarvey, D., LiVolsi, V. A. & Baloch, Z. W. Archived formalin-fixed paraffin-embedded (FFPE) blocks: A valuable underexploited resource for extraction of DNA, RNA, and protein. *Biopreservation and biobanking* **11**, 101-106 (2013). https://doi.org:10.1089/bio.2012.0052

204 Gustafsson, O. J., Arentz, G. & Hoffmann, P. Proteomic developments in the analysis of formalin-fixed tissue. *Biochimica et biophysica acta* **1854**, 559-580 (2015). https://doi.org:10.1016/j.bbapap.2014.10.003

205 Mason, J. T. Proteomic analysis of FFPE tissue: barriers to clinical impact. *Expert review of proteomics* **13**, 801-803 (2016). https://doi.org:10.1080/14789450.2016.1221346

206 Ting, L., Rad, R., Gygi, S. P. & Haas, W. MS3 eliminates ratio distortion in isobaric multiplexed quantitative proteomics. *Nature methods* **8**, 937-940 (2011). https://doi.org:10.1038/nmeth.1714

207 Savitski, M. M., Mathieson, T., Zinn, N., Sweetman, G., Doce, C., Becher, I., . . . Bantscheff, M. Measuring and managing ratio compression for accurate iTRAQ/TMT quantification. *Journal of proteome research* **12**, 3586-3598 (2013). https://doi.org:10.1021/pr400098r

208 Gil, J., Ramirez-Torres, A., Chiappe, D., Luna-Penaloza, J., Fernandez-Reyes, F. C., Arcos-Encarnacion, B., . . . Encarnacion-Guevara, S. Lysine acetylation stoichiometry and proteomics analyses reveal pathways regulated by sirtuin 1 in human cells. *The Journal of biological chemistry* **292**, 18129-18144 (2017). https://doi.org:10.1074/jbc.M117.784546

209 Zhang, Y., Muller, M., Xu, B., Yoshida, Y., Horlacher, O., Nikitin, F., . . . Yamamoto, T. Unrestricted modification search reveals lysine methylation as major modification induced by tissue formalin fixation and paraffin embedding. *Proteomics* **15**, 2568-2579 (2015). https://doi.org:10.1002/pmic.201400454

210 Tuveson, D. A., Weber, B. L. & Herlyn, M. BRAF as a potential therapeutic target in melanoma and other malignancies. *Cancer Cell* **4**, 95-98 (2003). https://doi.org:10.1016/S1535-6108(03)00189-2

211 Kiuru, M. & Busam, K. J. The NF1 gene in tumor syndromes and melanoma. *Laboratory investigation; a journal of technical methods and pathology* **97**, 146-157 (2017). https://doi.org:10.1038/labinvest.2016.142

212 Kalbasi, A. & Ribas, A. Tumour-intrinsic resistance to immune checkpoint blockade. *Nat Rev Immunol* **20**, 25-39 (2020). https://doi.org:10.1038/s41577-019-0218-4

213 Jonsson, G., Busch, C., Knappskog, S., Geisler, J., Miletic, H., Ringner, M., . . . Lonning, P. E. Gene expression profiling-based identification of molecular subtypes in stage IV melanomas with different clinical outcome. *Clinical cancer research : an official journal of the American Association for Cancer Research* **16**, 3356-3367 (2010). https://doi.org:10.1158/1078-0432.CCR-09-2509

214 Cirenajwis, H., Ekedahl, H., Lauss, M., Harbst, K., Carneiro, A., Enoksson, J., . . . Jonsson, G. Molecular stratification of metastatic melanoma using gene expression profiling: Prediction of survival outcome and benefit from molecular targeted therapy. *Oncotarget* **6**, 12297-12309 (2015). https://doi.org:10.18632/oncotarget.3655

215 Mollinedo, F. Neutrophil Degranulation, Plasticity, and Cancer Metastasis. *Trends in immunology* **40**, 228-242 (2019). https://doi.org:10.1016/j.it.2019.01.006

216 Ognibene, M., Pagnan, G., Marimpietri, D., Cangelosi, D., Cilli, M., Benedetti, M. C., . . . Pezzolo, A. CHL1 gene acts as a tumor suppressor in human neuroblastoma. *Oncotarget* **9**, 25903-25921 (2018). https://doi.org:10.18632/oncotarget.25403

217 Kobayashi, T., Ogawa, H., Kasahara, M., Shiozawa, Z. & Matsuzawa, T. A single amino acid substitution within the mature sequence of ornithine aminotransferase obstructs mitochondrial entry of the precursor. *Am J Hum Genet* **57**, 284-291 (1995).

218 Maurya, S. R. & Mahalakshmi, R. Mitochondrial VDAC2 and cell homeostasis: highlighting hidden structural features and unique functionalities. *Biol Rev Camb Philos Soc* **92**, 1843-1858 (2017). https://doi.org:10.1111/brv.12311

219 Wu, Z. Z., Wang, S., Yang, Q. C., Wang, X. L., Yang, L. L., Liu, B. & Sun, Z. J. Increased Expression of SHMT2 Is Associated With Poor Prognosis and Advanced Pathological Grade in Oral Squamous Cell Carcinoma. *Frontiers in oncology* **10**, 588530 (2020). https://doi.org:10.3389/fonc.2020.588530

220 Afshar-Kharghan, V. The role of the complement system in cancer. *The Journal of clinical investigation* **127**, 780-789 (2017). https://doi.org:10.1172/jci90962

221 Pio, R., Corrales, L. & Lambris, J. D. The role of complement in tumor growth. *Advances in experimental medicine and biology* **772**, 229-262 (2014). https://doi.org:10.1007/978-1-4614-5915-6_11

222 Rooney, M. S., Shukla, S. A., Wu, C. J., Getz, G. & Hacohen, N. Molecular and genetic properties of tumors associated with local immune cytolytic activity. *Cell* **160**, 48-61 (2015). https://doi.org:10.1016/j.cell.2014.12.033

223 Guo, R., Luo, J., Chang, J., Rekhtman, N., Arcila, M. & Drilon, A. MET-dependent solid tumours - molecular diagnosis and targeted therapy. *Nature reviews. Clinical oncology* **17**, 569-587 (2020). https://doi.org:10.1038/s41571-020-0377-z

224 Kohrman, A. Q. & Matus, D. Q. Divide or Conquer: Cell Cycle Regulation of Invasive Behavior. *Trends Cell Biol* **27**, 12-25 (2017). https://doi.org:10.1016/j.tcb.2016.08.003

225 Wang, S., Tang, L., Lin, J., Shen, Z., Yao, Y., Wang, W., . . . Liu, Y. ABCB5 promotes melanoma metastasis through enhancing NF-κB p65 protein stability. *Biochem Biophys Res Commun* **492**, 18-26 (2017). https://doi.org:10.1016/j.bbrc.2017.08.052

226 Ng, M. F., Simmons, J. L. & Boyle, G. M. Heterogeneity in Melanoma. *Cancers* **14** (2022). https://doi.org:10.3390/cancers14123030

227 Blessing, K., Sanders, D. S. & Grant, J. J. Comparison of immunohistochemical staining of the novel antibody melan-A with S100 protein and HMB-45 in malignant melanoma and melanoma variants. *Histopathology* **32**, 139-146 (1998). https://doi.org:10.1046/j.1365-2559.1998.00312.x

228 Aisner, D. L., Maker, A., Rosenberg, S. A. & Berman, D. M. Loss of S100 antigenicity in metastatic melanoma. *Human pathology* **36**, 1016-1019 (2005). https://doi.org:10.1016/j.humpath.2005.07.010

229 Bresnick, A. R., Weber, D. J. & Zimmer, D. B. S100 proteins in cancer. *Nature reviews. Cancer* **15**, 96-109 (2015). https://doi.org:10.1038/nrc3893

230 Xiong, T. F., Pan, F. Q. & Li, D. Expression and clinical significance of S100 family genes in patients with melanoma. *Melanoma research* **29**, 23-29 (2019). https://doi.org:10.1097/cmr.0000000000000512

231 Åberg, A. M., Bergström, S. H., Thysell, E., Tjon-Kon-Fat, L. A., Nilsson, J. A., Widmark, A., . . . Lundholm, M. High Monocyte Count and Expression of S100A9 and S100A12 in Peripheral Blood Mononuclear Cells Are Associated with Poor Outcome in Patients with Metastatic Prostate Cancer. *Cancers* **13** (2021). https://doi.org:10.3390/cancers13102424

232 Janka, E. A., Várvölgyi, T., Sipos, Z., Soós, A., Hegyi, P., Kiss, S., . . . Emri, G. Predictive Performance of Serum S100B Versus LDH in Melanoma Patients: A Systematic Review and Meta-Analysis. *Frontiers in oncology* **11**, 772165 (2021). https://doi.org:10.3389/fonc.2021.772165

233 Massi, D., Landriscina, M., Piscazzi, A., Cosci, E., Kirov, A., Paglierani, M., . . . Tarantini, F. S100A13 is a new angiogenic marker in human melanoma. *Mod Pathol* **23**, 804-813 (2010). https://doi.org:10.1038/modpathol.2010.54

234 Chen, H., Xu, C., Jin, Q. & Liu, Z. S100 protein family in human cancer. *American journal of cancer research* **4**, 89-115 (2014).

235 Ascierto, P. A., Kirkwood, J. M., Grob, J. J., Simeone, E., Grimaldi, A. M., Maio, M., . . . Mozzillo, N. The role of BRAF V600 mutation in melanoma. *Journal of translational medicine* **10**, 85 (2012). https://doi.org:10.1186/1479-5876-10-85

236 Lopez-Rios, F., Angulo, B., Gomez, B., Mair, D., Martinez, R., Conde, E., . . . de Castro, D. G. Comparison of testing methods for the detection of BRAF V600E mutations in malignant melanoma: pre-approval validation study of the companion diagnostic test for vemurafenib. *PLoS One* **8**, e53733 (2013). https://doi.org:10.1371/journal.pone.0053733

237 Hugdahl, E., Kalvenes, M. B., Puntervoll, H. E., Ladstein, R. G. & Akslen, L. A. BRAF-V600E expression in primary nodular melanoma is associated with aggressive tumour features and reduced survival. *British journal of cancer* **114**, 801-808 (2016). https://doi.org:10.1038/bjc.2016.44

238 Cheng, L., Lopez-Beltran, A., Massari, F., MacLennan, G. T. & Montironi, R. Molecular testing for BRAF mutations to inform melanoma treatment decisions: a move toward precision medicine. *Mod Pathol* **31**, 24-38 (2018). https://doi.org:10.1038/modpathol.2017.104

239 Ilmonen, S., Asko-Seljavaara, S., Kariniemi, A. L., Jeskanen, L., Pyrhönen, S. & Muhonen, T. Prognosis of primary melanoma. *Scand J Surg* **91**, 166-171 (2002). https://doi.org:10.1177/145749690209100206

240 Plym, A., Ullenhag, G. J., Breivald, M., Lambe, M. & Berglund, A. Clinical characteristics, management and survival in young adults diagnosed with malignant melanoma: A population-based cohort study. *Acta oncologica (Stockholm, Sweden)* **53**, 688-696 (2014). https://doi.org:10.3109/0284186x.2013.854928

241 Wei, W., Sun, Z., da Silveira, W. A., Yu, Z., Lawson, A., Hardiman, G., . . . Chung, D. Semi-supervised identification of cancer subgroups using survival outcomes and overlapping grouping information. *Statistical methods in medical research* **28**, 2137-2149 (2019). https://doi.org:10.1177/0962280217752980

242 Katlinskaya, Y. V., Katlinski, K. V., Yu, Q., Ortiz, A., Beiting, D. P., Brice, A., . . . Fuchs, S. Y. Suppression of Type I Interferon Signaling Overcomes Oncogene-Induced Senescence and Mediates Melanoma Development and Progression. *Cell reports* **15**, 171-180 (2016). https://doi.org:10.1016/j.celrep.2016.03.006

243 Raaijmakers, M. I., Widmer, D. S., Narechania, A., Eichhoff, O., Freiberger, S. N., Wenzina, J., . . . Levesque, M. P. Co-existence of BRAF and NRAS driver mutations in the same melanoma cells results in heterogeneity of targeted therapy resistance. *Oncotarget* **7**, 77163-77174 (2016). https://doi.org:10.18632/oncotarget.12848

244 Leon, K. E. & Aird, K. M. Jumonji C Demethylases in Cellular Senescence. *Genes* **10** (2019). https://doi.org:10.3390/genes10010033

245 Ohta, K., Haraguchi, N., Kano, Y., Kagawa, Y., Konno, M., Nishikawa, S., . . . Ishii, H. Depletion of JARID1B induces cellular senescence in human colorectal cancer. *International journal of oncology* **42**, 1212-1218 (2013). https://doi.org:10.3892/ijo.2013.1799

246 Chicas, A., Kapoor, A., Wang, X., Aksoy, O., Evertts, A. G., Zhang, M. Q., . . . Lowe, S. W. H3K4 demethylation by Jarid1a and Jarid1b contributes to retinoblastoma-mediated gene silencing during cellular senescence. *Proceedings of the National Academy of Sciences of the United States of America* **109**, 8971-8976 (2012). https://doi.org:10.1073/pnas.1119836109

247 Bayo, J., Tran, T. A., Wang, L., Peña-Llopis, S., Das, A. K. & Martinez, E. D. Jumonji Inhibitors Overcome Radioresistance in Cancer through Changes in H3K4 Methylation at Double-Strand Breaks. *Cell reports* **25**, 1040-1050.e1045 (2018). https://doi.org:10.1016/j.celrep.2018.09.081

248 Xu, W., Zhou, B., Zhao, X., Zhu, L., Xu, J., Jiang, Z., . . . Jin, H. KDM5B demethylates H3K4 to recruit XRCC1 and promote chemoresistance. *International journal of biological sciences* **14**, 1122-1132 (2018). https://doi.org:10.7150/ijbs.25881

249 Gresko, E., Ritterhoff, S., Sevilla-Perez, J., Roscic, A., Fröbius, K., Kotevic, I., . . . Schmitz, M. L. PML tumor suppressor is regulated by HIPK2-mediated phosphorylation in response to DNA damage. *Oncogene* **28**, 698-708 (2009). https://doi.org:10.1038/onc.2008.420

250 Huang, P. J., Lee, C. C., Tan, B. C., Yeh, Y. M., Julie Chu, L., Chen, T. W., . . . Tang, P. CMPD: cancer mutant proteome database. *Nucleic acids research* **43**, D849-855 (2015). https://doi.org:10.1093/nar/gku1182

251 Izzi, V., Davis, M. N. & Naba, A. Pan-Cancer Analysis of the Genomic Alterations and Mutations of the Matrisome. *Cancers* **12** (2020). https://doi.org:10.3390/cancers12082046

252 Sherry, S. T., Ward, M. H., Kholodov, M., Baker, J., Phan, L., Smigielski, E. M. & Sirotkin, K. dbSNP: the NCBI database of genetic variation. *Nucleic acids research* **29**, 308-311 (2001). https://doi.org:10.1093/nar/29.1.308

253 Park, S., Supek, F. & Lehner, B. Systematic discovery of germline cancer predisposition genes through the identification of somatic second hits. *Nature communications* **9**, 2601 (2018). https://doi.org:10.1038/s41467-018-04900-7

254 Marston, S. The Molecular Mechanisms of Mutations in Actin and Myosin that Cause Inherited Myopathy. *International journal of molecular sciences* **19** (2018). https://doi.org:10.3390/ijms19072020

255 Kronert, W. A., Bell, K. M., Viswanathan, M. C., Melkani, G. C., Trujillo, A. S., Huang, A., . . . Bernstein, S. I. Prolonged cross-bridge binding triggers muscle dysfunction in a Drosophila model of myosin-based hypertrophic cardiomyopathy. *Elife* **7** (2018). https://doi.org:10.7554/eLife.38064

256 Orgaz, J. L., Crosas-Molist, E., Sadok, A., Perdrix-Rosell, A., Maiques, O., Rodriguez-Hernandez, I., . . . Sanz-Moreno, V. Myosin II Reactivation and Cytoskeletal Remodeling as a Hallmark and a Vulnerability in Melanoma Therapy Resistance. *Cancer Cell* **37**, 85-103.e109 (2020). https://doi.org:10.1016/j.ccell.2019.12.003

257 McGrail, D. J., Pilié, P. G., Rashid, N. U., Voorwerk, L., Slagter, M., Kok, M., . . . Lin, S. Y. High tumor mutation burden fails to predict immune checkpoint blockade response across all cancer types. *Ann Oncol* **32**, 661-672 (2021). https://doi.org:10.1016/j.annonc.2021.02.006

258 Bassani-Sternberg, M., Bräunlein, E., Klar, R., Engleitner, T., Sinitcyn, P., Audehm, S., . . . Krackhardt, A. M. Direct identification of clinically relevant neoepitopes presented on native human melanoma tissue by mass spectrometry. *Nature communications* **7**, 13404 (2016). https://doi.org:10.1038/ncomms13404

259 Reynisson, B., Alvarez, B., Paul, S., Peters, B. & Nielsen, M. NetMHCpan-4.1 and NetMHCIIpan-4.0: improved predictions of MHC antigen presentation by concurrent motif deconvolution and integration of MS MHC eluted ligand data. *Nucleic acids research* **48**, W449-w454 (2020). https://doi.org:10.1093/nar/gkaa379

260 Puré, E. & Blomberg, R. Pro-tumorigenic roles of fibroblast activation protein in cancer: back to the basics. *Oncogene* **37**, 4343-4357 (2018). https://doi.org:10.1038/s41388-018-0275-3

261 Fitzgerald, A. A. & Weiner, L. M. The role of fibroblast activation protein in health and malignancy. *Cancer Metastasis Rev* **39**, 783-803 (2020). https://doi.org:10.1007/s10555-020-09909-3

262 Vangangelt, K. M. H., Tollenaar, L. S. A., van Pelt, G. W., de Kruijf, E. M., Dekker, T. J. A., Kuppen, P. J. K., . . . Mesker, W. E. The prognostic value of tumor-stroma ratio in tumor-positive axillary lymph nodes of breast cancer patients. *International journal of cancer* **143**, 3194-3200 (2018). https://doi.org:10.1002/ijc.31658

263 Souza da Silva, R. M., Queiroga, E. M., Paz, A. R., Neves, F. F. P., Cunha, K. S. & Dias, E. P. Standardized Assessment of the Tumor-Stroma Ratio in Colorectal Cancer: Interobserver Validation and Reproducibility of a Potential Prognostic Factor. *Clin Pathol* **14**, 2632010x21989686 (2021). https://doi.org:10.1177/2632010x21989686

264 Hagenaars, S. C., Vangangelt, K. M. H., Van Pelt, G. W., Karancsi, Z., Tollenaar, R., Green, A. R., . . . Mesker, W. E. Standardization of the tumor-stroma ratio scoring method for breast cancer research. *Breast Cancer Res Treat* **193**, 545-553 (2022). https://doi.org:10.1007/s10549-022-06587-3

265 Doma, V., Kárpáti, S., Rásó, E., Barbai, T. & Tímár, J. Dynamic and unpredictable changes in mutant allele fractions of BRAF and NRAS during visceral progression of cutaneous malignant melanoma. *BMC cancer* **19**, 786 (2019). https://doi.org:10.1186/s12885-019-5990-9

266 Cherepakhin, O. S., Argenyi, Z. B. & Moshiri, A. S. Genomic and Transcriptomic Underpinnings of Melanoma Genesis, Progression, and Metastasis. *Cancers* **14**, 123 (2022).